Performance of nanoclay infused plant fibre-reinforced hybrid biocomposites under impact loading.

Submitted in fulfilment of the requirements of the degree of
Doctor of Engineering in Mechanical Engineering
in the
Department of Mechanical Engineering, Faculty of Engineering, and the Built Environment at the Durban University of Technology

MUFARO MOYO
(21557681)

MARCH 2023

Supervisor: Professor K. Kanny

Co-Supervisor: Dr T. P. Mohan

DECLARATION

I hereby declare that this dissertation is my own work and effort. It has not been submitted anywhere for any award or any other degree and is also not being concurrently submitted for any other degree. Where other sources of information have been used, they have been acknowledged.

Signature of candidate: …… …….

Date: ……24 March 2023…….....

We/I endorse the declaration by the candidate.

Name of Supervisor	Signature	Date Signed
Prof. K. Kanny		3/04/23
Dr. T. P. Mohan		3/4/2023

DEDICATIONS

To my beloved children, this is for you, to inspire and challenge you academically. I believe it is a good bar you should aim to reach and go beyond. This thesis is a demonstration that it can be achieved despite whatever obstacles you may face in life.

To my family members for believing in me, being a source of inspiration, for your never-ending love, emotional and moral support, prayers, encouragement and for enduring all the long periods I spent away studying depriving you of family time and visits. This is the fruit we will cherish forever.

To my friends, relatives and all those who assisted me in various ways during the study period.

ABSTRACT

This study focused on developing sustainable and lightweight plant fibre-reinforced hybrid bionanocomposites with enhanced impact properties. Such biocomposites are envisaged as potential replacements for the non-sustainable conventional synthetic fibre-reinforced polymer composites in applications requiring resistance to impact loading. In this work, the hybrid bionanocomposites were fabricated using polylactic acid (PLA) as the biopolymer, kenaf fibre nonwoven mat as the biofibre and clay nanoparticles of different loadings as fillers. Clay nanoparticle loading of 0, 3, 5, and 7 wt% were used. The resultant kenaf/nanoclay/PLA hybrid bionanocomposites were tested for thermal decomposition, tensile properties, flexural properties, dynamic mechanical properties and impact properties. The medium velocity impact resistance was tested using a high speed gas gun. The structure-property relationships were characterised using a scanning electron microscopy (SEM), energy dispersive x-ray (EDX), fourier transform infrared (FTIR) spectroscopy and x-ray diffraction (XRD) techniques. The resultant kenaf/nanoclay/PLA hybrid bionanocomposites were found to be considerably lightweight with a positive buoyancy. Clay nanoparticle loading of 5 wt% was found to be the optimum. The results showed that the thermal stability and dynamic mechanical properties of the hybrid bionanocomposites improved with the addition of clay nanoparticles. The tensile strength and the flexural strength of the hybrid bionanocomposites improved by 19.1% and 9.8%, respectively, when clay nanoparticles were added. Infusion with clay nanoparticles improved the Young's modulus and flexural modulus by 41.5% and 34%, respectively. Addition of clay nanoparticles improved the energy absorption capability and impact strength of the hybrid bionanocomposites under low velocity impact loading by 92.9% and 98.7%, respectively. The clay nanoparticles also considerably enhanced the medium velocity impact resistance of the hybrid bionanocomposites as evidenced by improvement of the perforation threshold limit, energy absorption capability and damage resistance. The perforation threshold limit improved to 37 m/s which was equivalent to 42.3% increase, the energy absorption capability improved by 109% and the resistance to damage improved by 26.5%. The dominating damage mechanisms for the kenaf/nanoclay/PLA hybrid bionanocomposites were observed to be shear, matrix cracking, matrix crushing, fibre fracture, fibre/matrix debonding, shear plugging, bulging, interface debonding and delamination. Since the resistance to impact loading was established to be in the medium velocity impact range, the novel hybrid bionanocomposites have a potential to replace the non-biodegradable synthetic fibre-reinforced polymer composites in cushioning against secondary debris or blasts in the medium velocity impact range. They are also suitable for lightweight applications such as in the transportation sector for lightweight mass transit systems and unmanned aerial vehicles (UAV). The novel biodegradable kenaf/nanoclay/PLA hybrid bionanocomposite materials developed in this work are potential materials for the future which can positively contribute to sustainability and attainment of Sustainable Development Goals (SDG's).

ACKNOWLEDGEMENTS

I am very grateful and greatly indebted to my project supervisor Prof. K. Kanny and my Co-Supervisor Dr. T.P. Mohan for their much-valued supervision, help, patience, encouragement and guidance which made this research work a success. I sincerely appreciate your collaborative efforts which gave this work a sensible direction.

I am also deeply indebted to Prof. R. Velmurugan from the Indian Institute of Technology Madras (IIT Madras) for facilitating and allowing me to perform the medium velocity impact tests and other characterisations at IIT Madras. Thank you very much for hosting me in your Department of Aerospace Engineering, Composite Technology Centre and for rendering me all the necessary support during the time of experimentation. Many thanks also go to Prof. Velmurugan's Composite Technology Centre team, especially Dr Naresh Reddy who helped a lot during the period of performing the medium velocity impact tests and other characterisations. Many thanks to Dr. G. Balaganesan, Department of Mechanical Engineering, Mechanical Engineering Workshop, IIT Madras for the assistance in machining the projectiles used during the medium velocity impact tests and machining of the test specimens.

Dr. Myalowenkosi Sabela (Department of Chemistry, DUT) who was my roommate at the DUT Corlo Court Residence. Thank you for the various kind of assistance rendered, comradeship support and for teaching me how to use some software important in research. Many thanks to Dr. Thabo Falayi, Namibia University of Science and Technology, Department of Mining and Process Engineering, Windhoek, Namibia for the assistance rendered during the analysis of some results and proof reading part of my research work and journal papers.

The authority of the National University of Science and Technology (NUST), Zimbabwe for giving me a study leave which enabled me to undertake the PhD study. I also thank my colleagues in the Department of Fibre and Polymer Materials Engineering, NUST for all the various kind of assistance given, encouragement and for being a source of my motivation.

My colleagues and friends from the Composite Research Group, DUT, namely, Dr. Avinash Ramsooroop, Dr. Festus Mwangi, Dr. Ajay Rane, Dr Joseph Toyin Gbadeyan, Mr. John Olusanya, Mr. Kenneth Nkemdilim Okeke, Mr. Olusegun Adigun Afolabi, Mr. Sifiso Nkosi, Dr. Stanley Onwubu, Dr. Maleni Thakur, Ms. Sathie Chetty, Mr. Robert Khumalo and Mr. Fidel Zandu for all the help and advice. I will remain grateful for your assistance and words of encouragement.

These acknowledgements would be inadequate without expressing my appreciation for the financial support received from the DUT through the Research and Postgraduate Support, the National Research Foundation (NRF) of South Africa and the Council for Scientific and Industrial Research (CSIR) of South Africa for the financial support to cover experiments.

Finally, I give glory to the Almighty God for always taking care of my soul, making me strong when facing huge "storms of life" and for making me successfully cross different life rubricons.

TABLE OF CONTENTS

LIST OF FIGURES

LIST OF TABLES

LIST OF ABBREVIATIONS

FRPC	–	Fibre reinforced polymer composites
SFRPC	–	Synthetic fibre reinforced polymer composites
NFRPC	–	Natural fibre-reinforced polymer composites
NFRBPC	–	Natural fibre reinforced biopolymer composites
PLA	–	Polylactic acid
NaOH	–	Sodium hydroxide
MMT	–	Montmorillonite
UTM	–	Universal testing machine
DMA	–	Dynamic mechanical analyser
TGA	–	Thermogravimetric analyser
DSC	–	Differential scanning calorimetry
SEM	–	Scanning electron microscopy
EDX	–	Energy dispersive x-ray
XRD	–	X-ray diffraction
FTIR	–	Fourier transform infra-red
PCC	–	Phantom Camera Control
PHA	–	Polyhydroxyalkanoates
SPSS	–	Statistical Package for Social Sciences

PUBLICATIONS AND CONFERENCE PROCEEDINGS AND PRESENTATIONS

Below is a list of the publications that have been generated from this research.

Journal Papers and Conference Proceedings

- **Moyo M**, Kanny K, Velmurugan (2020), The efficacy of nanoclay in enhancing medium velocity impact resistance of kenaf/PLA biocomposites, Journal of Applied Nanoscience. https://doi.org/10.1007/s13204-020-01602-9
- **Moyo M**, Kanny K, Velmurugan (2020), Performance of kenaf non-woven mat/PLA biocomposites under medium velocity impact, Journal of Fibres and Polymers. Volume 21, 2642–2651. https://doi.org/10.1007/s12221-020-1130-z
- **Moyo M**, Kanny K, Mohan T. P (2020), Thermo-mechanical response of kenaf/PLA biocomposites to clay nanoparticles infusion, Materials Today: Proceedings Journal. Volume 38, 609-613. https ://doi.org/10.1016/j.matpr.2020.03.471
- **Moyo M**, Kanny K, Mohan T.P (2022), Effects of combined alkali treatment and clay nanoparticle infusion on thermo-mechanical response of kenaf/PLA biocomposites, South African Journal of Science and Technology, Volume 40, Issue 1, 137-141.
- **Moyo M**, Kanny K, Velmurugan R, Mohan T.P and Balaganesan G (2018), Energy absorption of kenaf/PLA biocomposites, Advances in Composites, Biocomposites and Nanocomposites Volume 3, ICCBN 2018 Conference Proceedings, edited by Krishnan Kanny, 2018, 367-377, ISBN: 978-1-919858-30-2.
- **Moyo M**, Cherop P. T, Kanny K, Mohan T.P, Kiambi S and Musonge P (2018), Kinetics of non-isothermal degradation of polylactic acid film, Advances in Composites, Biocomposites and Nanocomposites Volume 3, ICCBN 2018 Conference Proceedings, edited by Krishnan Kanny, 2018, 378-391, ISBN: 978-1-919858-30-2.

In Preparation Journal Papers

- **Moyo M**, Kanny K, Mohan T.P (2022), Influence of clay nanoparticles on tensile, flexural and low velocity impact resistance of sustainable kenaf/nanoclay/PLA bionanocomposites. Target Journal: Journal of Applied Nanoscience.
- **Moyo M**, Kanny K, Mohan T.P (2022), Properties of alkalized and nanoclay infused kenaf fibre and their influence on mechanical properties of resultant hybrid bionanocomposites. Target Journal: Journal of Fibers and Polymers.

Book Chapters

- **Moyo M**, Rane A, Joseph G, Kanny K (2022), Green Composites Based on Polyhydroxyalkanoates in the book titled, "Green micro – and nanocomposites for future", edited by Sabu Thomas, Abitha V. K., and Hanna J. Maria, Stanford Publishing, Chapter 5, pages 147-164. (In press).

Conference Paper Presentations

- **Moyo M**, Kanny K, Mohan T. P (2021), Oral presentation at the Conference of the South African Advanced Materials Initiative (CoSAAMI-2021), 18-22 October 2021, South Africa. Presentation was on effects of combined alkali treatment and clay nanoparticle on thermo-mechanical properties of PLA kenaf fibre-reinforced bionanocomposites.
- **Moyo M**, Kanny K, Mohan T. P (2020), Oral presentation at the International Symposium on Nanostructured, Nanoengineered and Advanced Materials (ISNNAM 2020), 6-7 August 2020, International Convention Centre, Johannesburg, South Africa. Presentation was on the effects on nanoclay on the thermo-mechanical response of kenaf/PLA biocomposites.
- **Moyo M**, Kanny K, Velmurugan R, Mohan T.P and Balaganesan G (2018), Oral presentation on "Energy absorption of kenaf/PLA biocomposites", Third International Conference on Composites, Biocomposites and Nanocomposites (ICCBN2018), 7 – 9 November 2018, Nelson Mandela Bay Stadium, Port Elizabeth, South Africa.
- **Moyo M**, Cherop P. T, Kanny K, Mohan T.P, Kiambi S and Musonge P (2018), Oral presentation on "Kinetics of non-isothermal degradation of polylactic acid film", Third International Conference on Composites, Biocomposites and Nanocomposites (ICCBN2018), 7-9 November 2018, Nelson Mandela Bay Stadium, PE, South Africa.
- **Moyo M**, Kanny K, Mohan T. P (2018), Oral presentation on "Thermal and morphological effects of nanoclay on plant fibres", 7th International Conference on Nanoscience & Nanotechnology in Africa (NanoAfrica 2018), 22 – 25 April 2018, Salt Rock Hotel, Durban, South Africa.
- **Moyo M**, Kanny K (2016), Oral presentation on "Effects of nanoclay impregnation on banana fibres for reinforcement of composites", First Indo-South Africa Research Workshop on Nanocomposite Materials and their Applications, 7-9 July 2016, Umfolozi Hotel Casino Convention Resort, Empangeni, Durban, South Africa.

Chapter 1 Introduction

1.1 Introduction

This study focused on developing and enhancing the properties of plant fibre-reinforced biopolymer hybrid biocomposites for applications where medium velocity impact resistance is required. The hybrid biocomposites were made using kenaf, PLA and clay nanoparticles. Currently, development of biocomposites with good or enhanced impact resistance is one of the priority research areas surrounding biocomposites made using biodegradable materials. The aim is to expand the application spectrum of natural plant fibre reinforced biopolymer biocomposites to high performance applications previously dominated by polymer composites reinforced with synthetic fibres. Synthetic fibre reinforced conventional polymer composites or bio-fibre reinforced synthetic composites are currently the most used composites for applications requiring good impact resistance [1-6]. The replacement with biocomposites in such applications addresses a myriad of challenges associated with synthetic fibre-reinforced polymer composites such as sustainability, high costs of production and end-of-life waste disposal challenges.

1.2 Background of the study

The development and design of synthetic fibre reinforced conventional polymer composites as replacements to steel structures was a great achievement as it brought about improvements such as lightweight, resistance to corrosive substances and high strength-to-low weight ratio. However, these synthetic fibre-reinforced polymer composites brought their own challenges around issues of sustainability, high costs of production, high energy for their production and not being satisfactorily light weight. The source of raw materials for the synthetic fibre-reinforced polymer composites are petroleum based which are non-renewable. There is environmental degradation and pollution during extraction and processing of raw materials and additionally in the production of the conventional polymer composites. The processing activities and manufacturing of polymer composites requires high energy and is expensive. The other major problem is that synthetic fibre-reinforced polymer composites are not biodegradable and hence have a post-use disposal challenge. Compelling evidence shows that synthetic fibre-reinforced polymer composites (conventional FRPC), significantly contribute to the global waste problem [7-15]. In the search for solutions to address the challenges associated with synthetic fibre-reinforced polymer composites, proposed initiatives such as recycling, landfill and incineration have been found to have their own challenges which include high costs of recycling, landfill taxes and production of greenhouse gases during incineration.

In addition, these proposed initiatives focus on waste only and leave out other challenges affiliated with the synthetic fibre-reinforced conventional polymer composites unaddressed. Underlining philosophical realignment needed is to develop sustainable solutions around fibre reinforced composites. This pointed towards the use of biomaterials to produce biocomposites that can biodegrade. However, these biocomposites are not void of challenges.

One of the major challenges of biocomposites is that they have inherently inferior properties to conventional synthetic fibre-reinforced polymer composites. These include poor resistance to impact loading, poor resistance to thermal loading and moisture absorption [2, 3, 16-23]. These challenges are currently limiting the application scope of natural plant fibre reinforced biopolymer biocomposites to low-end or non-structural applications where light external loading like soft knocks or very low impact loading are experienced. Earlier studies initiated on biocomposite research resulted in the development of biocomposites not suitable to be used where good resistance to impact loading properties are required [5, 20, 23-28]. Cruz and Fangueiro, 2016 [18], Pickering et al., 2016 [17], Vaisanen et al., 2017 [16] postulated the need for improving properties of natural plant fibres and the resultant natural fibre-reinforced biocomposites so that they possess adequate property characteristics for diversified uses. Literature reiterates about the growing keenness in using renewable materials in the development of biocomposites for structural uses [2, 16, 21-23, 29, 30]. Vaisanen et al., 2017 [16] describe the development and utilisation of natural plant fibre strengthened biopolymer biocomposites as the upcoming step in developing sustainable biocomposites that are affordable and resilient.

1.3 Problem Statement

Natural plant fibre-reinforced biopolymer biocomposites which are identifiable as befitting and sustainable substitutes for synthetic fibre reinforced conventional polymer composites have low impact properties and hence perform poorly under medium velocity impact loading.

1.4 Scope of the research

Although there are diverse classes of biopolymers, plant natural fibres and clay nanoparticles, PLA, kenaf and montmorillonite (MMT) cloisite clay nanoparticles, respectively, were chosen for this research. Even though there are several chemicals used in the surface treatment of natural plant fibres, NaOH was chosen for modifying kenaf fibres in this work.

1.5 Aim

To develop and enhance properties of nanoclay infused kenaf/PLA hybrid biocomposites for applications requiring medium velocity impact resistance.

1.6 Objectives

The objectives of this research and the associated work plans are shown in Figure 1.1.

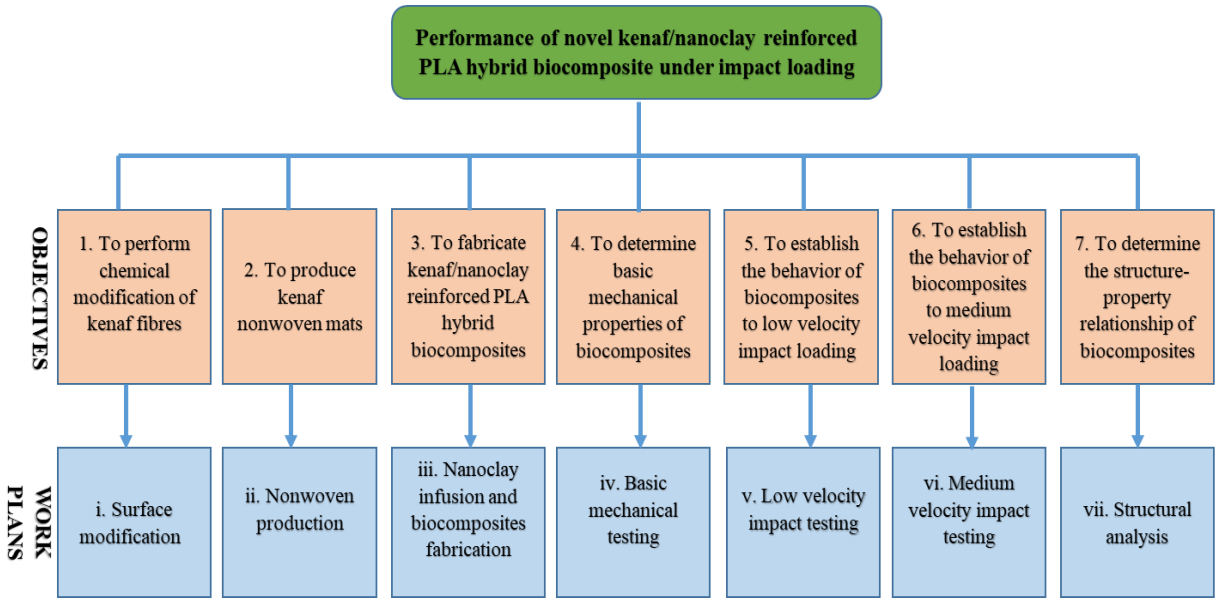

Figure 1.1 Objectives and work plans

The objectives and work plans shown in Figure 1.1 were achieved by performing various tests, characterisations and analyses of the nanoclay infused kenaf/PLA hybrid composite specimens.

1.7 Justification

This research positively contributes to sustainability through creation of completely biodegradable biocomposites which are cost effective, low weight and from renewable sources. It also creates an industry for low income countries whose communities can embark on the production of natural fibres which require low capital investment.

1.8 Contributions of the research work

This work contributes to the current body of knowledge in this field as follows;

- A novel hybrid bionanocomposite material suitable for use in application areas where resistance to medium velocity impact loading is required was developed. The use of biomaterials, namely kenaf and PLA and hybridisation with nanoclay makes the

material unique and novel. The material is also unique in that it is sustainable, lightweight and can float in water.

- Provides a means of enhancing natural fibre-reinforced biopolymer biocomposites properties using nanoparticles.
- Establishes the theory behind the behaviour of natural fibre-reinforced biopolymer biocomposites and their damage mechanisms under medium velocity loads. This could be used as benchmarks or points of reference for other future works on biofibre-reinforced biocomposites.
- Establishes the perforation threshold limit (ballistic limit) of model plant fibre-reinforced biocomposites.
- Establishes the optimum nanoparticles content for biocomposites intended for high-end applications.
- Establishes the damage mechanisms of the hybrid bio-nanocomposites.

1.9 Structure of the dissertation

This dissertation contains a total of eight (8) chapters, namely;

- Chapter 1 which is the introduction and contains the background, problem statement, scope, aim and associated objectives, justification, contribution of this research work and the outputs achieved in terms of journal papers, proceedings and conference papers.
- Chapter 2 which covers the literature reviewed in this work. This includes review on fibre-reinforced composite materials, their manufacturing processes, properties, testing, characterisation and applications. Review on application of nanotechnology in biocomposites production.
- Chapter 3 which constitutes the methodology. It describes the materials, research approach and methodology adopted in the fabrication, testing and analyses of the biocomposites.
- Chapter 4 which contains the results and discussions.
- Chapter 5 which summarises the results of published journal paper on the medium velocity impact behaviour of kenaf nonwoven fibre reinforced PLA biocomposites.
- Chapter 6 which summarises the results of published journal paper on the medium velocity impact behaviour of kenaf nonwoven reinforced/nanoclay/PLA hybrid bionanocomposites.

- Chapter 7 summarises the results of two journal papers on the effects of NaOH and clay nanoparticle infusion on thermal and mechanical properties of the hybrid bionanocomposites
- Chapter 8 consists of conclusion and recommendations and also points to future research directions related to the current work.

1.10 Conclusion

The focus of this study was on developing novel plant fibre-reinforced hybrid bio-nanocomposites with enhanced impact properties. The motivation behind was to develop sustainable and lightweight bio-nanocomposites with enhanced properties which make them to be suitable to replace the non-sustainable conventional polymer composites. The contributions of this work include development of novel, sustainable and lightweight hybrid bio-nanocomposites. The research also avails the theory surrounding the behaviour of hybrid bio-nanocomposites and their damage mechanisms when under medium velocity impact conditions. The theory could be applied as a benchmark or point of reference for any future research work on biocomposites exposed to impact conditions. The work also establishes the perforation threshold limit (ballistic limit) and optimum clay nanoparticle loading for the hybrid bio-nanocomposites. This information is currently not available in literature and hence will be of value to any upcoming research on biocomposites exposed to impact conditions. The findings of this research help in expanding the application spectrum of biocomposites from the current low end applications to high end applications where they can shield from secondary lasts and debris. In addition, the kenaf/nanoclay/PLA hybrid bionanocomposites can also be suitable for applications where lightweight and floatation are required. The hybrid bionanocomposites developed in this work would also positively contribute to the attainment of Sustainable Development Goals (SDG's) – Agenda 2030 in various ways and hence are potentially part of materials for the future. This dissertation is made up of eight (8) chapters.

Chapter 2 Literature Review

2.1 Introduction

Literature reviewed was on and related to matrices, fibres, fillers and other additives for composite materials, manufacturing processes for composite materials, types of composite materials, properties and applications. Also reviewed are applications of nanotechnology in the production and impact property characteristics of polymeric composite materials. The review of literature gave a deep understanding of the subject matter and revealed the research gaps.

2.2 Composite materials

Literature defines a composite in terms of a minimum of two distinctive phases or constituents in a material [31-33]. Hybrid composites result when at least two reinforcing materials are used [32]. Three major factors propelling the use of composites are weight curtailment, resistance to corrosion and part-count reduction [32]. Composites are lightweight materials because both the reinforcing fibres and the polymers used as matrices have low density. Composites to command a large market in industry displacing conventional materials such as steel [32-34]. Part-count reduction often translates into production, assembly, and inventory savings which in turn compensates for higher material cost [32, 33]. Composite materials are classified based mainly on reinforcement, laminate configuration and hybrid structure [32].

2.2.1 Reinforcement

This classification of composites considers the nature of the reinforcing material. The frequently used reinforcement materials are continuous long fibres, discontinuous fibres and particles and whiskers [32-35]. Figure 2.1 shows the different reinforcement materials for composites.

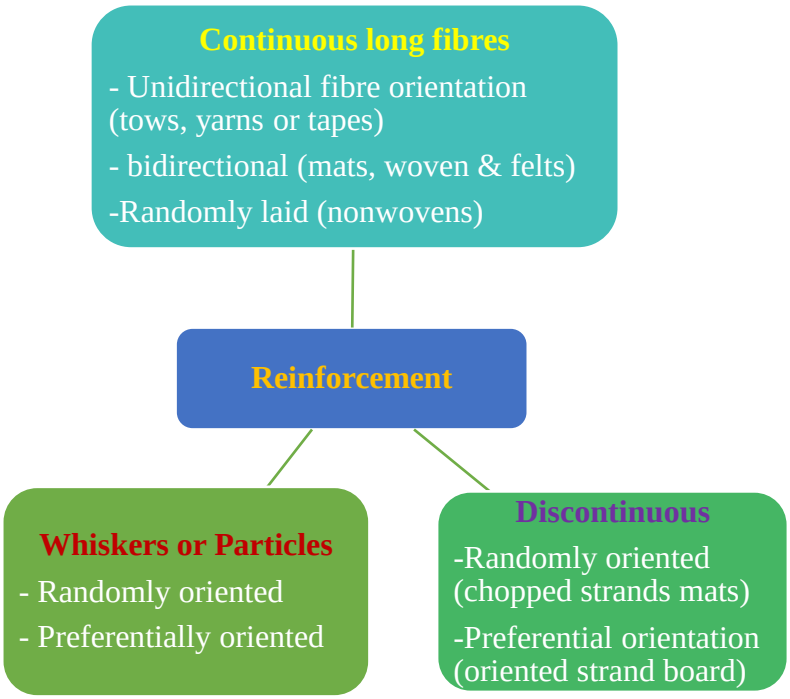

Figure 2.1 Reinforcement materials for composites

Fibre reinforcement is the most preferred in composites because it offers a lot of benefits. Fibre reinforced composite materials are multi-phased materials consisting of reinforcement material in form of fibres bonded to a polymer matrix forming distinct interfaces [32, 36, 37]. However, fillers or other additives can be included in the matrix during production of the composites [37].

2.2.2 Laminate configuration

The lamina or laminate could be unidirectional or bulk composites [32]. Unidirectional arranged lamina could be single lamina (called layer or ply) or several lamina (laminae). Laminae consist of similar material and orientation. A laminate contains multiple stacked laminae and connected together with other laminae of different material and orientation. Bulk composite materials have unidentifiable laminae and they include bulk compounded composites and particulate-reinforced polymer composites [32].

2.3 Matrix

Matrix also referred to as resin, is a substance that binds fibres together. The functions of a matrix are shown in Figure 2.2. The decomposition temperature of the reinforcement fibres influences the selection of the matrix [17]. Most natural fibres, for instance, are thermally

unstable above 200 ºC, although under some scenarios they could be processed but for a short period at temperatures slightly higher than their decomposition temperatures [17].

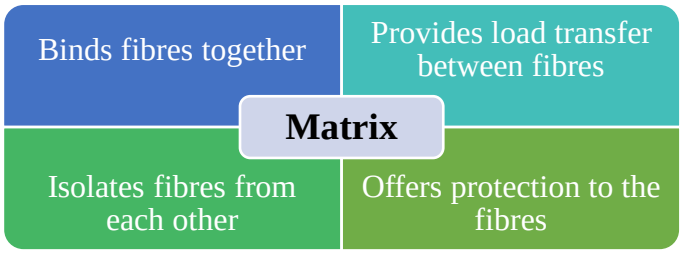

Figure 2.2 Functions of matrix in composites

Matrices dictate the response of the composite material to degradative conditions that eventually lead to failure of the structure [28, 32, 33, 37, 38]. Degradative effects include;

- Delaminated effects
- crack development and propagation
- moisture absorption
- damage due to impact
- thermal creeping
- chemical destruction.

The matrix also holds the fibre orientation and position in the composite material for carrying the loads and distribution of the stress among the fibres thereby providing resistance to crack development and propagation due to plastic flow at the cracked tips [28, 39]. Although matrices play a minor role in determining the capability of a composite material in carrying the tensile load, its selection influences compressional, interlaminar and in-plane shear property characteristics of the composite structure [37, 38].

Common types of matrices for composite are polymer matrix, metallic matrix, ceramic matrix and in some cases carbon [28, 37]. Ceramics and metal matrix materials are commonly used in environments with high temperatures, for instance, motor parts of engines [28]. Polymer matrices are the most preferred matrix materials in the production of fibre-reinforced composites [28, 37, 38]. Polymer matrices are broadly divided into non-biodegradable polymers and biodegradable polymers with a further classification on whether they are thermoset polymers or thermoplastic polymers as shown in Figure 2.3.

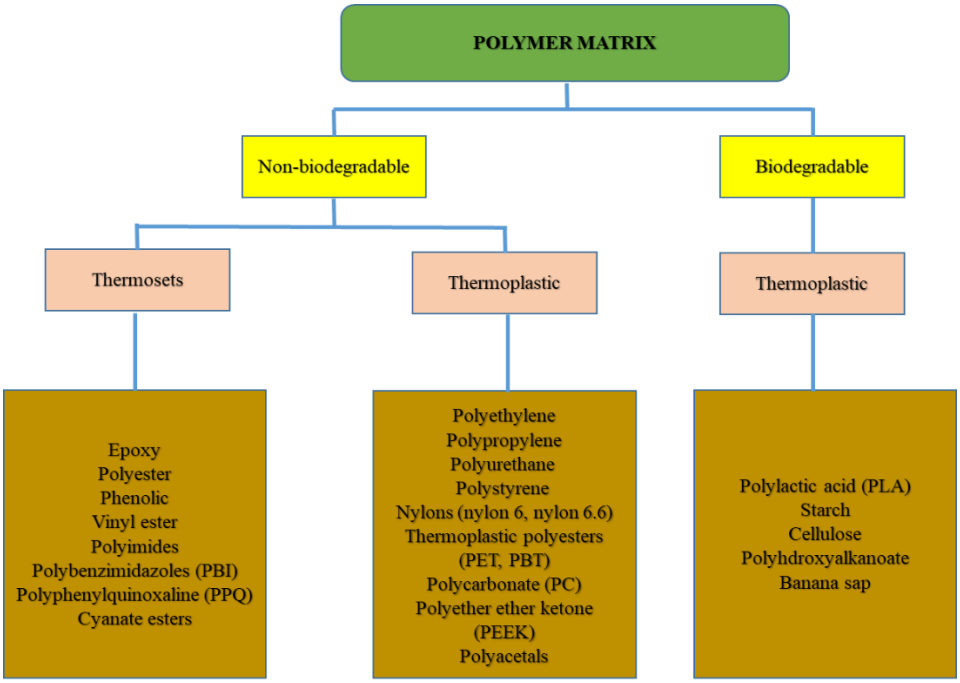

Figure 2.3 Classification of polymer matrices

2.3.1 Non-biodegradable polymer matrix

This group comprises of non-biodegradable petroleum based thermoset and thermoplastic polymers. They are referred to as conventional polymers [40]. They are well established worldwide for various applications because of their long durability, high modulus and elevated specific strength [41]. They could be either thermoset polymer matrix or thermoplastic polymer matrix. Their discussion is the next sections.

2.3.2 Thermoset polymer matrix

Thermoset matrix (resin) is a polymeric material in a liquid form which can be irretrievably get changed by curing [28]. They are applied as matrix materials in continuous (long) fibre reinforced conventional composites due to their low viscosity which makes them easy to process [37, 38]. Their uniqueness is on ability to form three-dimensional crosslinked networks by curing [38]. When working with thermoset matrices, joining of molecules is achieved by crosslinking [37]. After the crosslinking process, heat application cannot melt the thermoset polymeric material [37]. However, the thermoset polymeric material could be softened at high temperature if the crosslinking was low [37]. Thermosets are frequently applied in high performance and advanced composite materials for applications such as aerospace, automotive, wind turbine blades where remarkably high strength, modulus and chemical stability are a priority [38]. They have high resistance to thermal loading, dimensional stability, high rigidity,

high creep resistance, good resistance to chemicals, corrosives and solvents [28]. However, thermoset matrices have major drawbacks of brittleness at room temperature, poor toughness, and low elongation (elasticity) after having been hardened [28]. Epoxy resin, polyester matrix, vinyl esters and phenolic matrices are reportedly the most widely employed matrices in the production of natural plant fibre-reinforced composite materials [42].

2.3.3 Thermoplastic polymer matrix

Thermoplastic matrices are extremely common and cheaper than thermosets [28]. They are usually employed on short fibre-reinforced composites which can be produced through extrusion, for instance, injection moulding [37]. It has been reported that there is an increasing interest in making continuous fibre reinforced thermoplastic composite materials because of their inherent favourable properties like lightweight and mouldability into varied shapes [37, 38]. In a thermoplastic matrix material, individually existing molecules are not chemically connected together. They are, instead, joined by intermolecular forces (weak secondary bonds), that is, hydrogen bonding and van der Waals bonds [37]. Heat application to a solid thermoplastic matrix breaks down the intermolecular forces temporarily leading to the molecules to flow (move relative to each other) forming a new configuration when under pressure [37]. Upon cooling, the molecules get frozen in the new layout and the secondary bonds are then restored which result in a new solid shape [17, 37]. Therefore, thermoplastic polymeric matrices could be softened by heat application, melted and reshaped (or post-formed) multiple times [17, 37].

Thermoplastic polymers have advantages over thermoset polymers of higher impact strength and fracture resistance or toughness which translate to excellent damage tolerance properties to the composite material [28, 37]. Thermoplastic polymeric matrices generally have higher ratio of strain-to-failure than thermoset polymeric matrices and this provides good resistance to microcracking of matrix in composite materials [37]. Thermoplastic polymeric matrices also have benefits of infinite storage (shelf) life at room temperatures, short time for fabrication and postformability, for instance, by thermoforming [28, 37]. Thermoplastic composites can be easily recycled and reformed [28]. However, impregnating the reinforcing fibres in thermoplastic resin is challenging as the resins are naturally in a solid state [28].

2.3.4 Challenges of non-biodegradable polymer matrix

Some of the major challenges associated with the non-biodegradable polymer matrices are that the fossil fuels, which are the sources of these polymers are getting depleted and have environmental impact during extraction and processing [38, 42-44]. The polymers do not biodegrade and hence they accumulate as waste and pollute the environment after post-use disposal [40-42, 45-47]. Recycling of these polymers is expensive and hence their disposal is often dependent on combustion or incineration which produces toxic and hazardous substances and gases [45]. Consequently, these concerns are important driving factors for researchers to come up with alternatives to the petroleum based polymers.

2.4 Biodegradable polymer matrix

Growing concerns on and calls for sustainability triggered a paradigm shift with regards to the development and uses of biodegradable polymers (biopolymers) as composite matrices. Biopolymers are defined as polymers derived from renewable sources or living organisms and their biodegradability is influenced by the polymer's physical and chemical microstructure [39, 45]. Biopolymers are favourable candidates in replacing the synthetic polymers from an ecological angle and sustainability opinion [17, 38]. Biopolymers are divided into natural biodegradable polymers and synthetic biodegradable polymers depending on their origin [40, 47, 48].

2.4.1 Natural biodegradable polymer matrix

Natural biodegradable polymers are obtained from renewable sources, namely, plants, animals or microorganisms such as bacteria. Figure 2.4 shows different divisions of natural biodegradable polymers.

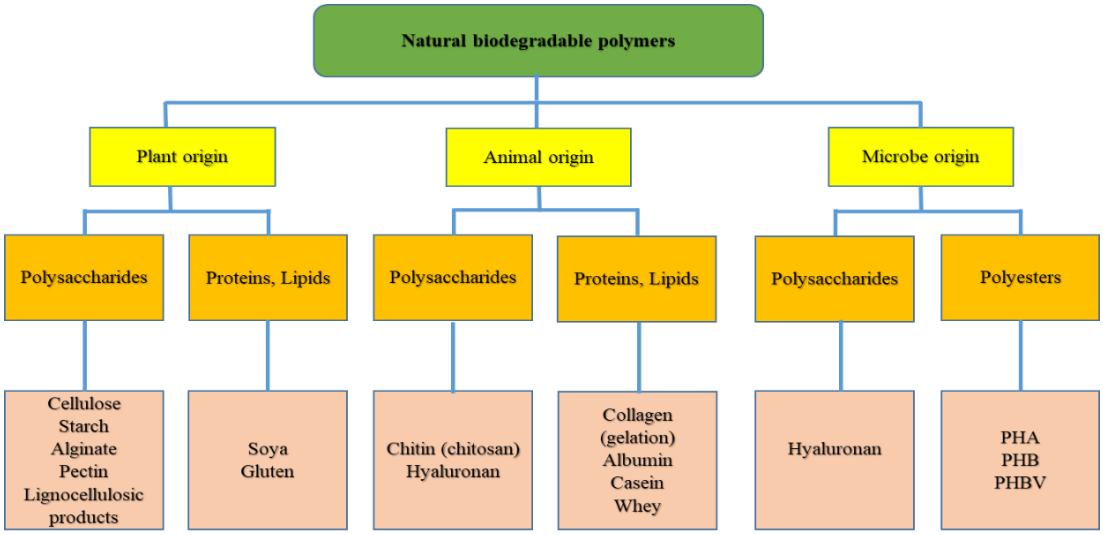

Figure 2.4 Natural biodegradable polymers

The classifications shown in Figure 2.4 were done by referencing to literature on natural biodegradable polymers [39, 40, 43-45, 47-53]. The extracted natural biopolymers can be polysaccharides, proteins, lipids or polyesters and the specific examples of these are shown in Figure 2.4. The agro-based polymers (such as polysaccharides, proteins and lipids) are acquired by fractionation from biomass and the polyester polymers (such as PHA, PHB and PHBV) are obtained by the fermentation process from biomass substances or genetically modified plants [44]. The utilisation of biomass in composite production results in biomass beneficiation. The utilisation of the naturally available huge raw materials results in the reduction of waste materials and carbon dioxide released in the atmosphere and promotes complete biodegradation [48]. Reinforcing biomass-derived matrices with biomaterials gives green composites [44, 48, 54].

2.4.2 Synthetic biodegradable polymer matrix

These are acquired from non-renewable petroleum based sources. They are defined as polymers modified from naturally occurring polymers or synthesized chemically from synthetic polymer monomers in a way that makes them to naturally degrade without leaving residual substances harmful to the environment [45]. Figure 2.5 shows different divisions of synthetic biodegradable polymeric matrices.

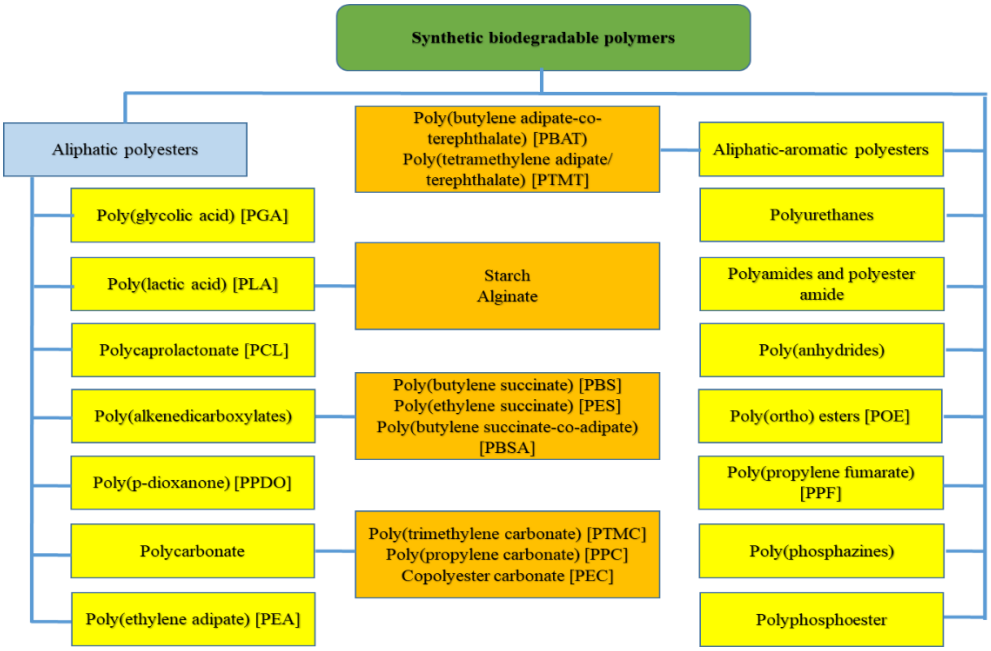

Figure 2.5 Synthetic biodegradable polymers

The classifications shown in Figure 2.5 were done by referencing to literature on synthetic biodegradable polymers [39, 40, 43-45, 48-50, 55-57]. Synthetic biodegradable polymers are synthesised from monomers obtained from biomass (such as PLA) and others synthesised by the petrochemical processes [44]. Numerous studies show that PLA is a clear front-runner and the most widely employed biopolymer in manufacturing of composite materials due to its properties which are comparable to those of synthetic polymer matrices [17, 38]. Table 2.1 shows properties of selected polymer matrices.

Table 2.1 Properties of selected polymer matrices
(Sources [4, 16])

Matrix	**Density (g/cm^3)**	**Tensile strength (MPa)**	**Young's modulus (GPa)**	**Melting temperature (^oC)**	**Thermal conductivity ($W.m^{-1}.K^{-1}$)**	**Total heat release (kJ/g)**
Polyethylene	0.9	14.8	0.83	115	0.51	41.7
Polypropylene	0.9	40.3	1.92	130	0.22	41.3
Polyacrylonitrile	1.2	57.1	2.73	300	1.03	13.4
Polycarbonates	1.2	69.9	2.60	157	0.18	20.2
Polystyrene	1.1	40.2	3.03	240	0.04	38.9
Polymethyl methacrylate	1.2	46.8	2.23	130	0.21	24.4
Polyvinyl chloride	1.4	51.4	2.42	160	0.18	11.4
Polyvinyl acetate	1.2	39.7	1.71	200	0.32	21.7
Polylactic acid	1.2	50.3	3.54	160	1.14	14.1
Polyethylene terephthalate	1.4	55.4	2.73	260	0.16	15.2

2.4.3 Polylactic acid

Polylactic acid (PLA) is part of the aliphatic polyesters family with origin from α-hydroxy acids [40]. It is not regarded as a new polymeric material. Production of PLA started with Jules Pelouze in early 1845 by condensation of lactic acid using a distillation process forming low-molecular weight PLA and lactide [58]. A century later, Wallace Carothers who was a DuPont scientist discovered the production of PLA by heating in a vacuum [58]. However, this process was found infeasible for the industrial scale production of high purity PLA because of the high costs associated with the purification process. Consequently, it was limited to the manufacturing of devices, such as sutures, drug carriers and implants, for the medical sector. In 1992, Cargill, a company which was also involved in PLA research and development since set up a pilot plant [58]. Cargill Dow Polymer LLC joint venture was formed in 1997 by Cargill and Dow for commercialisation of PLA under the Ingeo brand [58]. This was a landmark in the history of PLA as it enabled large-scale production and use of PLA biopolymer. This stimulated an expansion in PLA research, inventions and publications. For this reason, PLA is viewed as one of the most promising sustainable material due to its compostability and its renewability since it is acquired from renewable sources such as starch and sugars [40].

2.4.4 Synthesis and production of PLA

2-hydroxy propionic acid which is a lactic acid (LA) monomer is used in the production of PLA by either the direct polycondensation (DP) process route or the ring-opening polymerisation (ROP) process route [58]. Figure 2.6 shows the two routes that can be used in the production of PLA.

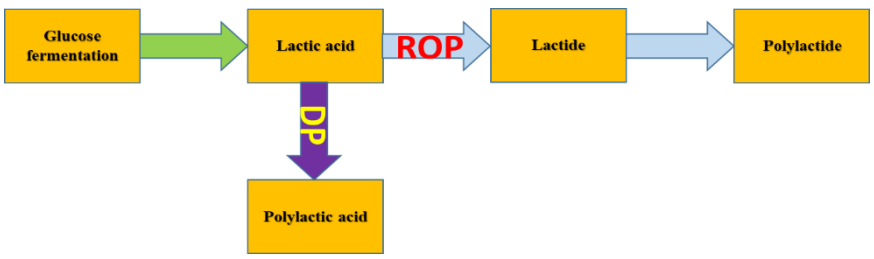

Figure 2.6 PLA production routes

Fermentation of sugar gives LA which is then converted to PLA using the DP route or lactide and then polylactide using the ROP route. Though the terms polylactic acid and polylactide could be interchangeably applied, scientifically they are different. Polylactic acid refers to the PLA produced from LA [58]. LA is produced from non-fossil renewable agricultural feedstock

or biomass such as corn, potato, sugar-beet, cane molasses [59]. Other sources include cellulosic non-food biomass and crops (such as switchgrass) and agricultural waste [59]. NatureWorks, currently, commands the largest single production facility share for LA producing about 180000 metric tonnes per year from corn as the feedstock [58]. The LA produce from NatureWorks is converted largely to Ingeo PLA [58]. The largest producer of LA is Purac but its products are used in beverage, food and pharmaceutical sectors [58]. Figure 2.7 shows the PLA global production capacity.

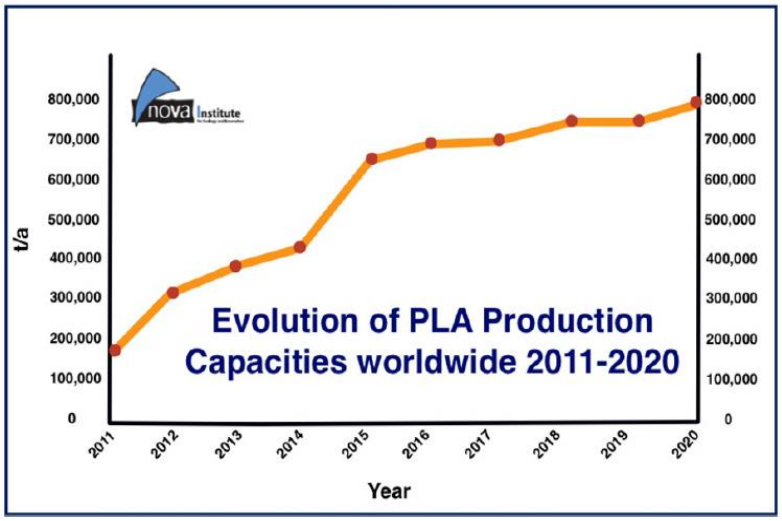

Figure 2.7 2011 to 2020 PLA global production capacity

(Source: [59-61])

Figure 2.7 shows that PLA production in t/a (tonnes/year) is increasing enormously. This is due to the increased demand on PLA products.

2.4.5 Properties of PLA

PLA's optical purity strongly impacts the properties of the polymer like structural, mechanical, thermal and barrier characteristics [59]. PLA consisting of above 90% L-content tends to be crystalline or semicrystalline whilst grades with lower optical purity tend to be amorphous [59]. Properties of PLA vary according to [58];

- Polymer structure
- Degree or level of crystallinity,
- Formulation of the material (for instance, availability of blends, inclusion of plasticizers and composites)

- Molecular weight
- Configuration (orientation).

The polymer structure influences the PLA's mechanical and thermal characteristic properties. The crystallinity parameter affects PLA's mechanical characteristic properties [58]. PLA 3051D has a Tg between 55 – 65 ^{o}C, melting temperature of around 180 – 184 ℃ and tensile strength of about 48 MPa and are almost identical to other polyester polymers like PET [40, 45, 62]. Biodegradable and non-biodegradable plasticisers lower the Tg and improve ductility and processability [58]. Blending PLA with other materials culminates in property changes. In this study, particular interest is on the blending of PLA with organo-modified clay nanoparticles. Previous studies showed that addition of cloisite 30B at 5 wt.% to PLA increased modulus but adversely affected tensile strength and elongation [58]. Hybridising PLA with cloisite 30B and paraloid EXL2330 at 5 wt% and 20 wt%, respectively, significantly improved impact strength and percentage elongation, reduced tensile strength and no changes on the modulus when compared to the control neat PLA [58]. NatureWorks reported that use of 35-80% rubber (high content) blendex 338 impact modifier or polyurethane improves the impact strength [58]. Biomax strong has been reported to lessen PLA's brittleness as well as enhancement of impact strength and other properties like melt stability and flexibility [58].

PLA's thermal properties are low due to absence of the benzoic ring [40]. Table 2.2 below summarises mechanical properties of some PLA grades from NatureWorks.

Table 2.2 Mechanical properties of some PLA grades from NatureWorks

Property	**Unit**	**Ingeo 2003D**	**Ingeo 3801X**	**Ingeo 8052D**
Strength (Tensile)	MPa	53.2	--	--
Strength (Yield)	MPa	60.1	25.9	48
Young's modulus	GPa	3.6	2.9	-
Elongation	%	6.1	8.1	2.5
Impact Strength (Notched)	J/m	12.8	144	16
Strength (Flexural)	MPa	--	44	83
Modulus (Flexural)	GPa	--	2.85	3.8

Source [58]

Ingeo 2003D PLA grade is employed as a general purpose extrusion PLA grade for applications in the food sector. Ingeo 3801X polymer is suitable for injection moulding requiring high heat

and impact performance. Ingeo 8052D PLA grade is designed for packaging applications, for instance, packaging of fresh farm produce like vegetables and meat [58]. Ingeo biopolymer 10361D is derived from renewable resources and used as a binder or adhesive-grade resin [63]. It has Tg ranging between 55 – 60 ºC [63]. Figure 2.8 shows PLA's chemical structure.

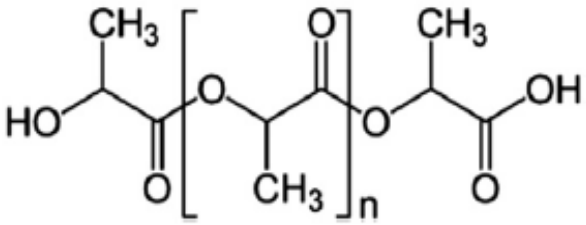

Figure 2.8 Chemical structure of PLA

PLA is hydrophobic due to the existence of methyl groups (–CH3) in its structure as shown in Figure 2.8 [40, 45]. Consequently, it is more resistant to hydrolysis. The carbonyl group (C=O) in PLA weakens its chemical and water resistance properties leading to its degradation by hydrolysis [40]. Hydrolytic degradation of PLA could take place after it has absorbed only 1% moisture which demonstrates its biodegradability and eco-friendliness [40]. Matrix porosity and polymer crystallinity influence the degradation rate [45]. PLA experiences three principal types of degradative processes, namely, chemical hydrolytic, enzymatic and microbial degradation [40].

Chemical hydrolytic degradation happens when the C=O bond of PLA is attacked by the water molecule. Enzymatic degradative effect takes place in the PLA's amorphous part to preferentially attack the ester bonds of LA [40]. The enzymes that degrade PLA belong to the same group with enzymes that degrade silk fibroin and hence same conclusions can be made for the microbial degradation [40].

Solubility of PLA can be performed using the following [58];

- trichloromethane (chloroform) – $CHCl_3$.
- dichloromethane (methylene chloride) – CH_2Cl_2.
- 1,4 dioxane (simply called dioxane) – $C_4H_8O_2$.
- acetonitrile abbreviated as MeCN (methyl cyanide) – $H_3C{-}C{\equiv}N$.
- 1,1,2-trichloroethane – $C_2H_3Cl_3$
- dichloroacetic acid (bichloroacetic acid) – $CHCl_2COOH$

Solubility is also performed by heating usually to boiling points [58] using:

- acetone,
- toluene (toluol),
- ethylbenzene

Generally, PLA does not dissolve in water, alcohols (selected) and alkanes. PLA that is highly crystalline is resistant to solvent attack by acetone solvent, ethyl acetate compound and tetrahydrofuran (THF). Amorphous PLA is easily dissolved in many and varied organic solvents like benzene, chlorinated solvents, dioxane, THF and methyl cyanide (acetonitrile) [58, 64].

The life-cycle of PLA biopolymer shown in Figure 2.9 shows some of the benefits associated with PLA.

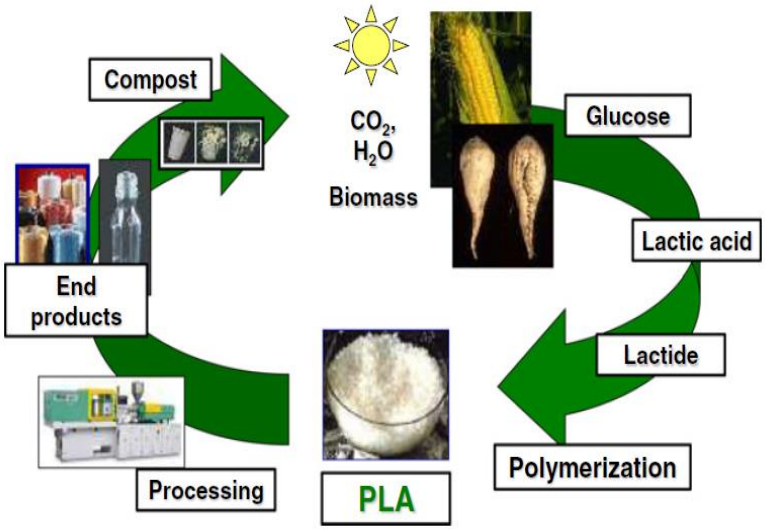

Figure 2.9 PLA life cycle
(Source: [59])

The PLA life cycle allows the biological to complete the circle. The biological systems use solar energy, water and carbon dioxide during photosynthesis. The biomass from products such as corn and sugar-beet is then used in the manufacturing of PLA which is then applied in the production of biodegradable and compostable materials. The compost from PLA provides nutrients to the biological systems thereby facilitating a healthy photosynthesis process and plant growth. The cycle goes on and on like that. The PLA life cycle results in the reduction of carbon footprint.

However, PLA is not void of challenges and hence it has some limitations on certain applications. Some of the challenges of PLA include poor toughness (brittleness) and poor thermal stability [45, 64]. The chain mobility and crystallization can be improved by plasticization [45].

2.4.6 Applications of PLA

Figure 2.10 shows some of the applications of PLA.

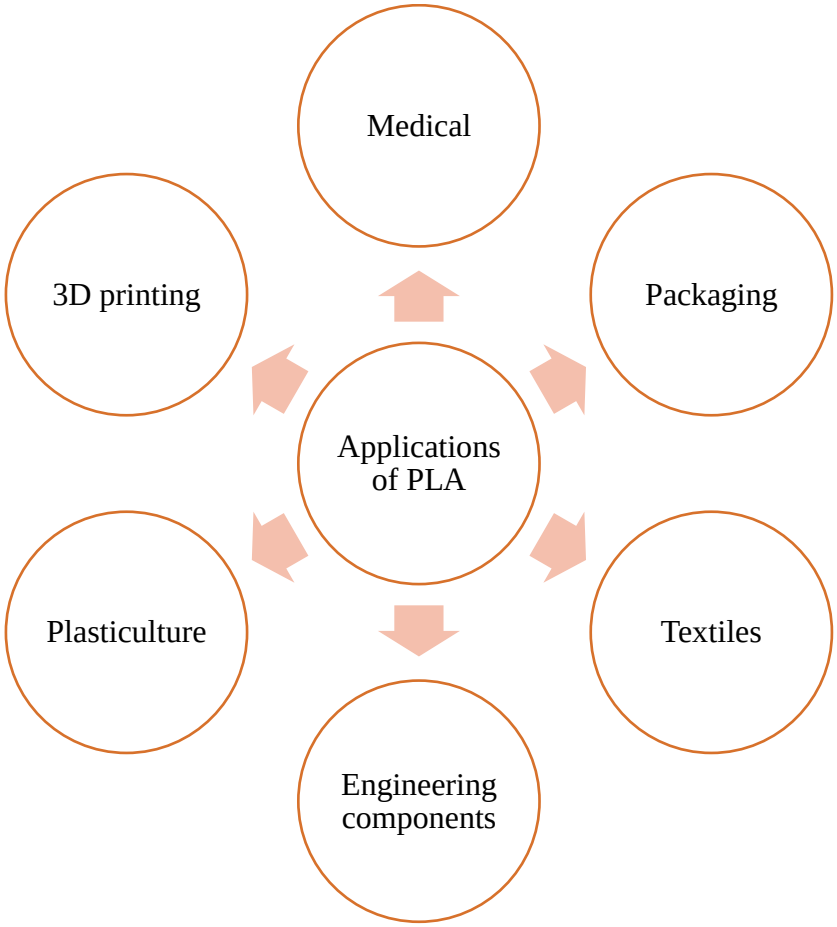

Figure 2.10 Applications of PLA

Although PLA possesses properties desirable for applications in consumer goods, it has some challenges for multipurpose applications just like any other polymeric material. As a result, researchers are continually trying to expand the application spectrum of PLA through different initiatives. Some of the initiatives include blending the PLA biopolymer with some resins and compounding the PLA biopolymer with fillers like fibres, micro-particles and particles in the nano-scale range [65].

2.5 Fibres

The fibres employed as reinforcement in the production of composites are usually of high strength, stiffness and modulus [32, 36, 37]. Figure 2.11 shows the main functions of fibres in fibre-reinforced composites.

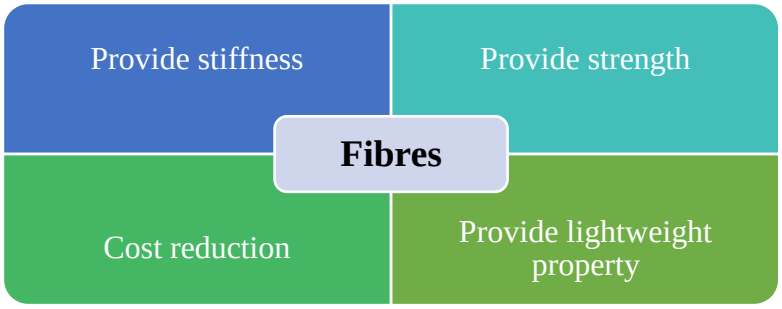

Figure 2.11 Functions of fibres in composites

The choice of fibre type to be used as reinforcement is a trade-off among considerations such mechanical properties, environmental properties and cost [32]. The fibres used in the reinforcement can be synthetic fibres or natural fibres and in cases of some hybrid composites, a combination of synthetic fibres and natural fibres.

2.5.1 Synthetic Fibres

These are artificial (man-made) fibres and are the conventional reinforcing fibres in making composite materials reinforced using fibres. Common synthetic fibres used as reinforcements in the making composites are glass fibre, carbon fibre and aramid fibres [6, 32, 33, 35]. Glass fibres are in the forefront in terms of usage as polymer reinforcement. About 90% of all fibre-reinforced polymer composites are made of glass fibres [6]. E-glass (electrical glass grade) is a very popular glass form. A-glass which is an alkali glass type, C-glass which is a chemical resistant glass type and R-glass (S-glass) which is the high strength type of glass are other types of glass fibres [6]. Carbon fibre has high strength and offers biggest strength and modulus properties [6]. Carbon fibres are independent of moisture and maintain their tensile strength even at elevated temperatures [6]. Aramid fibres find uses where high strength, high impact resistance and lightweight are a priority. Kevlar is the commonly used aramid fibre in the manufacturing of fibre-reinforced composites with high impact resistance [6]. Other synthetic fibres used as reinforcement materials include silica fibres, quartz fibres, boron fibres, ceramic fibres, basalt fibres and metallic fibres [32, 33, 35]. Although this group of fibres has good mechanical properties, literature shows that they have some drawbacks [3, 18, 19, 66]. The major challenges associated with synthetic fibres are shown in Figure 2.12.

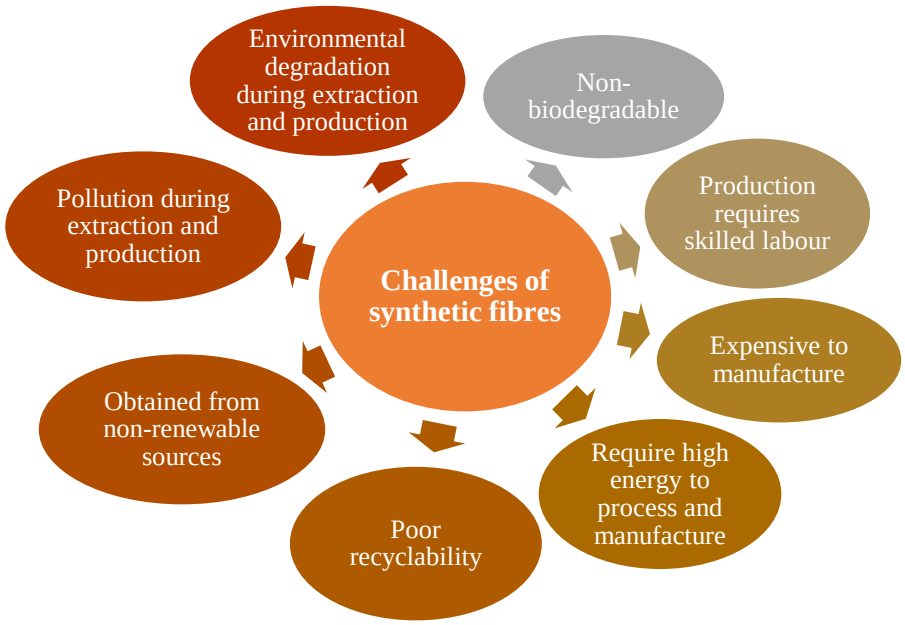

Figure 2.12 Challenges of synthetic fibres

Figure 2.12 shows that synthetic fibres:

- are non-biodegradable and hence are not environmentally friendly. This poses a threat to safe post-use disposal.
- need high investment in processing and production equipment making the fibres generally expensive.
- require skilled labour during the extraction of the raw materials and their processing into final product. This means there is need to invest in human capital development of skilled personnel to handle the synthetic fibre production processes unlike in the production of natural fibres were low level skills are required.
- require high energy during processing and manufacture which increases the production costs. Also, they are not suitable for poor countries which have energy challenges.
- are obtained from non-renewable petroleum resources. These petroleum sources are getting depleted and hence the need for alternatives cannot be overemphasized.
- have extraction and production processes which cause pollution and environmental degradation. Mining of petroleum contributes to environmental degradation in various ways such as production of toxic and non-toxic wastes which become part of the environment. Also, by-products such as volatile organic compounds and the industry's emissions of greenhouse gases pollute the environment.

- have poor recyclability and hence they are mostly landfilled after use. This is a challenge because of the high landfill costs and that landfill space is shrinking everywhere. Incineration releases toxic gases and hence cannot be an alternative.

Synthetic fibres' mechanical properties are good. Table 2.3 shows mechanical properties of selected synthetic fibres commonly used as reinforcing materials in the manufacture of fibre-reinforced composites.

Table 2.3 Mechanical properties of selected synthetic fibres and cost [5, 16, 17, 26, 28, 38, 67, 68]

Fibre	Density (g/cm^3)	Elongation (%)	Tensile strength (MPa)	Young's modulus (GPa)	Cost ($/kg)
E-glass	2.6	2.5-3.0	2000-3500	70-76	1.60
S-glass	2.5	2.8	4570	86.0	4.80
Carbon	1.7	1.4-1.8	4000	235	15-22
Aramid	1.4	3.3-3.7	3000-3150	63-67	11-25

2.5.2 Natural Fibres

Natural fibres are fibres which occur naturally. They are acquired from different parts of the plants, animals or minerals and hence are divisible into plant, animal and mineral fibres. Plant fibres are cellulosic in nature and animal fibres consist of proteins such as keratin and collagen [17, 28]. Figure 2.13 shows the categories of natural fibres.

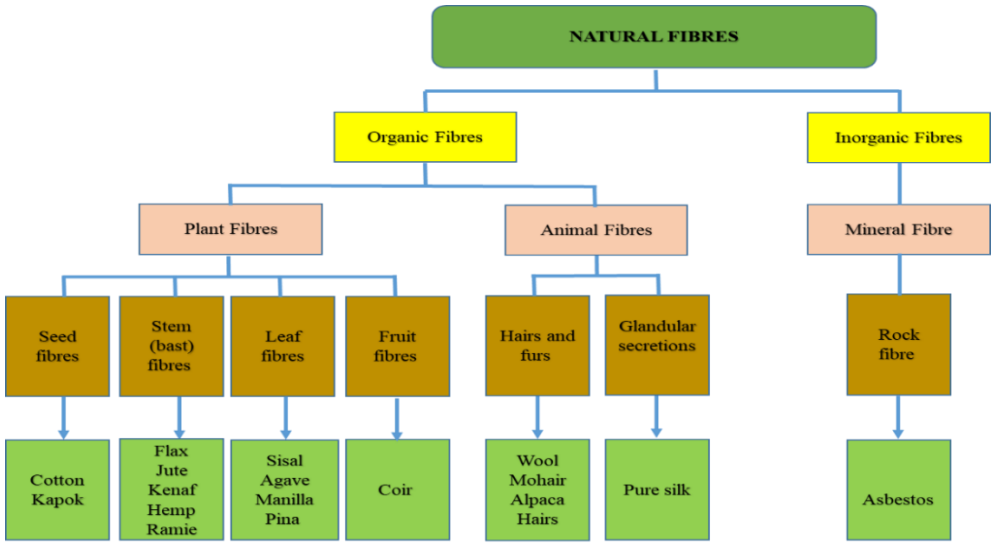

Figure 2.13 Classes of natural fibres

Plant fibres are the most commonly applied natural fibres in composite reinforcement [28]. The most common and promising sustainable fibres for use as reinforcement in the production of composites are kenaf, sisal, jute, coir, flax and hemp [28, 67]. Consequently, their annual production statistics and producing countries are of importance to industries that use plant fibres as reinforcing materials. Table 2.4 shows natural fibres annual production, costs and largest producers.

Table 2.4 World annual production of selected natural fibres, cost and largest producers [16, 20, 26, 28, 38, 68-71]

Fibre	**Species**	**World production (10^3 tons)**	**Cost ($/kg)**	**Largest producers**
Cotton	Gossypium	2500	1.50-2	China, India and USA
Coir	Cocos nucifera	100	0.50	India and Sri Lanka
Flax	Linum usitatissimum	830	3.11	Canada, France and Belgium
Hemp	Cannabis sativa	214	1.55	China, France and Philippines
Jute	Corchorus capsularis	2500	0.90	India, China and Bangladesh
Kenaf	Hibiscus cannabinus	970	0.38	USA, India, South Africa and Bangladesh
Ramie	Boehmeria nivea	100	1.52	China, Brazil, Philippines and India
Sisal	Agave sisalana	378	0.65	Tanzania and Brazil
Pina	Ananas comosus	74	0.10	Philippines, Thailand, Indonesia and India
Banana	Musa indica	200	0.81	India and Brazil

The growth and utilisation of natural fibres bring social and economic benefits to developing countries. The living conditions of the small-scale farmers and low-income employees are supported and improved by embarking on cultivation of plants for natural fibre production. India's jute industry, for instance, directly employs about 260 000 workers and supports the living style of about 4 million families [71]. A similar scenario existed in Bangladesh in 2008 where about 750 000 farmers were involved in the cultivation of jute plants and 2.5 million workers were employed in the jute processing mills [71]. These scenarios show the benefits brought about by cultivation of plants for natural fibre production and having mills for

processing of natural fibres. The living conditions of the people are uplifted and national unemployment rate gets reduced.

Figure 2.14 shows some of the major advantages of natural fibres.

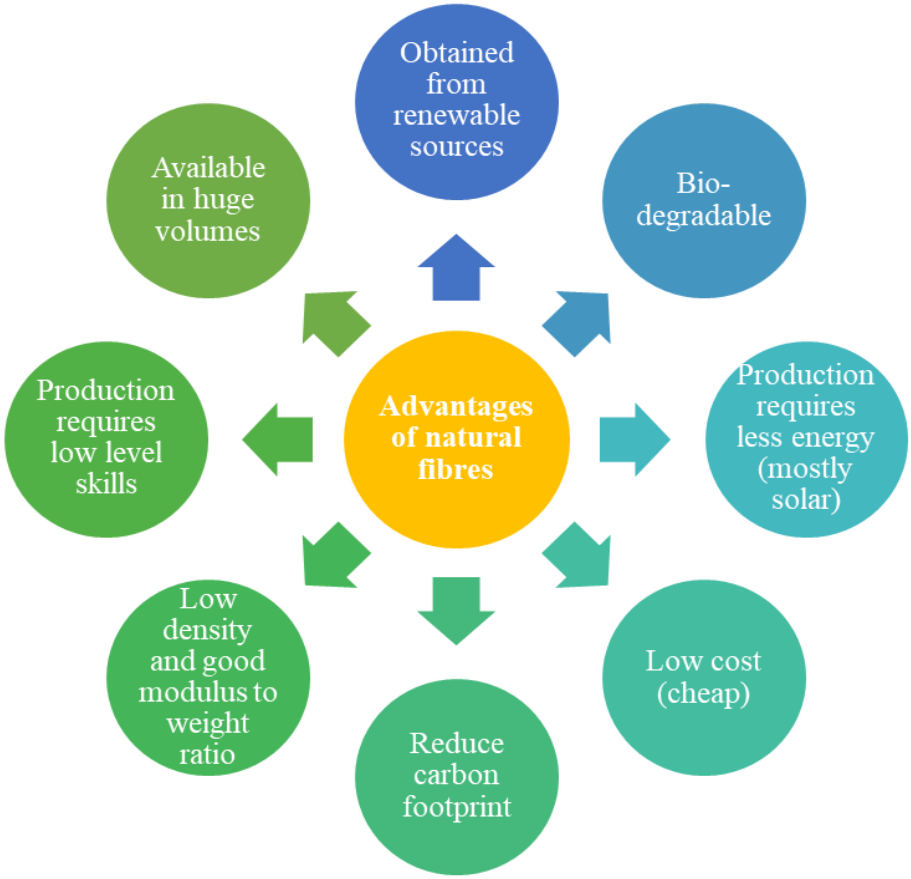

Figure 2.14 Advantages of natural fibres

Natural fibres are environmentally friendly because they are biodegradable unlike synthetics like carbon, glass and aramid fibres [72]. They are obtained from renewable sources such as plants which replenish themselves or cultivated by man and are produced in large volumes. Low energy is required in the production of natural fibres and it is mostly solar energy. They do not add the burden to the national electricity grids thereby not compounding the ever-increasing energy demand. Natural fibres cheaper than synthetics as they are obtained at low costs. Low cost investment and equipment are required in the production of natural fibres, unlike in the production of synthetics which require high cost of investment and sophisticated equipment. The level of knowledge required in the manufacturing of natural fibres is low compared to that required in the manufacturing of synthetic fibres. Consequently, they can be easily produced by poor countries. Natural fibres can contribute more to weight reduction than synthetic fibres because they have much lower densities than synthetic fibres. The density of

natural fibres ranges from as low as 1.25 g/cm^3 to as high as 1.5 g/cm^3 whilst that of E-glass and carbon fibres are 1.8 g/cm^3 and 2.1 g/cm^3, respectively [37]. Literature reported that the ratio of modulus to weight of some natural fibres is higher than that of some synthetic fibres such as E-glass fibres [37]. This is an indication that such natural fibres could compete with E-glass in designs where stiffness is critical [37]. Growing of plants results in the reduction of carbon footprint since the plants use carbon dioxide during photosynthesis and release oxygen. Ultimately, this reduces greenhouse gases and hence global warming.

Working with natural fibres requires an understanding of their chemical properties and mechanical properties. Plant natural fibres are lignocellulosic in nature and consist of cellulose component, hemicellulose component, lignin component, pectin and waxes [26, 71]. Table 2.5 shows the chemical compositional status of selected natural fibres and the quantities of the different components.

Table 2.5 Chemical compositional status of selected natural fibres [4, 26, 28, 38, 68, 71, 73, 74]

Fibre	**Cellulose (wt%)**	**Hemicellulose (wt%)**	**Lignin (wt%)**	**Pectin (wt%)**	**Ash (wt%)**	**Waxes (wt%)**	**Moisture content (%)**	**Micro-fibrillar angle (degrees)**
Cotton	83-91	3.0-5.7	0.7–1.6	0.6	-	0.6	7.85-8.5	20–30
Coir	32-43	0.15-0.25	40-45	3.4	2.7-10.2	-	10-12	30-39
Flax	71	18.6-20.6	2.2	2.3	5-10	1.7	8-12	5-10
Hemp	57-77	14-22.4	3.7-13	0.9	0.8	0.8	6.2-12	2.62
Jute	45-71.5	13.6-21	12-26	0.2	0.5-2	0.5	12.5-13.7	8.0
Kenaf	31-57	18-24	15-21	0.6	2-4	0.8	6.2-12	2-6.2
Ramie	68.6-91	5-16.7	0.6-0.7	1.9	-	0.3	7.5-17	7.5
Sisal	47-78	10-24	7-11	10	0.6-1	2	10-22	10-22
Pina	70-80	18.8	12.7	1.1-1.2	0.9-1.2	3.2-4.2	11.8	8-15
Banana	60-65	6-8	5-10	-	9.6	11	10-15	11-12

Natural plant fibres are lignocellulosic in nature and their chemical composition is chiefly consists of cellulose (α-cellulose), hemicelluloses and lignin [44, 72, 75]. Other constituents of natural plant fibres are waxes, pectin, ash and moisture content.

The cellulose component is strong and stiff and endows the fibre surface with many hydroxyl (-OH) groups thereby making them naturally hydrophilic [44, 53, 72, 76]. It is made up of a long chain of anhyhdroglucose polymer units that are interconnected forming microfibrils [44, 72]. Figure 2.15 shows the cellulose structure.

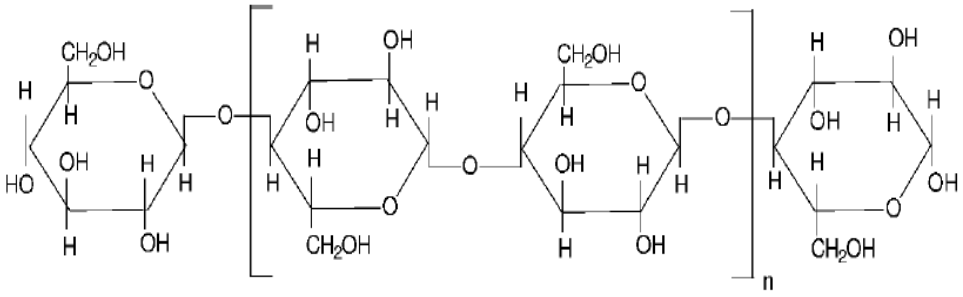

Figure 2.15 Structure of cellulose
Source: [72]

The -OH groups facilitate the development of intra-molecular hydrogen bonding in the macro-molecule and inter-molecular hydrogen bonding among other cellulose macromolecules and hydroxyl groups from air [72]. Figure 2.16 shows hydrogen bonding in natural plant fibres.

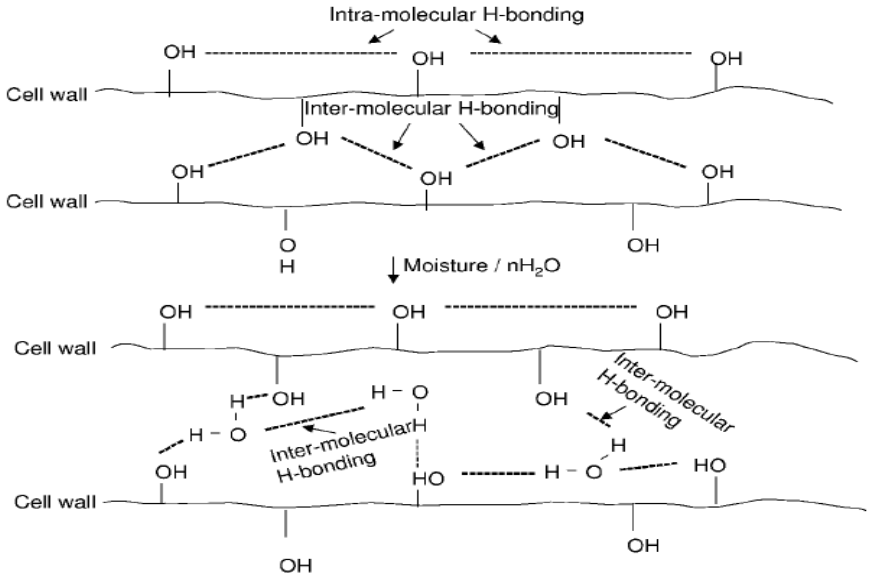

Figure 2.16 Schematic view of hydrogen bonding in natural plant fibres
Source: [72]

Cellulose is the major component of all natural fibres of plant origin and the cellulose fibrils are along fibre length [44]. Cellulose contributes to strength (both tensile and flexural) and rigidity, that is, inflexibility or stiffness [44, 77]. The cellulose's nature and crystallinity influence the reinforcing efficiency of the natural plant fibre [44]. Cellulose determines the mechanical properties of natural plant fibres.

Hemicellulose, which is not a form of cellulose, is very hydrophilic, hydrolysable in acids, soluble in alkali and functions as matrix that supports the cellulose microfibrils [44, 48, 53]. It increases the fibre's capacity to absorb water [75]. Lignin is a three-dimensional complex hydrocarbon copolymer containing aliphatic and aromatic constituent components which are completely insoluble in many solvents and cannot be disintegrated to monomeric components [44, 48]. It is amorphous and very hydrophobic and gives rigidity to plants [44, 48]. Groups identified in lignin are hydroxyl, carbonyl and methoxyl [44, 48]. Lignin is regarded as a thermoplastic polymeric component with a melting temperature and glass transition temperature of (T_g) of 170 ^oC and 90 ^oC, respectively [44]. Acids do not hydrolyse lignin, however, it is soluble in hot alkali, condensable easily in phenol and can be readily oxidised [44]. It is difficult to isolate lignin from the plant fibres [78]. Pectins, an umbrella name for heteropolysaccarides, provide flexibility to the plant fibres and in most cases contain various alcohol types [44, 78]. Pectins side chains are normally crosslinked with calcium ionic components and arabinose sugars and pectins structure is complex [77]. The carboxylic groups make pectins the most hydrophilic components in the natural plant fibres and highly prone to fungal attack [79]. Waxes consist of different types of alcohols [44, 48]. Removal of the noncellulosic components like the hemicellulose component, lignin component, pectins and waxes has an influence on the mechanical properties of natural plant fibres and interfacial bonding with matrix components [80].

The natural plant fibre structure generally consists of the primary wall, secondary wall and the central canal called lumen as shown in Figure 2.17.

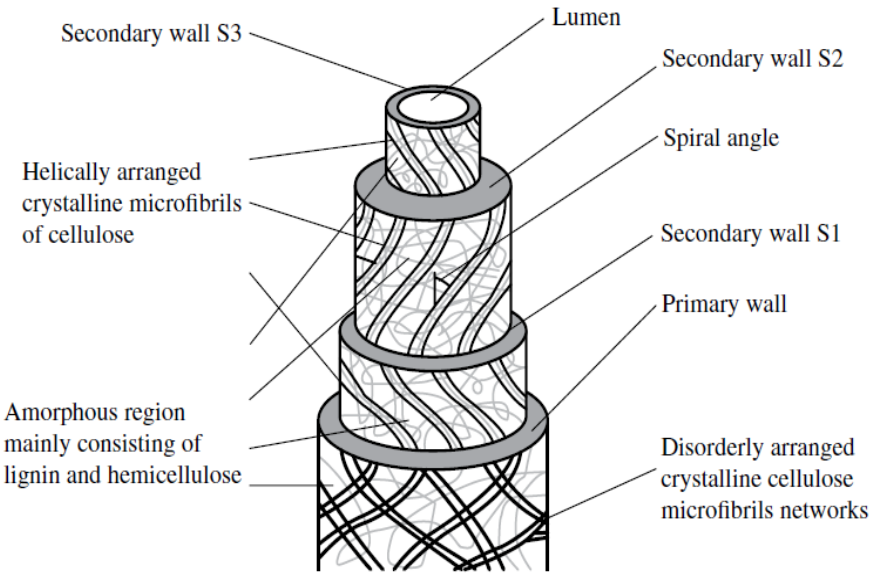

Figure 2.17 Structure of natural plant fibre
(Source: [48, 81, 82])

The primary wall is the first wall layer to be deposited during cell growth and it encircles the secondary wall. The primary wall is consisted of hemicellulose, pectin and lignin [80]. The secondary wall section consists of 3 layers, namely, the external secondary wall S1, the thick secondary wall S2 and the internal secondary wall S3 as shown in Figure 2.17. The crystalline cellulose fibrils in the thick secondary wall S2 influence the fibre's mechanical properties [80, 83]. Wall layer S2 contains of a series of helically wound microfibrils and the angle between the fibre axis and the microfibrils is called microfibrillar angle and it varies from fibre to fibre [28, 48]. Microfibrillar angle is believed to have a link to and influences fibre stiffness [28]. Spiral orientation of microfibrils leads to fibres that are more ductile than fibres with parallel orientated microfibrils which tend to be more rigid and inflexible [28]. Secondary wall S3 also contains crystalline cellulose [80].

Table 2.6 shows the physical and mechanical properties of selected natural fibres.

Table 2.6 Physical and mechanical properties of selected natural fibres [4, 5, 16, 17, 20, 26, 28, 38, 67, 68, 70, 71, 73]

Fibre	Physical properties			Mechanical properties			
	Density (g/cm^3)	**Diameter (µm)**	**Moisture absorption (%)**	**Tensile strength (MPa)**	**Young's modulus (GPa)**	**Elongation at break (%)**	**Decomposition temperature (°C)**
Cotton	1.5-1.6	12-38	7.9-8.5	287-597	5.5-12.6	3.0-10.0	232
Coir	1.15-1.46	100-460	10	95-230	4.0-6.0	15.0-30.0	285-465
Flax	1.4-1.53	40-600	8-12	745-1500	27.6-80	1.2-3.2	220
Hemp	1.4-1.5	25-500	6.2-12	550-900	70	1.0-1.35	215
Jute	1.3-1.46	25-200	12.5-13.7	393-800	10-30	1.5-1.8	215
Kenaf	1.4	30-50	9-12	223-930	14.5-53	1.5-2.7	229
Ramie	1.5	35-60	7.5-17	220-938	44-128	2.0-3.8	240
Sisal	1.33-1.5	50-200	10-22	400-700	9.0-38.0	2.0-14	205-220
Pina	1.5	105-300	11.8	413-1625	1.5	1.0-3.0	255-395
Banana	1.35	160-200	8.7-12	500	12	1.5-9	220

However, natural fibres are not void of problems. Figure 2.18 shows some of the major challenges associated with natural fibres.

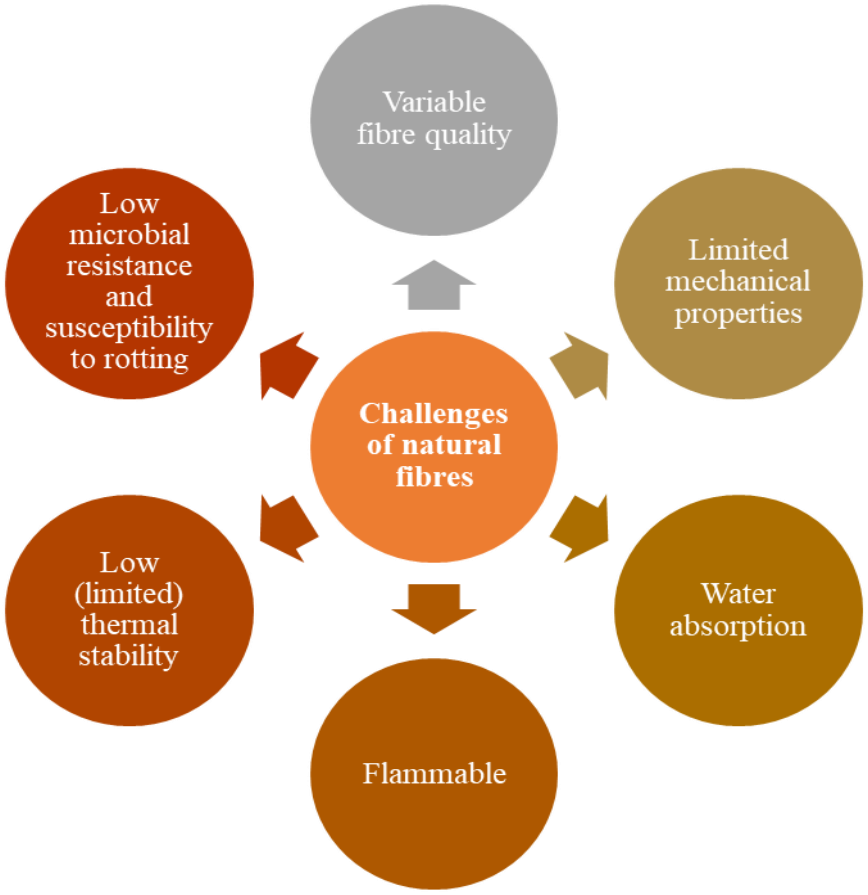

Figure 2.18 Major challenges associated with natural fibres

Natural fibres have inconsistent or variable properties. Their physical properties vary according to factors such as harvesting season, farming region, soil conditions and weather conditions [84]. Low resistance to microbial attack and being prone to rotting is another major challenge of natural fibres. This is a challenge during long-term storage, when fibres are being transported especially by ships and composite fabrication [84]. However, on the biodegradability aspect, susceptibility to rotting and being prone to microbial attack are advantages. Natural fibres limited or low thermal stability which affects the processing temperatures. The recommended processing temperature is up to 200 ^{o}C above which most natural plant fibres start to degrade [84]. Heat causes alterations in the physical and chemical structure of the fibres. These changes could be depolymerisation, dehydration, oxidation, decarboxylation, hydrolysis and recrystallization [84].

2.5.3 Kenaf fibre

Kenaf also called hibiscus cannabinus L. is a quick growing plant belonging to the Malvaceae family and indigenous to Africa [85-89]. It has economic and horticultural importance since it is herbaceous and also a source of lignocellulosic materials or fibre materials [85-87, 90, 91].

It is a 3rd world crop after bamboo and wood and has been propagated as a renewable source of industrial fibres annually [89, 90, 92]. It requires less than six months to get to a plant size suitable for practical applications [92]. Retting process is used in the extraction of kenaf fibre [87, 93]. The properties (mechanical, chemical and physical) of kenaf fibres are shown in Tables 2.4 and 2.5, respectively. It is of importance to mention here that different scholars reported different kenaf cellulose content. Some reported cellulose content of 52-59% [85, 94], alpha cellulose of 65% [87] and others reported 60-80% cellulose [95]. In terms of functional groups, FTIR peaks appeared at wavenumber 3390 and 1190 cm^{-1}, for O-H group stretching and O-H group bending frequencies, respectively, whilst a peak at 2910 cm^{-1} was for $–CH_2$ stretching frequency [85]. The peaks at wavenumber 1739 and 1650 cm^{-1} represented the C=O (carbonyl) group for hemicellulose's acetyl group and aldehyde group in lignin, respectively [85].

2.6 Fillers and other additives

Other materials such as fillers can be included so as to improve specific properties, processability, dimensional stability and reduce costs [32]. Some examples of fillers include calcium carbonate ($CaCO_3$), clay nanoparticles, mica and solid and or hollow glass micro spheres [37]. Fillers and other additives are added to the polymer matrix for the following purposes [37];

- Cost reduction (most fillers cost lower than the matrix)
- Control viscosity
- Produce smoother surface
- Reduce mould shrinkage
- Improve some properties.

2.7 Fibre-reinforced composites manufacturing processes

Different manufacturing processes (fabrication methods) are employed in the manufacture of fibre-reinforced composites. The choice on manufacturing process to use depends on factors such as [32];

i. matrix type,
ii. fibres
iii. temperature required for part formation and curing of the matrix
iv. cost associated with the process.

All manufacturing processes have some limitations on the structural design. For this reason, designers have to understand the advantages and limitations of each manufacturing process prior to selection of the process to use for composite part production. Some of the common composite manufacturing methods include hand lay-up, prepregs layup, spray layup, compression moulding, injection moulding, bag moulding, autoclave processing, resin transfer moulding (TRM), pultrusion, vacuum assisted resin transfer moulding (VARTM) and filament winding [4, 17, 32, 36]. The basic unit operations involved during the manufacturing process are [32];

i. placement of the fibres along the required orientations
ii. fibre impregnation (by the resin or matrix)
iii. consolidation process of impregnated fibres (by removal of excess resin, volatile substances and air)
iv. curing (solidification) of the polymeric matrix
v. extraction process or removal from the mould
vi. finishing process (final operations like trimming).

2.7.1 Hand layup

This method is described as the most basic and oldest method of manufacturing composites [4, 28, 32, 35]. It is also called wet layup. This process is done manually where layers of fabrics or plies are placed in the mould and matrix applied forming a laminated stack [28, 32, 35]. The wet composite is squeezed, brushed or rolled by use of hand rollers for even distribution of the resin, removal of entrapped air and consolidation of composite layers to desired thickness [28, 32]. Four steps followed in hand layup are;

- Preparation of mould
- Gel coating
- Layup
- Curing.

Hand layup is a labour intensive process and dependent on operator skills. It has a limitation on the volume of fibre loading or the number of plies to use. However, the process is versatile, has low cost tooling and long fibres can be used making it attractively good for structural applications in industries like the marine and aerospace industries [4, 28, 32, 35].

2.7.2 Prepregs layup

Prepregs are defined as sheets of fibres impregnated with a pre-set quantity of homogenously distributed matrix [32, 37]. The major difference between prepregs layup and the hand layup is that fibre impregnation is done prior to moulding in the prepregs layup method [32]. Prepregs are widely used in the fabrication of high performance aerospace parts and complex geometries [32]. Fibres for prepregs layup can be in form of woven fabrics, continuous rovings and non-woven mats [32, 37]. Both the thermoset matrices and thermoplastic matrices could be used in this method [32, 37]. The dimensions of the prepreg sheets can be varied. Literature shows that the width can be varied from less than 25 mm to 457 mm and if the sheet width exceeds 457 mm, then they will be no longer called prepregs but broadgoods [32, 37]. The resin content could be between 30% and 45% by weight [37]. In this method, solvents are used to control the liquid resin's viscosity and a release film or waxed paper is used as a mould release agent during curing [32, 37].

Production of thermoplastic prepregs is much harder than producing thermoset prepregs. This is due to the thermoplastic resins' high viscosity which makes it more difficult to properly wet the fibres than when using the low-viscosity thermoset resins [32, 37]. Nevertheless, it is possible to produce thermoplastic prepregs and several commercial techniques have been developed for making thermoplastic prepregs [37]. Prepregs made using thermoplastic resins are available in most of the fibre forms [32]. They should be heated in order for them to be tacky and drapable [32]. In the case of thermoplastic resins, curing is done by simply cooling down at room temperature [32].The major advantages of thermoplastic prepregs is that they could be stored for an infinite period without the need for specialised storage facilities and can be consolidated with easiness into laminated products by heat and pressure application [37]. The storage time (shelf life) of the resin before moulding is important. In the case of epoxy, the shelf life is 6 – 8 days at 23 ^{o}C and can be stored for up to 6 months or more if storage temperature is -18 ^{o}C whilst prepregs made using thermoplastic matrices have unlimited storage period under non-specialised storage facilities [37].

Incorporation of fibres into thermoplastic resins can be achieved using the following techniques [37];

- Impregnation by hot melting. This technique is ideal for semicrystalline thermoplastic matrices without any suitable solvents for impregnation in solution form. Examples of

such thermoplastics are PEEK and PPS. Amorphous polymers can also be used in this technique.

- Solution method of impregnation. It is ideal for polymeric matrices that have good dissolution solvents. Examples are amorphous polymers, like polysulfone and polyethylenimine (PEI). The choice on solvent is predominantly governed by the solubility of the polymer, chemical structure and molecular weight. The boiling temperature of the solvent influences the solubility of the polymer. Solvents with low boiling temperatures are preferred because solvents with high boiling points are difficult to remove the prepregs. Removal of the solvent from the prepregs is a very critical issue since entrapped solvents create high void content in the final laminate which adversely affects the properties. Thermoset prepregs made by this technique are drapable and tacky whilst thermoplastic prepreg materials are not sticky (tacky) [37]. Thermoplastic prepregs are not that flexible making it difficult to drape them into contoured mould surfaces [37]. Spot welding along the outside edges is one way that was used to deal with the challenges of lack of stickiness of thermoplastic prepregs [37].
- Liquid impregnation. In this technique, low molecular weight monomeric units or prepolymers (precursors) are used in coating the fibres. It is commonly applied in linear aromatic condensation-thermoplastic imide (LARC-TPI) and other thermoplastic polyimides. Dissolving of the precursor in the solvent is done to lower the viscosity. Prepregs made by this technique are drapable and tacky. This technique has difficulties in removing the residual solvent and by-products from the prepregs during the laminate consolidation process.
- Film stacking. This technique is principally used for woven fabric materials or random fibre mats that are interleaved between the unreinforced thermoplastic polymeric sheets. Heating and pressing are done to force the thermoplastic matrix into the reinforcement layers thereby forming a prepreg sheet.
- Fibre mixing. This technique uses commingling, wrapping, or coweaving to intimately mix thermoplastic fibres with reinforcement fibres. Commingled and wrapped fibres can be made into 2- or 3-dimensional hybrid fabrics by weaving, knitting, or braiding. The thermoplastic fibres in the hybrid fabrics are then melted and spread to cause wetting of the reinforcement fibres at the stage of laminate consolidation during moulding. Using hybrid fabrics has principal advantages of high flexibility and

drapability over contoured moulds, whereas the other techniques are ideal for relatively flat surfaces. This technique, however, needs the thermoplastic polymer to be in filament form for it to be possible to mix the fibres. This is the case for PEEK and PPS thermoplastic polymers which can be spun into monofilaments. Commingled roving and fabrics can be made using PP and PET fibres.

- Dry powder coating. In this technique, thermoplastic powders that are charged and fluidized are used for coating the reinforcement fibres. After fluidizing, the fibres are oven heated to melt the polymer coating on the fibre surface.

Some of the advantages of prepregs include [32];

- Possibility for high volume fraction of fibres
- Ability to have uniformity in terms of fibre distribution
- Simplicity in terms of manufacturing.

However, the process has major drawbacks like [32];

- slowness and labour intensiveness
- needs curing equipment which is normally expensive
- added cost of making prepregs.

2.7.3 A brief introduction of other composites manufacturing processes

Other composite manufacturing process commonly used are:

- Spray layup which is an extension of hand layup technique which automatically reinforces materials in form of chopped fibres only [4, 35, 36].
- Compression moulding which is generally employed for both thermoplastic and thermoset resins with either loosely chopped or mats of short fibres or mats of long fibres which are either haphazardly oriented [4, 17, 32].
- Injection moulding which uses short fibres of length of up to 30 mm as reinforcing material and is suitable for mass production, making thick specimens and gives accurate product dimensions [35, 36].
- Bag moulding method which is predominantly employed in the aerospace field where high rate of production is not a critical factor [37].

- Autoclave fabrication process which is an extended form of the vacuum bag method and provides a larger pressure than in the vacuum bag technique thereby causing greater compression and elimination of voids [32].
- Resin transfer moulding (RTM) where multiple layers of dry woven mats or continuous strand mats are put at the bottom half of a 2-part mould with a catalysed liquid resin being injected into the closed mould [17, 28, 32, 36, 37].
- Pultrusion which is a continuous moulding process applied in the manufacturing of long and straight structural components of constant cross-sectional area [32, 35-37].
- Vacuum assisted resin transfer moulding (VARTM) which allows high fibre volume fraction and produces parts with few voids and good surface finish [4, 32].

Filament winding which produces axisymmetric hollow parts by having a series of continuous uncured resin-impregnated roving or monofilament materials wound on a mandrel that rotates mandrel [32, 35-37].

2.8 Fibre-reinforced polymeric composites (FRPC)

The development of single engineering materials such as metals, ceramics and polymers culminated in these materials being combined together forming composites. Previous studies presented composites as alternatives to many conventional materials [6, 27, 31, 96]. Generally, composites are manufactured using a matrix and a reinforcing (filler) material. Classification of composite materials is done according to the content, that is, consideration of the base (matrix) material and the material used as reinforcement [97]. The three main categories of composite materials are particulate reinforced composites, SMC and fibre-reinforced composites [97]. This review in the next sections focused on fibre-reinforced composites which are relevant to this research work.

Fibre-reinforced composite materials are composed of matrix reinforced with fibres. Fibre length is used in the sub-classification of fibre-reinforced composites. Reinforcement with long fibres gives continuous fibre-reinforced composites, while reinforcement with short fibres gives discontinuous fibre reinforcement composites [97]. The emergence of fibre-reinforced composites resulted in conventional materials facing stiff competition in terms of weight savings and cost. The continued keenness in fibre-reinforced composites resulted in a marginal growth in their production and application. Some of the benefits of fibre-reinforced composites include; lightweight, high specific strength, flexural strength, damping properties, durability,

stiffness, thermal stability, electromagnetic interference shielding and resistance to wear, impact and corrosion [4, 5, 27, 36, 37, 96]. These attractive properties have led fibre-reinforced composite materials to get applications in areas such as aerospace, marine, construction, biomedical, mechanical, automobile, military, packing, sports sector, and other manufacturing industrial sectors [4, 5, 27, 36, 37, 96].

The reinforcement fibres could be synthetic fibres or natural fibres. Reinforcement with synthetic fibres gives synthetic fibre reinforced polymer composites (SFRPCs) which are traditionally termed as conventional fibres. Likewise, reinforcement with natural fibres gives natural fibre reinforced polymer composites (NFRPCs). Reinforcement of a single matrix with at least two or more materials gives hybrid fibre reinforced polymer composites [97].

2.9 Synthetic fibre-reinforced polymer composites (SFRPC)

SFRPC are made by reinforcing polymer matrices using synthetic fibres. Thermoset polymers are the most commonly used matrices. Some of the resins used include epoxy, polyester, polypropylene and the synthetic fibres used as reinforcement materials include glass, carbon and aramid fibres [98-105]. These are major types of fibre reinforced composites and generally considered as conventional fibre-reinforced composites. The market growth of fibre reinforced composite products is much consolidated and dominant in the European region. Some of the European countries with notably and consistent market growth are Germany, the United States of America (USA), Spain, France, Italy and Portugal [106]. In 2019, the USA's market for composites was estimated to be $26.7 billion and is expected to reach $33.4 billion by year 2025 based on the forecasted compound annual growth rate (CAGR) of 3.8% [107]. Glass, carbon and aramid fibres are the commonly used synthetic fibres for reinforcement. Epoxy and polyester polymeric matrices are the commonly used resins. Consequently, the following review focuses on polymer composites manufactured using either glass or carbon or aramid as reinforcing materials.

2.9.1 Glass fibre-reinforced polymer composites (GFRPC)

GFRC have a lion's share in the composites market followed by carbon fibre-reinforced composites. According to the 2017 Composite Market Report, GFRCs account for approximately 95% of the total share of composites [106]. In Germany, the market growth for GFRCs increased from 2% for the pre-2017 period to 5% in 2017 [106]. In the U.S.A, market

growth for GFRCs grew by 1.7% to 1.2 million tonnes with a market value of $2.2 billion in 2019 [107]. According to the prognosis of Mazmudar et al. (2020), the USA market for GFRCs could reach 1.4 million tonnes by 2025 with a CAGR of 2.4% [107]. Chief suppliers of glass fibre in the USA which account for above 50% total output by value are Owens Corning company, CPIC, Jushi company, Johns Manville company and Nippon Electric Glass [107]. The major consumers of glass fibre in the USA which represent about 69% of total usage have been reported to be the transportation (including the automotive), construction, tank and pipe sectors [107]. The Mazmudar et al. (2020) report indicated that the market for glass fibres is driven by increase in construction for residential and commercial purposes, continued growth in activities for gas and oil, waste/wastewater infrastructure and demand for lightweight vehicles [107]. In the GFRCs, glass fibres offer excellent strength, impact resistance, thermal stability, durability and friction and wear properties [97]. The transport market constituting of mass transit systems and automobiles is anticipated to be one of the largest USA markets in the next 5-10 years [107]. Key vehicle manufacturers have earmarked considerable investment in composite technology to reduction in weight and carbon emission to below legislated levels [107]. GFRCs carry a post-use disposal problem after their service life [97].

2.9.2 Carbon fibre-reinforced polymer composites (CFRPC)

CFRPCs are extensively used in areas such as the automotive sector, aerospace industry and other weight sensitive industries [97, 108-110]. They are employed in structural applications replacing conventional materials such as steel, alloys and aluminium [10, 108, 111]. The load-bearing applications of CFRPCs are classified into two sectors, namely, the advanced technology sector and the general engineering and transportation sector [108]. The high-technology applications cover aerospace sector and nuclear engineering whereas the general engineering sector and transportation sector cover bearings, fan belts, gears and automotive bodies [108]. Due to the increased production of CFRPCs, the worldwide demand per annum for carbon fibres sky-rocketed from about 16-55 kilo-tonnes in the last decade and demand was expected to reach 140 kilo-tonnes by year 2020 [109, 112, 113]. The market growth, fuelled by increments in carbon fibre usage in the aerospace sector, wind turbine blade materials and other industrial uses, is around 10-12% per year [107, 110, 113]. However, there is an estimation that by the year 2022, there might be a supply shortfall of virgin carbon fibres of around 24000 tonnes worldwide [110]. This shortfall can be covered by a number of ways such

as using recycled carbon provided that the limitations of current recycling technologies could be solved as well as having suitable alternatives to the carbon fibre.

2.9.3 Aramid fibre-reinforced polymer composites (AFRPC)

Kevlar is the most commonly used aramid fibre in the production of aramid fibre-reinforced polymer composites (AFRPCs) with high impact properties and high degree of tensile strength properties [97, 114]. However, due to the anisotropic nature of polymer composites reinforced with kevlar, they possess low compressional strength than polymer composites reinforced with glass and/ or carbon fibres [97]. AFRPCs made using kevlar have structural applications in the aerospace sector, bullet-proof vests and high strength ropes for offshore oil rigs [114].

2.9.4 Other synthetic fibre-reinforced polymer composites

This category involves those composites reinforced with synthetic fibres such as boron, basalt, polyacrylonitrile-F and metallic fibres. Basalt fibres have better physical and mechanical properties than glass fibres [97].

2.9.5 Major challenges of synthetic fibre-reinforced polymer composites

Despite the SFRPCs having many advantages on good properties, they are not void of challenges. In general, SFRPCs have challenges in addressing the following critical issues which are pertinent to modern day materials science and engineering;

- Energy requirements
- Cost of production
- Environmentally friendliness
- End of life (EoL) directives and post-use disposal challenges
- Carbon footprint
- Millennium Development Goals (MDGs), especially on sustainability.

It is reported that one major challenge of carbon fibre is that its manufacturing process is expensive, energy intensive and emits hazardous by-products which have environmental and human health ramifications [110]. Some of the gases are CO, CO2, NH3, HCN, NOx and VOCs and they should be managed during the manufacturing process [110].

Literature shows that SFRPCs significantly contribute to the annual large volumes of waste being created globally [9, 112, 113]. The life-span of CFRPCs used in the manufacturing of aerospace, automotive and wind turbine components is estimated to be up to 30 years [113]. The demand for carbon fibre is estimated to get to 117 kilotonnes by year 2022 [110, 113, 115, 116]. Pakdel et al. 2021, explained that this increase will result in dramatic increase in CFRPCs waste in future [110]. Other researchers also raised the same concern on increased CFRPCs wastes in the future posing challenges on environmentally friendly management of composites after their useful service life [9, 113]. Considering the projected growth in demand for CFRPCs, the amount of waste from EoL CFRPC components is expected to significantly increase in the future. It is reported that the large demand of FRPC materials culminated in huge amounts of waste materials, a majority of which are non-decomposable [110, 117]. The cumulative CFRPCs waste from the turbine sector, for example, is projected to reach 483 kilo tonnes by 2050 in Europe alone [118]. Other industries such as the automotive and aerospace sectors are also witnessing an increase in the use of carbon fibre. Meng et al. (2018) reported that the total value of carbon fibres used in the automotive sector is projected to have a value of USD 6.3 billion in 2021 [119]. Though there are efforts to deal with SFRPCs wastes such as recycling, incineration and landfilling, still problems exist as these waste management systems do not solve other problems and also brought new challenges. Countries, especially those in the European Union (EU) have come up with legislative measures restricting waste disposal methods such as incineration and landfilling [112]. Landfilling is the least preferred method of waste disposal in the EU and has been banned in some countries like Germany [14]. The other restriction is the ELV directive (End of Life Vehicles directive) which put strict restrictions that from 2015 onwards, all new vehicles were expected to be 95% reusable or recyclable [112, 120-122]. Concerns of the same nature were raised for composites used in the aerospace sector. In the aircraft production sector, between 30 to 50% of the fibre-reinforced polymer is manufacturing scrap [123-126]. Biggest concern in this industry is that between 6000 and 8000 aircrafts are going to reach the end of their useful service life by year 2030 [110, 119, 124-126]. This is definitely going to create a significant amount of composite waste. In 2017, scrap from industrial production of CFRPCs and CFRPC waste due to end-of-life and short application life like in wind energy components shot up [9]. Figure 2.19 shows the global carbon fibre demand and estimated carbon fibre waste.

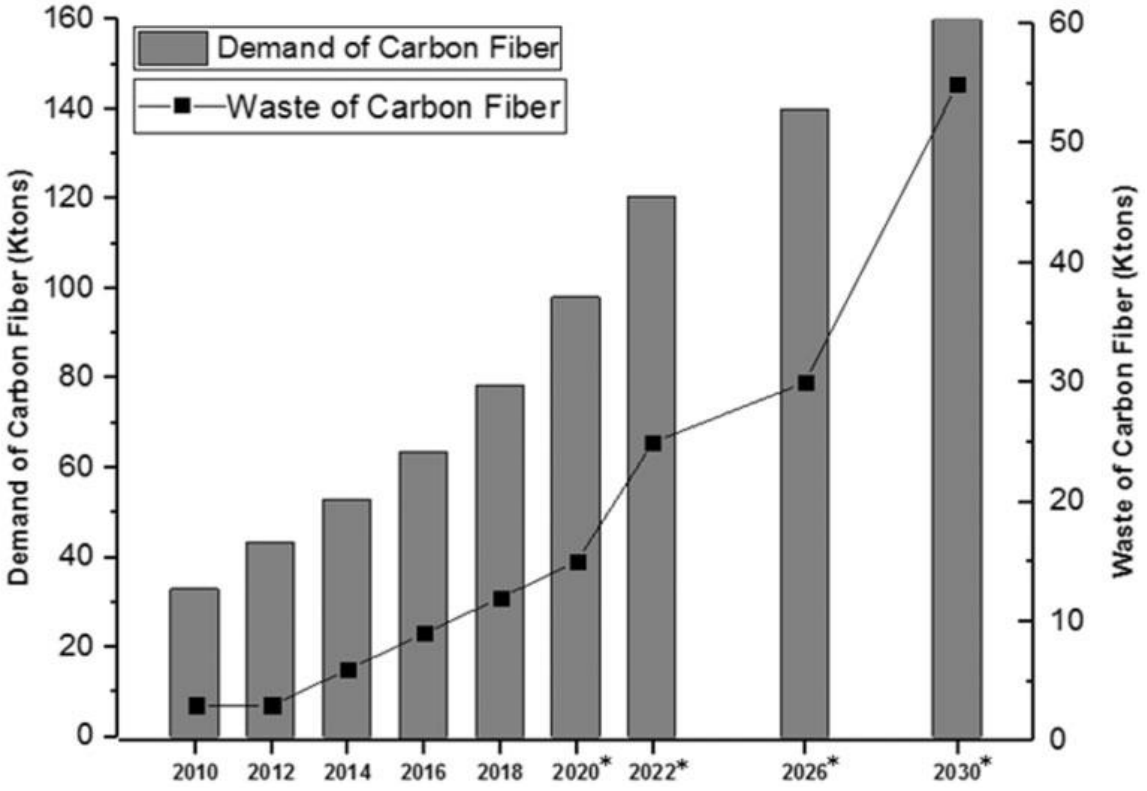

Figure 2.19 Global carbon fibre demand and estimated carbon fibre waste
Source: [109]

SFRPCs such as CFRPCs are described as energy intensive materials and hence ideal candidates for recycling [112]. Lab scale recycling reported the possibilities of using microwave heating, fluidised bed, chemical recycling, mechanical recycling and incineration in recycling SFRPCs [112]. However, recycling SFRPCs is met with major limitations outlined as [112];

- Cross-linked thermoset polymers which are used as matrices during production cannot be remoulded or remelted.
- Hybrid SFRPCs have an added complexity of creating a complex multiphase type of waste making recycling more difficult.
- Lack of standardisation on the composition of the SFRPCs creates a wide variation among waste materials.
- It is technically challenging to identify the various compositions thereby making the selection and separation among different wastes problematic.

2.10 Natural fibre-reinforced polymer composites (NFRPC)

Tightening legislation on environmentally unfriendly materials and sustainability triggered a new era in composite manufacturing. The new paradigm shift pointed towards recyclability and replacement of synthetic fibres with biofibres (natural fibres) in the production of fibre-reinforced composites. Previous studies report on the growing interest in using regenerative or renewable materials [28, 127-129]. NFRPCs have been recognised as ideal alternatives to SFRPCs [28, 120, 127-130]. Reinforcement with natural fibres reduces component weight by about 40% when compared to glass fibres [97, 120]. In addition, NFRPCs have reduced cost, environmental pollution, toxicity and recyclability [97]. These economic and environmental benefits of NFRPCs make them predominantly better over SFRPCs for modern applications [97]. Reinforcement of thermoset matrices with short and long natural fibres has manifested in high-performance applications [131]. A logical starting point was suggested to be the reinforcement of recyclable thermoplastic resins with biodegradable plant fibres [120]. Extrapolations based on the 2011-2016 projections indicated an estimated worldwide growth of 10% in the NFRPCs [2]. Sisal, jute, kenaf, flax and oil palm are among some of the natural fibres used as reinforcing fibres [2]. The NFRPCs are broadly classified into partially biodegradable and completely biodegradable composites [72]. Further classifications are based on the type of the matrix used as shown in Figure 2.20.

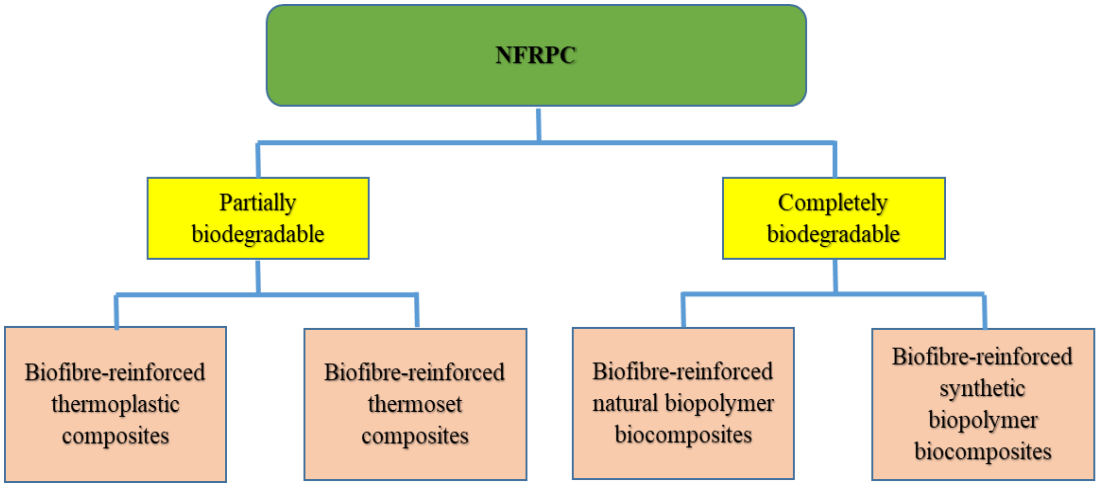

Figure 2.20 Classification of NFRPCs

Some scholars classify NFRPC into green composites, semi-green composites and hybrid composites based the quantities of the natural materials and reinforcement materials used to produce the composites [4, 132-135]. Figure 2.21 shows the life cycle of NFRPCs.

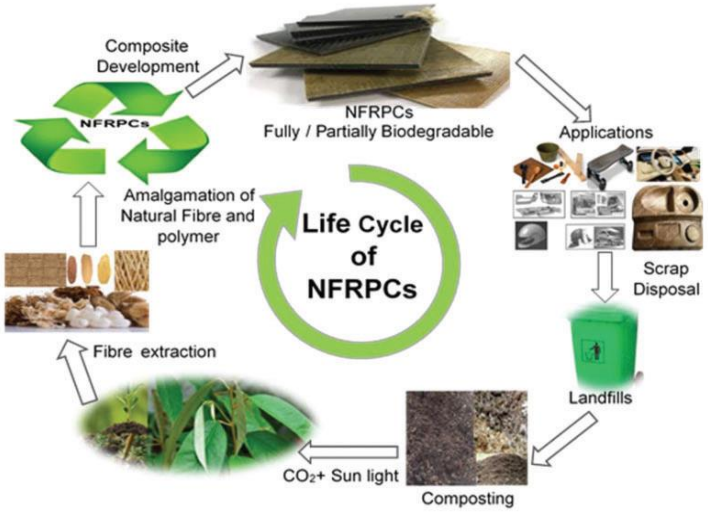

Figure 2.21 Life cycle of NFRPCs
Source: [136]

2.10.1 Partially biodegradable NFRPC

This group consists of natural fibre-reinforced synthetic polymer composites (NFRSPC) having a non-biodegradable thermoplastic or thermoset polymer as the matrix and biofibre as the reinforcement. Such composites are defined as semi-green composites [132, 135, 137, 138].

2.10.2 Completely biodegradable NFRPC

This group consists of natural fibre-reinforced biopolymer biocomposites (NFRBBC) having a biodegradable natural or synthetic biopolymer as the matrix and biofibre as the reinforcement. This is a green composites group consisting of matrices and reinforcement materials obtained from natural or renewable sources [132, 135, 137, 138]. This is the new era of biocomposites where constituent materials, the matrix and the reinforcement materials are both biomaterials. Biocomposites (biodegradable) have been defined as composites that consist of biodegradable polymer matrix and biomaterial such as biofibres as the reinforcement [72]. These were triggered by the need for sustainability. This group of biocomposites support sustainability by use of biopolymer matrices that are obtained from natural sources like carbohydrates and vegetable oils [21, 139]. Development of 100% biodegradable biocomposites are ongoing attempts [4]. These types of fibre-reinforced composites are attractive as they are biodegradable, use materials obtained from renewable sources, use materials that require less energy to produce and cheap to obtain [4, 5, 38, 73, 140]. Despite their ability to address sustainability issues surrounding fibre-reinforced composites, biofibre-reinforced biopolymer biocomposites have challenges of meaning the mechanical properties [2, 3, 16-23, 141]. Mechanical properties of the biocomposites are affected by factors like polymer matrix type,

type of reinforcement fibres, origin and form of fibres, fibre distribution and dispersion in the matrix, fibre/matrix interactions and composite fabrication technique [141, 142]. The major challenges being faced in the development of 100% biodegradable biocomposites with high mechanical properties include [4, 16, 17, 143, 144];

- high moisture absorption property of biofibres
- tedious extraction process of biofibres
- low wettability of biofibres
- poor thermal stability for both the fibres and the biopolymers
- weak fibre to resin interfacial bonding.

These undesirable properties adversely affect the biocomposite materials' ultimate mechanical properties. Consequently, tremendous efforts are currently being put on developing biocomposites with improved properties [4].

2.10.3 Applications of NFRPC

NFRPCs have made inroads in the production of materials for use in automobile, medical, military, building, packaging, sports and construction industries [145, 146]. They are frequently used in the automobile sector due to its requirement for low cost, light weight and eco-friendly materials [2, 147, 148]. Use of NFRPCs reduces the cost of automobile manufacturing and automobile weight by about 20% and 30%, respectively [2, 148]. Weight reduction has an ultimate result of reduction in fuel consumption. The biocomposites have been incorporated in the production of interior parts such as [149];

- vehicle seats
- door liners for vehicles
- vehicle door panels
- backrests.

Car producers like Daimler Chrysler, Ford, Toyota, Bavarian Motor Works – BMW AG, Volkswagen, General Motors and Mercedes Benz are leading in the use of NFRPC [150, 151]. Car manufacturers in German are currently focusing on the production of car and trucks biobased composite body parts for exterior applications [148, 152, 153].

2.10.4 Hybrid fibre-reinforced polymer composites

These are formed by reinforcing a single matrix with at least two or more reinforcement materials [137, 138, 154-156]. Hybridisation also refers to the use of fillers in FRPCs [154],

nanoengineered composites, nanocomposites and fibre-metal laminates [157]. Nanoengineered composites consist of a matrix, fibres and nanoparticles and nanocomposites consist of a matrix and at least two nanoparticle types [157]. Fibre-metal laminates consist of a matrix, fibres and thin metallic sheets [157]. The concept of hybridisation has been in existence for centuries and it positively influences mechanical, physical and thermal property characteristics of the resultant product. Hybridisation has become one of the highly prioritised research area [154]. Figure 2.22 shows a classification of hybrid composites.

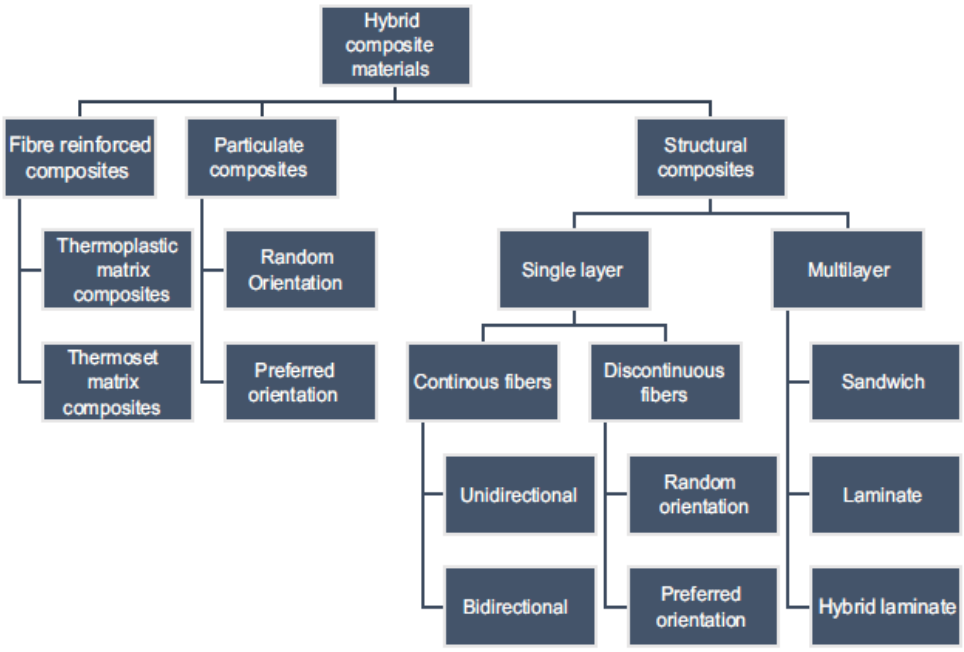

Figure 2.22 Classification of hybrid composites
Source [156]

Figure 2.22 shows that hybrid composites are of three classes. One of the classes is made using the common thermoset and thermoplastic resins reinforced with fibres. Another class is made using various fibre orientations. The last class is of structural hybrid composites made using single layers or multiple layers.

2.11 Impact behaviour

There is increased use of composites in transportation, ship structures, infrastructure, power industry, sporting good, military ground and air vehicles. Consequently, the understanding of impact behaviour is of utmost importance to designers and end users of composite materials [158]. Major focus currently is on replacing conventional SFRPCs with NFRPCs and natural fibre-reinforced biopolymer composites [159, 160]. Impact analysis is generally categorised

into four groups. Figure 2.23 shows the different categories of impact loading that can be used in the determination of the impact behaviour of materials.

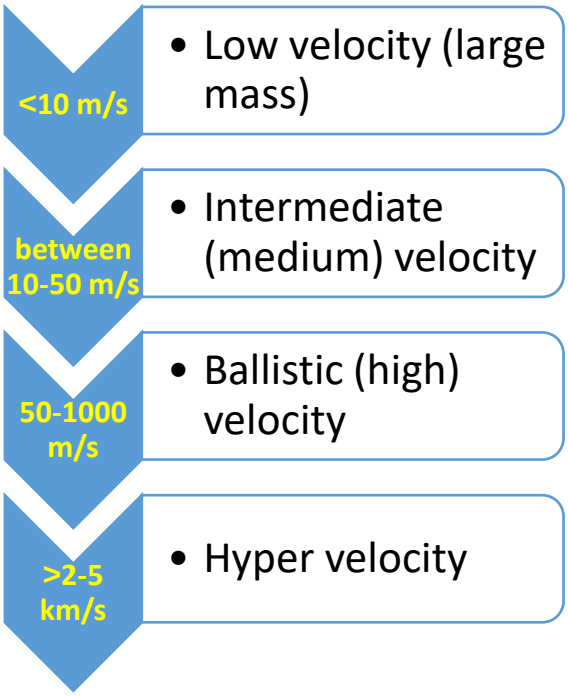

Figure 2.23 Velocity ranges for different impact loading
(Source: [158])

Impact behaviour of materials could be established at low velocity level, intermediate (medium) velocity level, high (ballistic) velocity or hyper velocity level as shown in Figure 2.23. The hyper velocity impact is for projectiles moving at very high velocities causing the target material to behave like a fluid [158]. Hyper velocity impact is often used in the development of protection from micrometeoroids and personnel in the low earth orbit [158]. Impact damage studies of composites focuses on [158]:

- dynamics of impact loads
- mechanisms of sustained damages
- damage resistance
- characteristics of post impact loading residual properties.

2.11.1 Low velocity impact

Low velocity impact (LVI) results from impacts of tool drops and has long impact durations with quasi-static response and global plate motion. LVI causes internal damage to reinforced polymer composites which reduces their performance properties and service life. The failure modes are dependent on the loading conditions and the failure modes and energy absorption

capabilities depend on stiffness, size and boundary conditions of the specimen [158]. The impact is imparted using a swinging pendulum, a rotating flywheel, dropping weight or a gas-gun driven projectile [158]. Izod, charpy and drop weight impact testing are the most typical equipment for low velocity impact analysis. The modes of failure in LVI are [158, 161]:

- matrix cracking
- delamination or debonding due to interlaminar stresses
- fibre breakage and buckling
- penetration.

Low velocity impact studies in literature focused mainly on SFRPCs, NFRPCs and hybridised polymer composites. Some of the published studies were on glass/epoxy composites [162-164], basalt/epoxy composites [165], kevlar/epoxy sandwich composite structures [166], hybrid composites made using carbon, glass and epoxy and sometimes natural fibres [167-169], carbon/epoxy composites [168-173].

2.11.2 Medium velocity impact

Medium velocity impact consists of foreign object debris on runways and roads, tornado and hurricane debris, secondary blast debris and hailstorms [158, 174]. It has short impact durations with dominant responses being flexural and shear waves. Olsson and Paget (2001) studied the response and damage mechanisms of 3mm thick carbon/epoxy laminated composites under medium velocity impact loading of a 10 g impactor at 37 and 47 m/s [174]. Dorival et al. (2016) studied the medium velocity impact behaviour of foam/carbon kevlar composite structures at 110 m/s using a steel impactor [175]. Trellu et al. (2020) studied the effect of medium velocity impact on carbon fibre composites using a 28g steel impactor [176]. Other studies on medium velocity focused on sandwich panels with different cores [177, 178]. There is no reported work on medium velocity impact studies on completely biodegradable biocomposites.

2.11.3 High velocity impact

High velocity impact usually emanates from effects of explosive warhead and small firearm fragments with dilatational wave as the dominant response [158]. Ballistic impact leads to localised damage due to the very little time available for the structure to respond to the stress waves propagating through the thickness of the material [158]. Boundary conditions effects, consequently, should be ignored since the impact passes well before the stress waves get to the boundary. There are numerous studies on ballistic (high) velocity impact studies on fibre-

reinforced composites. Some of the ballistic impact testing standards adopted internationally include the MIL-STD-662F, NIJ Standard-0101.06, 2008, NATO STANAG 2920 PPS 2003, ASTM 3062 and others [179-184].

Most of these studies are on GFRPCs [185-190], CFRPCs [102, 104, 186, 191-194], kevlar fibre-reinforced composites [105, 195-203], nanocomposites [104, 204-208] and hybrid composites [209-215]. There is little information on studies focusing on the ballistic impact of completely biodegradable natural fibre-reinforced biocomposites. Ballistic impact studies on composites that have natural fibres are on hybrid composites where a natural fibre was used as one of the reinforcing material or for composites where the natural fibre was used to reinforce a non-biopolymer matrix. Typical studies include ballistic studies on composites made using polypropylene matrix reinforced with flax fabrics, hemp fabrics and jute fabrics [216], curaua fibre/nanoclay reinforced polyester composites [217], hybridised kenaf/kevlar composites [212, 218] and manicaria saccifera fibre-reinforced PLA composites [219]. Luz et al. (2020) performed a comparison between the ballistic performance of composites with natural fibres and conventional materials employed in armour materials [220].

2.12 Nanotechnology in composite materials

Nanotechnology is also being applied in fibre-reinforced composites for the production of polymer nanocomposite materials. Polymer nanocomposites are a result of breakthroughs made on nanotechnology and nanomaterials [221]. Nanofillers are doping agents in the nanoscale range which are dispersed in the matrix [222]. Fillers in the nanoscale range such as clay nanoparticles, carbon nanotubes, calcium carbonate, nano diamonds (ultra-disperse diamonds), nano metal oxides, and graphene are used in the modification of the matrix to enhance the properties of the resultant composite material [221-223]. Most of the work reported in literature is on epoxy based polymer nanocomposites [99, 101, 104, 163, 187, 205-207, 224-230] and polyester based polymer nanocomposites [217, 231-238]. The published work focussed mostly on SFRPCs and partially biodegradable polymer composites and their hybrids. There is little reported work on completely biodegradable bio-nanocomposites. Mihai and Ton-That (2019) reported the limitedness of studies on the use of cellulosic fibres to reinforce PLA/nanoclay matrix [140]. Presently, montmorillonite clay (MMT) and organically modified montmorillonite (OMMT) are receiving the highest consideration in the modification of thermoplastic and thermoset polymers [239].

2.12.1 Clay nanoparticles

They are acquired from alkaline volcanic ash by a hydrothermal process and are composed of fine crystals of mixed metallic ions [240]. Mining and mineral-processing waste can also be a source of clay nanoparticles [241]. Clays are mainly based on phyllosilicates like the hydrous silicates of aluminum, magnesium, iron and zinc [240]. Microscopically, clays appear in a platelet fashion with layers consisting of silica (SiO_2) and alumina (Al_2O_3) [240]. The clay families include [240]:

- kaolinite/kaolin family with chemical formula $Al_2[Si_2O_5](OH)_4$
- halloysite family which show a tube-shaped structure with empirical formula $Al_2Si_2O_5(OH)_4.2H_2O$
- MMT family which combines many minerals and has a large quantity of SiO_2 and a small quantity of Al_2O_3
- laponite family which is a synthetic clay and its chemical structure is $Na^{+0.7}[(Si_8Mg_{5.5}Li_{0.3})O_{20}(OH)_4]^{-0.7}$
- layered double hydroxide clays which referred to as hydrotalcite with a large amount of water with chemical structure $[M^{2+}_{(1-x)}+M^{3+}_{(x)}(OH)_2]X^+(An^-)_{x/n}\cdot mH_2O$.

2.12.2 Clay nanoparticles dispersion mechanisms

The structure of nanoclays (dispersion) in resins can be characterised by intercalation or exfoliation as shown in Figure 2.24.

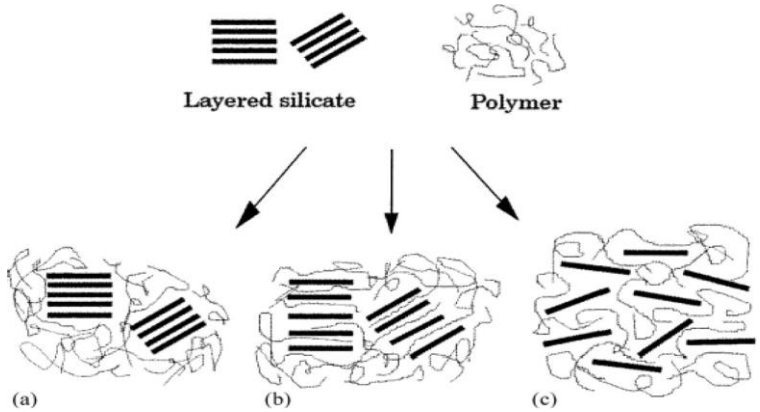

Figure 2.24 Dispersion mechanism of clay nanoparticle in resin
(a) microcomposite material (b) intercalation (c) exfoliation
(Source: [242])

In the microcomposite scenario, polymer molecules do not percolate into the galleries between layers and hence the d-spacing would be nearly identical to the pristine state [241, 242].

Intercalated structure is formed when multiple polymer chains are pushed between the interlayers culminating in the expansion of the interlayer d-spacing [241, 242]. In exfoliated nanocomposites, there is extensive percolation of the polymer, delamination of the layered structure and significant expansion of the d-spacing [242]. This diminishes the interaction forces between the layers with a typical separation distance of 10 nm or more [242]. Stirring and ultrasonication have been identified as the most facile and efficient methods of exfoliating clays [241]. Exfoliation results in a remarkable increase in nanocomposite properties [241, 242].

2.13 Composite materials floatation

There is a strong emphasis on cutting down the weight of composites so as to gain the advantages associated with lightweight materials or structures. In May 2015, the team from Deep Springs Technology announced about their researchers who had created a new very lightweight metal matrix composite that could float on water whilst retaining its heat resistance and strength [243]. The novel composite had a density of 920 kg/m^3 (0.92 g/cm^3) compared to 1000 kg/m^3 (1 g/cm^3) for water [243]. Such lightweight composites have been envisaged as real game changers in the development of lightweight polymer composites as economical alternatives to the heavy metal components in automobile and marine industry [243]. Amphibious vehicles could benefit from composites that are lightweight and have high buoyancy [243]. The lightweight structures have become in the transport vehicle manufacturing with major objectives of improving performance by reducing vehicle weight, lowering fuel and oil consumption and reduction in emissions [244]. The push now is for sustainable lightweight structures and major interest is in natural fibre-reinforced biocomposites [244-246]. The emphasis placed on lightweight structures or lightweight composite materials means that the need for determining the lightweight properties of the composites cannot be over-emphasized. Material density is one of the parameters that can be used in determining the weightlightness of composites as well as determining the buoyancy or floatation of the material. Some of the ways of determining the density and hence floatation of the composites have been given in literature [247-250]. The resultant of buoyancy tests could be positive, negative or neutral buoyancy. When an object floats in a liquid, buoyancy is said to be positive. Negative buoyancy is when an object sinks in a liquid and neutral buoyancy results when an object neither sinks nor floats. There is scanty literature on how nanoparticles affect the density of composite materials. Guo et al. (2006) research on how nanoparticles density and cell morphology [251].

2.14 Conclusion

The review of literature focused on classification of composite materials, matrices and reinforcement materials, fibres, fillers and additives, manufacturing processes for composites, FRPC, nanotechnology in composites, applications of composite materials and impact properties of materials. Production, properties and applications of kenaf, PLA and nanoclay were also reviewed. It was noted from the review that natural fibre-reinforced biocomposites have poor mechanical properties which limits their applications. Their current applications are mostly those that do not demand high mechanical properties. Consequently, current research is focusing on finding ways of improving the mechanical properties of natural fibre-reinforced biocomposites so as to widen their application to high performance or structural applications. Focus is also put on developing completely biodegradable biocomposites for sustainability since the current so called biocomposites are partially biodegradable. The current research, therefore, aims to develop completely biodegradable biocomposites for high performance applications. The next chapter discusses the methodology used in this study.

Chapter 3 Research Design and Methodology

3.1 Introduction

This chapter discusses the materials, equipment and procedures adopted in this work. Testing, testing standards, characterisations and analyses performed in this work are also discussed in this chapter. Figure 3.1 shows a summary of the experimental design followed in this work and the nature of testing, characterisation and analyses performed.

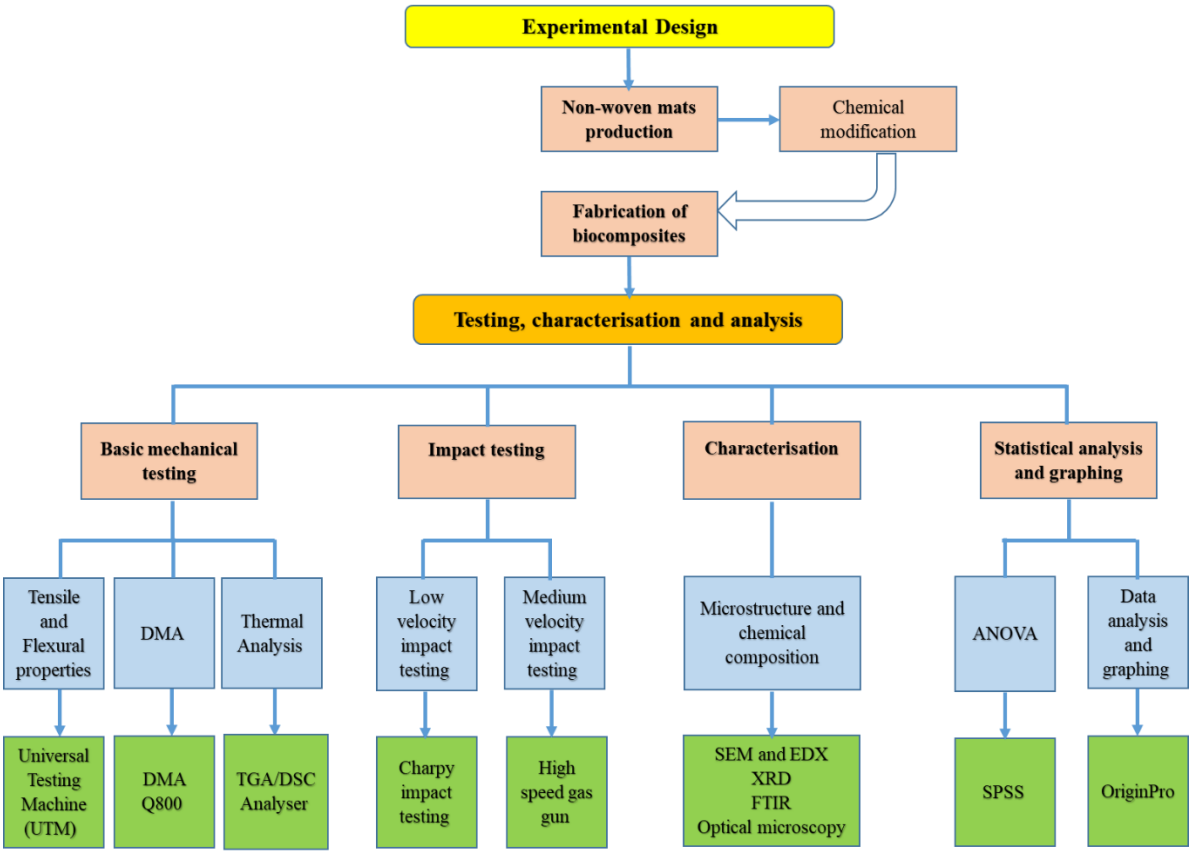

Figure 3.1 Experimental design summary

3.2 Materials

The materials used in this research work are as follows:

- Kenaf fibres of average length 50 mm and thickness 3 mm, sourced from Bangladesh,
- PLA 10361D (Ingeo biopolymer in granular form) from NatureWorks, USA,
- MMT Cloisite 30B clay nanoparticles of particle size ≤ 70 nm from Sigma-Aldrich (sourced through the South African agent),
- Non-woven mats (NWM) made using kenaf fibres and fabricated at the CSIR (Council for Scientific and Industrial Research) in Port Elizabeth, South Africa,

- Polytetrafluoroethylene (PTFE) non-sticking high temperature coated glass cloth from Keip Bros, South Africa,
- Sodium hydroxide (NaOH)
- Acetone

Pictures of kenaf fibre nonwoven mat, polylactic acid, clay nanoparticles and PTFE glass cloth are shown in Figure 3.2.

Figure 3.2 Materials for biocomposite fabrication

Figure 3.2a is the kenaf non-woven mat (kenaf NWM), Figure 3.2b is the PLA biopolymer, Figure 3.2c is the MMT nanoclay and Figure 3.2d is the PTFE coated glass cloth.

3.3 Fabrication of biocomposites

The production of kenaf fibre-reinforced biocomposites infused with clay nanoparticles methods included production of non-woven mats, surface modification and the actual fabrication of the biocomposites.

3.3.1 Production of kenaf non-woven mats

Non-woven mats were made using kenaf fibres. The fibre length was an average of 50 mm. The average weight of the non-woven mats was ± 250 gsm and thickness of 3 mm. The fabrication of the kenaf non-woven mats was done at the CSIR, Port Elizabeth, Nonwoven Unit (South Africa) using a needle-punching process. The needle-punching process produces randomly laid nonwoven fabric structures.

3.3.2 Surface modification of kenaf non-woven mats

Untreated and treated non-woven mats were used in this work. Literature reported that modification of fibres brings about positive effects that improve the interfacial adhesion [18, 81, 252-255]. Chemical modification was chosen in this work among all other available fibre modification techniques. This is because chemical modification is relatively cheap and easily performed [80]. Sodium hydroxide (NaOH) was used as the surface modification chemical.

The chemical treatment conditions used in this work were selected based on literature [254-260]. The modification method and procedures have been published in the South African Journal of Science and Technology (2022), Volume 40 Issue 1, pages 137-141, in the paper titled "Effects of combined alkali treatment and clay nanoparticle infusion on thermo-mechanical response of kenaf/PLA biocomposites", by **Moyo Mufaro**, Kanny Krishnan and Mohan T.P. 2% (m/v) NaOH was used to treat the mats at room temperature for 2 days. Drying of treated mats done initially at room temperature for 1 day followed by drying at 80 ^{o}C in an oven for 2 hours.

3.3.3 Fabrication of the biocomposites

The biocomposites were fabricated using the prepregs layup method. This method was chosen as the most suitable one for this work based on literature which showed that the prepregs layup method is ideal for parts to be used in high performance applications like in aerospace parts [32, 37]. In addition, the prepregs layup method is compatible with both thermoset and thermoplastic polymeric matrices and fibres in form of woven fabrics, nonwoven mats and continuous rovings [32, 37]. Fabrication of the biocomposites was done in the following manner:

a) Fabrication of neat biocomposites which were used as controls. The neat biocomposites consisted of PLA biopolymer reinforced with:
    i. Untreated non-woven mats (NWM), and
    ii. NaOH treated non-woven mats.
b) Fabrication of hybrid biocomposites. The hybrid biocomposites consisted of PLA biopolymer reinforced with:
    i. Untreated non-woven mats and infused with clay nanoparticles, and
    ii. NaOH treated non-woven mats and infused with clay nanoparticles.

3.3.4 Fabrication of untreated kenaf NWM reinforced PLA biocomposites

The methodology for fabricating the untreated kenaf NWM reinforced PLA biocomposites has been published in the Journal of Fibers and Polymers (2020), Volume 21, Issue 11, pages 2642-2651, in the paper titled "Performance of kenaf non-woven mat/PLA biocomposites under medium velocity impact", by **Moyo Mufaro**, Kanny Krishnan and Velmurugan Raman. In summary, the procedure involved preparation of the PLA resin, impregnation of the nonwoven fibre mats and curing at high temperatures. These stages are described below:

- Preparation of the PLA resin

  Initial oven drying of PLA granules at 60 ^{o}C prior to dissolution in acetone. This was done to get rid of moisture. 20% (m/v) polylactic acid was dissolved in acetone solvent. Mechanical stirring at 500 rpm was used to aid in the complete dissolution of PLA.

- Impregnation of the nonwoven fibre mats

  This stage was for the preparation of kenaf nonwoven mat/PLA biocomposite prepregs. The kenaf nonwoven mats were impregnated with the PLA biopolymer resin. Optimised fibre weight of 20% which is equivalent to fibre volume fraction of approximately 21% was used. The PTFE glass coated non-sticking cloth separator was employed as the release agent. The resin impregnated nonwoven mats were dried for 48 hours at room temperature. This also allowed for the evaporation of the acetone. The prepregs components had an aerial density of 250 g/m^2 and 500 g/m^2 and the dimensions were length of 300 mm and width of 300 mm.

- Curing at high temperature under pressure

  The dried kenaf NWM/PLA prepregs were oven cured under pressure at a temperature of 165 ^{o}C for 5 minutes. The PTFE glass coated non-sticking cloth separator was employed as the release agent during the curing process. Specimens for various tests were prepared from the cured kenaf NWM/PLA biocomposites.

3.3.5 Fabrication of treated kenaf NWM reinforced PLA biocomposites

The procedure and stages of fabrication were the same as those discussed under 3.3.4. The only difference is that in this case kenaf nonwoven mats treated with NaOH were used instead of the untreated ones so as to form treated kenaf NWM/PLA biocomposites. The method has been published in the South African Journal of Science and Technology (2022), Volume 40 Issue 1, pages 137-141, in the paper titled “Effects of combined alkali treatment and clay nanoparticle infusion on thermo-mechanical response of kenaf/PLA biocomposites”, by **Moyo Mufaro**, Kanny Krishnan and Mohan T.P.

3.3.6 Fabrication of untreated kenaf NWM/nanoclay/PLA hybrid biocomposites

The methodology for fabricating the untreated kenaf NWM/nanoclay/PLA hybrid biocomposites was published in the Journal of Applied Nanoscience (2021), volume 11, Issue

1, pages 441-443, in the paper titled "The efficacy of nanoclay loading in the medium velocity impact resistance of kenaf/PLA biocomposites", by **Moyo M**ufaro, Kanny Krishnan and Velmurugan Raman. Figure 3.3 is an illustration of the fabrication stages for the untreated kenaf NWM/nanoclay/PLA hybrid biocomposites.

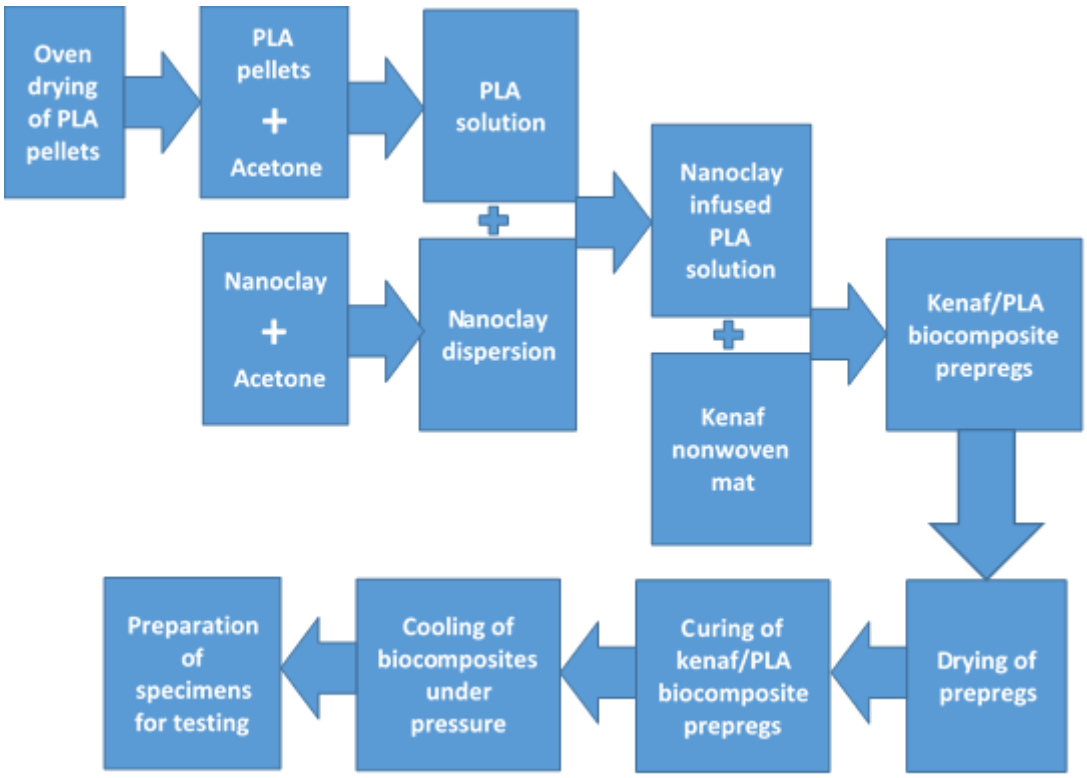

Figure 3.3 Fabrication process the hybrid bio-nanocomposite

In summary, the procedure involved preparation of the PLA resin, preparation of the nanoclay dispersion, impregnation of the nonwoven mats with nanoclay doped PLA resin and curing at high temperatures. Below is a description of the stages:

- Preparation of the PLA resin

  This was performed exactly as discussed under 3.3.4.

- Preparation of the nanoclay dispersion

  Montmorillonite (MMT) cloisite clay nanoparticles were dispersed in acetone. The homogeneity of the nanoclay dispersion in acetone was achieved by continuous magnetic stirring. The homogeneously dispersed clay nanoparticles in acetone then added to the PLA resin and stirred mechanically at 500 rpm for 30 minutes. The stirring was done so as to promote formation of a homogenous nanoclay-doped PLA

resin. In this work, clay nanoparticle content levels of 0, 3, 5 and 7 wt% m/m (nanoclay/PLA) were used.

- Impregnation of the nonwoven mats
  This stage was performed exactly as discussed under 3.3.4. The only difference is that in this case, the kenaf nonwoven mats were impregnated with homogeneously dispersed clay nanoparticle-doped PLA resin instead of the neat PLA resin so as to form untreated kenaf NWM/nanoclay/PLA hybrid biocomposites.

- Curing at high temperatures under pressure
  This stage was also performed exactly as discussed under section 3.3.4.

3.3.7 Fabrication of treated kenaf NWM/nanoclay/PLA hybrid biocomposites

The procedure and stages of fabrication for the treated kenaf NWM/nanoclay/PLA hybrid biocomposites were exactly the same as those discussed under 3.3.5. The only difference is that in this case NaOH treated kenaf nonwoven mats were used instead of the untreated ones so as to form treated kenaf NWM/nanoclay/PLA hybrid biocomposites.

3.4 Basic mechanical testing

Basic mechanical testing of the specimens fabricated in this work consisted of thermal analysis, dynamic mechanical analysis (DMA) tests, tensile strength testing and testing for flexural properties.

3.4.1 Thermal decomposition analysis

Thermal decomposition behaviour of the biocomposites was analysed using a thermogravimetric analyser (TGA). This was performed on a combined differential scanning calorimeter and thermogravimetric analyser, model SDT Q600 V20.9. ASTM E 1131 – 08 was followed in performing the thermal decomposition analysis [261]. Specimens were heated at a rate of 10 °C/min in the presence of nitrogen that was flowing at 100 ml/min from a temperature of 20 °C to 600 °C. The thermogravimetric (TG) and derivative of thermogravimetric (DTG) data was generated using the TA instruments software Advantage v5.5.20 whilst plotting of graphs was done using OriginPro software.

3.4.2 Dynamic mechanical analysis

Dynamic mechanical analysis (DMA) of the biocomposites was conducted on a dynamic mechanical analyser (DMA) Q800 V21.2. The tests were carried out according to ASTM D4065-01 [262]. DMA was done in three-point bending mode on a support span of length 50mm at a frequency of 1Hz and amplitude of 20 µm. Heating temperature was ramped from 25 ^{0}C (room temperature) to 80 ^{0}C at a rate of 3 ^{0}C/min. Specimen dimensions of 60 mm x 10 mm x 3 mm were used and three specimens were tested per sample. The glass transition temperatures (T_g) were determined from the midpoint of the loss modulus peak and tandelta peak based on literature [263-266].

3.4.3 Flotation test

Simple flotation test was performed following the Archimedes (buoyancy) method using water. The tests were performed following ASTM D792-20 and as outlined in literature by Saadati et al. (2019) and Amiri et al. (2017) [247-249]. The tests were performed in an open bucket with a diameter of 350 mm and depth of 350 mm. The specimen dimensions were of length 173 mm and width 173 mm. The bucket was filled with water (boiled and then cooled) and specimens were manually immersed in water and left for 2 minutes. The quick removal of specimens from the water was to avoid any possible chances of water absorption. This was in line with suggestions from literature [248]. The theoretical densities of the hybrid composites were determined following the rule of mixtures given by Equation 3.1:

$$\rho = \frac{v_a \rho_a}{V} + \frac{v_b \rho_b}{V} + \frac{v_c \rho_c}{V} \tag{3.1}$$

where; ρ is the composite density; ρ_a, ρ_b and ρ_c are constituents a, b and c densities, respectively; V is the composite volume; v_a, v_b and v_c are constituents a, b and c volumes, respectively.

$v_a/V = V_a$ which is the volume fraction of the constituent a and the same applies to the volume fraction of the constituents b and c. Therefore, the density of the composite becomes:

$$\rho = V_a \rho_a + V_b \rho_b + V_c \rho_c \tag{3.2}$$

Since this work deals with fibre-reinforced matrix;

$$\rho = V_f \rho_f + V_m \rho_m \tag{3.3}$$

where; V_f and V_m are volume fractions of the fibre and matrix, respectively; and ρ_f and ρ_m are the densities for the fibre and matrix, respectively. However, $V_f + V_m = 1$, and hence;

$$\rho = V_f \rho_f + (1 - V_f)\rho_m \quad (3.4)$$

Therefore, the theoretical density of the composites is determined by Equation 3.5:

$$\rho = V_f(\rho_f - \rho_m) + \rho_m \quad (3.5)$$

3.4.4 Tensile strength testing

Testing for tensile strength of the biocomposites was performed following ASTM D3039 [267]. The tests were conducted on a universal testing machine (UTM), Model: MTS Criterion Model 43 and computer-controlled by MTS Suite software. The machine has a capacity 30 kN (in both the tension and compression modes), sensitivity of 2.214 mV/V and data acquisition rate of 10 Hz. The crosshead speed was 2 mm/min. The length, width and thickness of the biocomposite specimens for tensile strength tests were 250, 25 and 3 mm, respectively. The gauge length was 150 mm. Five specimens were tested for each of the biocomposite samples and relevant calculations on mean tensile strength values, strain at break and Young's modulus were done. Figure 3.4 demonstrates how the specimens were mounted on the UTM machine.

Figure 3.4 Biocomposite specimen under tensile test

Young's modulus was taken on the linear slope of the curve, between two specific strains. Excel was used in determining the gradients and hence the Young's modulus for the biocomposites.

3.4.5 Flexural tests

Flexural tests were done to determine the flexural strength and stiffness of the biocomposite materials. A three-point bending flexure test was performed following ASTM D790-03 test standard [268]. The method used a supported beam with a span-to-thickness ratio of 16:1, with centre loading support span, developed for design applications as shown in Figure 3.5.

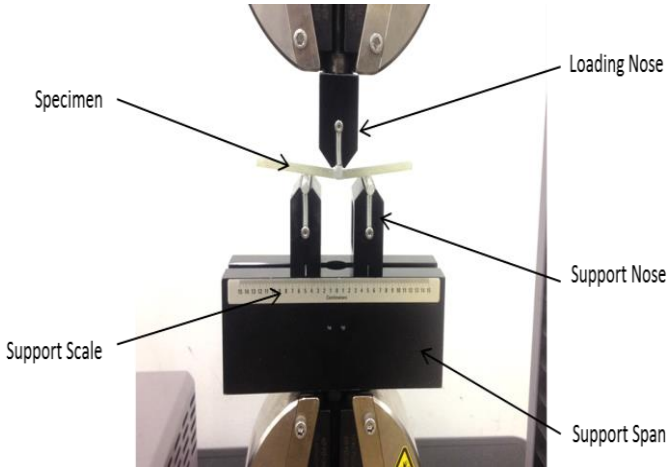

Figure 3.5 Composite specimen under flexural test

The nominal thickness was 3 mm, width was 12.7 mm and span length was 48 mm. The total length of each specimen was 128 mm. The biocomposite specimens were deflected until they ruptured in the outer surface and in instances where rupture was not going to be achieved, the test would be stopped when a maximum strain of 5% was reached. The rate of straining was 0.01 mm/mm/min. Five specimens of each biocomposite sample were tested and the average values of flexural strength and modulus determined. The rate of crosshead motion was calculated using Equation 3.6 [268] and set on the machine:

$$R = \frac{ZL^2}{6d} \tag{3.6}$$

where:

R is the rate of crosshead motion (in mm/min),

L is the support span (in mm),

d is the depth (thickness) of the beam in mm,

Z is the rate of straining of the outer (exterior) fibre (in mm/mm/min) and it is taken as 0.01.

Using Equation 3.6, the rate of crosshead motion to be used during the tests was 1.3 mm/min. The tests were conducted in a displacement control mode. The test was to be terminated when

the maximum strain experienced by the outer (exterior) surface of the biocomposite specimen had reached 0.05 mm/mm and the deflection at which this strain occurs is calculated using Equation 3.7 [268].

$$D = \frac{rL^2}{6d} \tag{3.7}$$

where:

D is the midspan deflection (in mm),

r is the strain in mm/mm and is taken as 0.05,

L is the support span (in mm), and

d is the thickness (depth) of specimen in mm.

Using Equation 3.7, the midspan deflection was 6.4 mm.

Flexural stress (σ_f) was calculated using Equation 3.8 [268]:

$$\sigma_f = \frac{3PL}{2bd^2} \tag{3.8}$$

where;

σ_f is the stress (in MPa) at the exterior surface at the mid-span of the specimen

P is the load (in N) at a given point on the load versus deflection curve

L is the support span (in mm)

b is the specimen width (in mm)

d is the thickness (depth) of specimen (in mm).

Flexural strain (ε_f) was calculated using Equation 3.9 [268]:

$$\varepsilon_f = \frac{6Dd}{L^2} \tag{3.9}$$

where,

ε_f is the flexural strain in the exterior surface (mm/mm)

D is the maximum deflection of the centre of the specimen (mm)

d is the thickness (depth) in mm

L is the support span in mm.

The modulus of elasticity, E_B (tangent modulus of elasticity) is determined using Equation 3.10 [268]:

$$E_B = \frac{L^3 m}{4bd^3} \tag{3.10}$$

where,

E_B is the bending modulus of elasticity (MPa),

L is the support span in mm,

b is the specimen width in mm,

d is the thickness (depth) in mm, and

m is the gradient of the initial straight-line portion of the load versus deflection curve, with units N/mm of deflection.

3.5 Impact testing of the biocomposites

Impact testing of the biocomposites involved low velocity impact tests and medium velocity tests. Medium velocity was selected because natural fibres have inherently low impact properties and hence their resultant composites were expected to have medium velocity impact resistance. Also included under impact testing is damage analysis of the damaged biocomposites after impact tests.

3.5.1 Low velocity impact testing

The fracture toughness of the biocomposites was determined through Charpy impact analysis. This analysis is also called Charpy V-notch impact analysis. It is a high-stain rate standardised test for determining the level of energy absorption by materials when fracturing. Materials' toughness and their temperature-dependent brittle to ductile transition curves can be determined using this test. Testing was performed on a Hounsfield Balanced Impact Machine (HBIM) at room temperature. The testing was done with reference to ASTM D6110-10 [269]. In this work, specimen dimensions of length 50 mm, width 10 mm and notch width of 2 mm were used. A length of 50 mm was used because the HBIM at the Durban University of Technology (DUT) can accommodate specimen length of 50 mm. There is published work where similar dimensions were used [270]. The thickness for the specimens was 3 mm and the V-notch was of root radius 0.25 ± 0.05 mm, 45° ± 1°. The notch acted as a stress concentration

point to initiate failure. The impact strength was calculated using both the ASTM D6110 standard in J/m and the ISO 179 in kJ/m^2.

3.5.2 Medium velocity impact testing

Medium velocity impact tests were conducted on a single stage high speed laboratory gas gun. The methodology for medium velocity impact testing of the biocomposites has been published in the Journal of Fibers and Polymers (2020), Volume 21, Issue 11, pages 2642-2651, in the paper titled, "Performance of kenaf non-woven mat/PLA biocomposites under medium velocity impact", by **Moyo Mufaro**, Kanny Krishnan and Velmurugan Raman and also published in the Journal of Applied Nanoscience (2021), volume 11, Issue 1, pages 441-443, in the paper titled, "The efficacy of nanoclay loading in the medium velocity impact resistance of kenaf/PLA biocomposites", by **Moyo Mufaro**, Kanny Krishnan and Velmurugan Raman. Figure 3.6 shows the laboratory gas gun used.

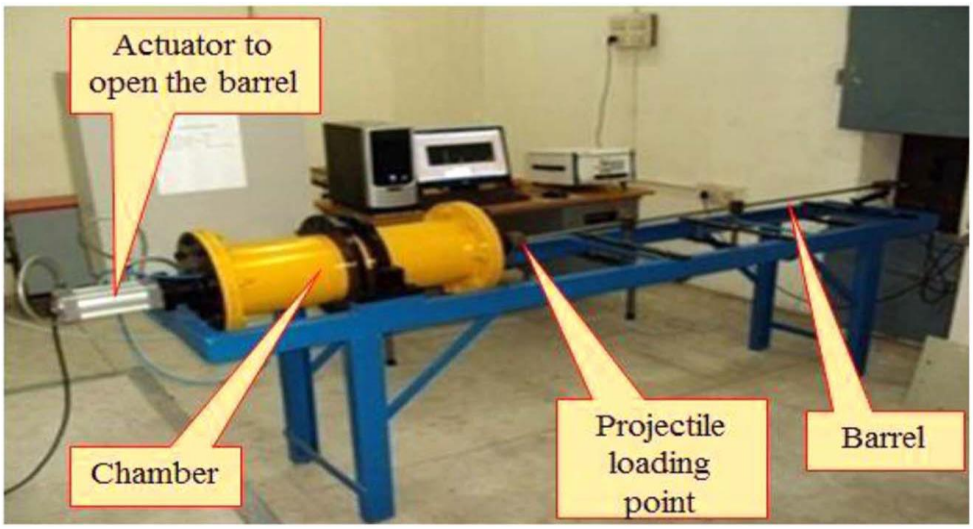

Figure 3.6 High speed laboratory gas gun

In summary, the square target biocomposites of 150 mm x 150 mm were clamped at the four corners and impacted with a projectile. The projectile was hemispherical in shape and made of mild steel. The projectile had a diameter of 15.5 mm, mass of 7.34 g, and length of 15.5 mm. A high-speed Phantom V611 video camera was integrated with the laboratory gas gun setup to capture the videos of the projectile trajectory (path) and motion. The trajectory and motion of the projectile were necessary in the analysis and evaluation of impact velocity and after post-impact velocity. Evaluations or assessments were on energy containment capability, damaged areas, damage mechanisms and establishment of perforation threshold of the various biocomposites specimens. Impact velocities of 20 m/s, 25 m/s, 35 m/s, 45 m/s, 65 m/s, 85 m/s

and 100 m/s were selected for the tests. The different impact velocities were obtained by varying the gas gun's chamber air pressure. It is important to mention here that impact velocities that were higher than the perforation threshold limit were incorporated so that the true nature of the biocomposites behaviour under medium velocity could be established.

The Vision Research software was used in the evaluation of the projectile trajectory, motion and velocities. The software was Phantom Camera Control (PCC) 2.8. Figure3.7 shows a captured and evaluated projectile trajectory. Figure 3.7a shows the trajectory that was captured and then evaluated just before contact and Figure 3.7b shows trajectory that was captured and evaluated after perforation (penetration).

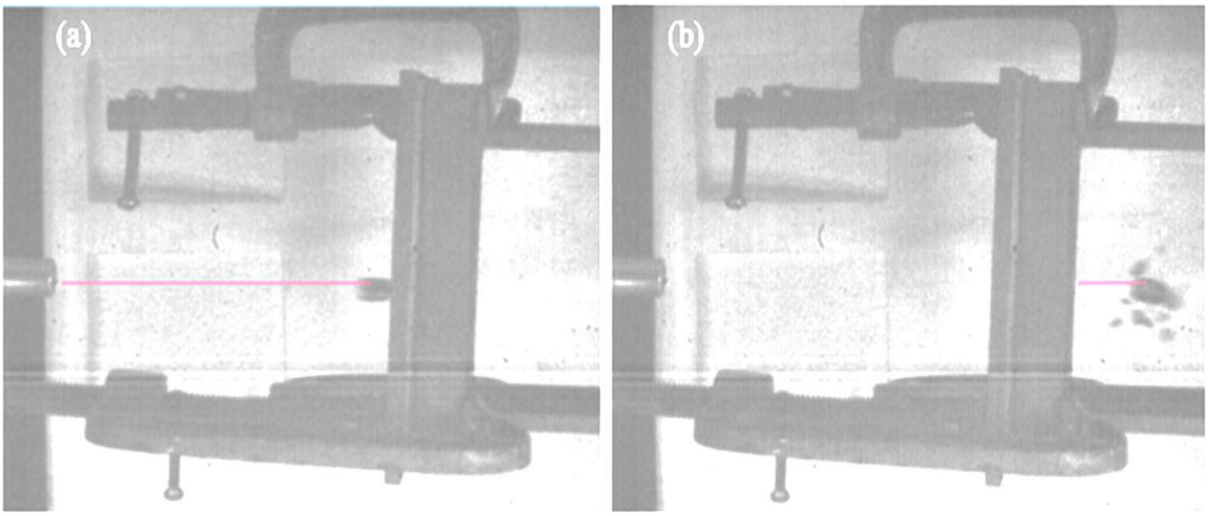

Figure 3.7 Captured and evaluated projectile trajectory

The coloured lines in Figure 3.7 were drawn using the PCC 2.8 software during the evaluation process of the velocities of the projectile just before the impact and after the penetration.

The kinetic energy formula shown in Equation 3.11 was used as the basis for the determination of the projectile's impact and residual energies.

$$\mathrm{KE} = \frac{1}{2} m_p {v_p}^2 \tag{3.11}$$

Where: KE is the kinetic energy, m_p and v_p are the projectile mass velocity, respectively.

The projectile's impact energy was calculated using Equation 3.12:

$$E_i = \frac{1}{2} m v_i^2 \quad (3.12)$$

Where E_i is the impact energy of the projectile at the point of impacting the target biocomposite and v_i is the impact velocity of the projectile at the point of impacting the target biocomposite established using the PCC software.

The residual energy of the projectile was calculated using Equation 3.13:

$$E_r = \frac{1}{2} m v_r^2 \quad (3.13)$$

Where E_r is the projectile's residual energy after penetrating the target biocomposite and v_r is the projectile's residual velocity after penetrating the target biocomposite established using the PCC software. It is worth mentioning here that if no penetration was achieved by the projectile, the target biocomposite would have absorbed all the impact energy of the projectile. Therefore, the residual velocity is considered as zero.

The difference between E_i and E_r is the Energy Absorbed (E_A) by the target biocomposite and can be calculated using Equation 3.14:

$$E_A = \frac{1}{2} m(v_i^2 - v_r^2) \quad (3.14)$$

The perforation threshold velocity (V_p) of the target biocomposite was determined using Equation 3.15:

$$V_{pt} = \sqrt{\frac{2E_{pt}}{m}} \quad (3.15)$$

Where; V_{pt} is the perforation threshold velocity of the target biocomposite and E_{pt} is the perforation energy of the projectile. E_{pt} is obtained from the plots of residual energy versus impact energy as the intercept of the equation for the relationship between the residual and the impact energies.

3.5.3 Damage analysis

Non-destructive evaluation (NDE) of the impacted specimens was conducted visually and microscopically. The analysis was on both the front (impacted) sides and back (non-impacted) sides. A Canon Camera model EOS 550D containing an image stabiliser function was used in photographing of the impacted specimens.

An optical microscope, BX51M Olympus was used in microstructural analysis of the damage on the biocomposite specimens. The microscope had an Analysis Docu Software as its integral part for intelligent image acquisition followed by image archiving and image processing. A magnification level of five times (5X) was used. It was possible to have greater magnifications but best images (resolutions) were obtained with a magnification of 5X. The measurements of the crack width were taken at different positions and then averaged.

Damage on the biocomposites tested under medium velocity were almost circular. As a result, the damaged area was obtained using Equation 3.16:

$$A = \pi r^2 \tag{3.16}$$

with A being the damaged area of the biocomposite and the radius of the damage is r.

3.6 Characterisation of fibres and biocomposites

The characterisations on the biocomposites focused on microstructural characterisation and analysis, chemical composition and functional groups analysis and crystallographic analysis.

3.6.1 Microstructural analysis

A scanning microscope (SEM) was used in performing microstructural analysis on the biocomposites. The evaluations were on observing the microstructural changes caused by clay nanoparticles added to the biocomposites. A Zeiss SEM of model SEM-EVO HD15 was used in this work. The Energy Dispersive X-ray (EDX) component was an integral part of the SEM. EDX was used for compositional analysis and mapping showing the distribution of clay nanoparticles in the biocomposite laminates. AZTEC V1.1 NanoAnalysis Software was used in operating the EDX. Gold coating was done on the specimens using a gold-sputtering process done on a Quorum model Q150RES sputter coater. This was done to make the specimens conductive.

3.6.2 XRD analysis

Crystallographic analysis on the biocomposites was achieved using an x-ray diffraction equipment (XRD equipment). Bruker D8 Discover powder XRD was used and it was operated at 40 kV and 40 mA. The rate of scanning was 2^o min^{-1} on specimen layer of thickness 0.1 mm with 2θ values being varied from 5^o to 80^o. X'Pert HighScore Plus software was used in the analysis of the XRD data. OriginPro software was used in determining the area of crystalline peaks and the area of all peaks (crystalline + amorphous regions) which are necessary in the calculation of crystallinity level. Equation 3.17 was used in calculating crystallinity level:

$$\% \text{ Crystallinity} = \frac{Area\ of\ crystalline\ peaks}{Area\ of\ all\ peaks} \times 100 \qquad (3.17)$$

3.6.3 FTIR analysis

Perkin Elmer Spectrum 1000 FTIR spectrometer was used in analysing the chemical structure of untreated, NaOH treated and clay nanoparticle infused fibres. The machine was fitted with an ATR (universal attenuated total reflectance) accessory. Recording of the spectra was in the range of 350 cm^{-1} to 4000 cm^{-1} wavenumber and with a resolution of 2 cm^{-1}.

3.7 Statistical analysis and graphing

IBM SPSS version 20 was used to carry out statistical analysis on the experimental data obtained in this work. The analysis was on the analysis of variance (ANOVA). OriginPro was also used to carry out some data analysis and graphing.

3.8 Conclusion

This chapter discussed the materials, equipment and procedures used in carrying out this research work. Major materials used in the fabrication of the hybrid bio-nanocomposites are PLA biopolymer, kenaf fibre nonwoven mats and clay nanoparticles. The experimental design consisted of production of the kenaf fibre nonwoven mats, chemical treatment of the nonwoven mats and fabrication of the kenaf/nanoclay/PLA bio-nanocomposites. Tests were performed on the basic mechanical properties (thermal decomposition, tensile, flexural and dynamic mechanical properties), low velocity impact resistance and response to medium velocity impact performed using a gas gun. Structure-property relationships were characterised using SEM, EDX, FTIR, XRD and optical microscopy techniques. ANOVA and other statistical analysis of data and graphing were performed using SPSS and OriginPro.

Chapter 4 Results and Discussion

4.1 Introduction

This chapter presents and discusses in detail the results of this work. Published results are discussed in summary.

4.2 Results on fibre testing and analysis

The results on fibres consist of thermal decomposition results, FTIR results, microscopic analysis (SEM and EDX) results and results on tensile strength.

4.2.1 TGA results for untreated and treated kenaf fibres only

The TGA results for untreated and treated kenaf fibres only are shown in Figure 4.1.

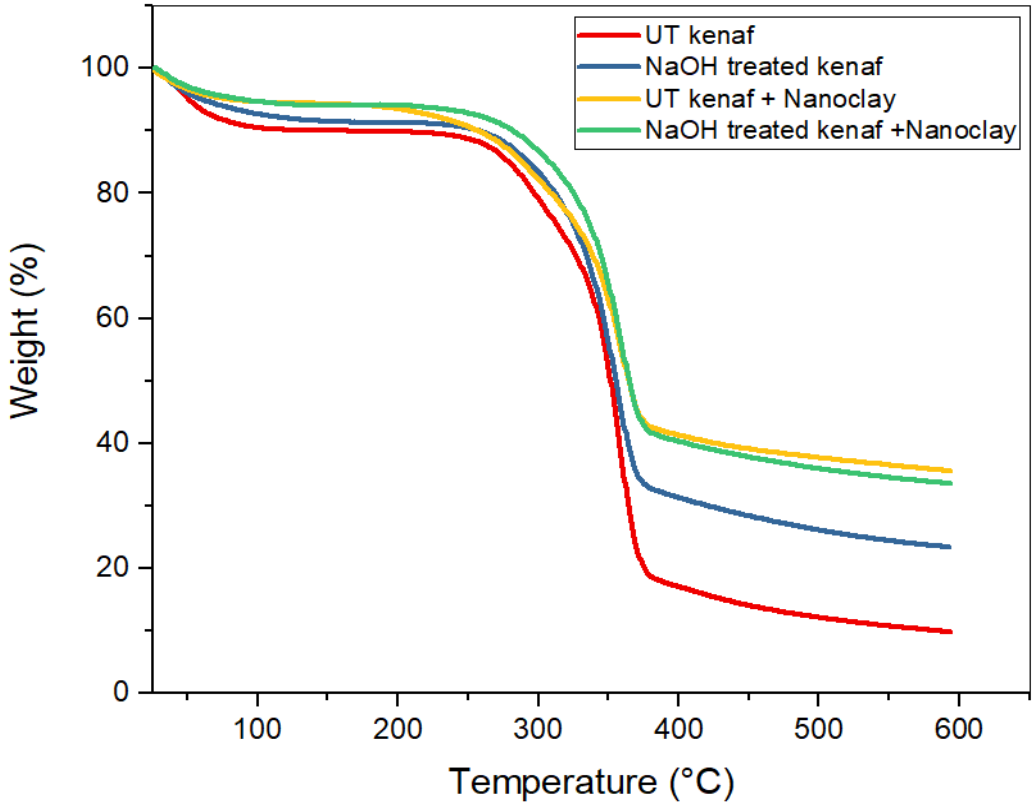

Figure 4.1 TGA thermogram for treated and untreated kenaf fibres only

Key: UT = Untreated

Figure 4.1 shows that the thermal decomposition of kenaf fibres begins with mass loss below 100 ^{o}C, followed by major decomposition between 200 ^{o}C and 400 ^{o}C and the remaining inorganic components after 400 ^{o}C. Moisture and volatiles decompose below 100 ^{o}C and in this case, most of the decomposition that occurred below 100 ^{o}C is attributed to moisture since kenaf fibre is a natural fibre which retains some moisture at room conditions. Figure 4.1 shows that the residual mass increased with introduction of treatments. This is clear from 400 ^{o}C up

to the end of the decomposition at 600 ºC. This is an indication that the treatments increased the thermal decomposition stability of the kenaf fibre.

A DTG graph (derivative graph of the TGA data) was plotted in order to observe all the peaks for the thermal decomposition of kenaf fibre. Figure 4.2 shows the DTG thermogram for thermal decomposition of untreated and treated kenaf fibres only.

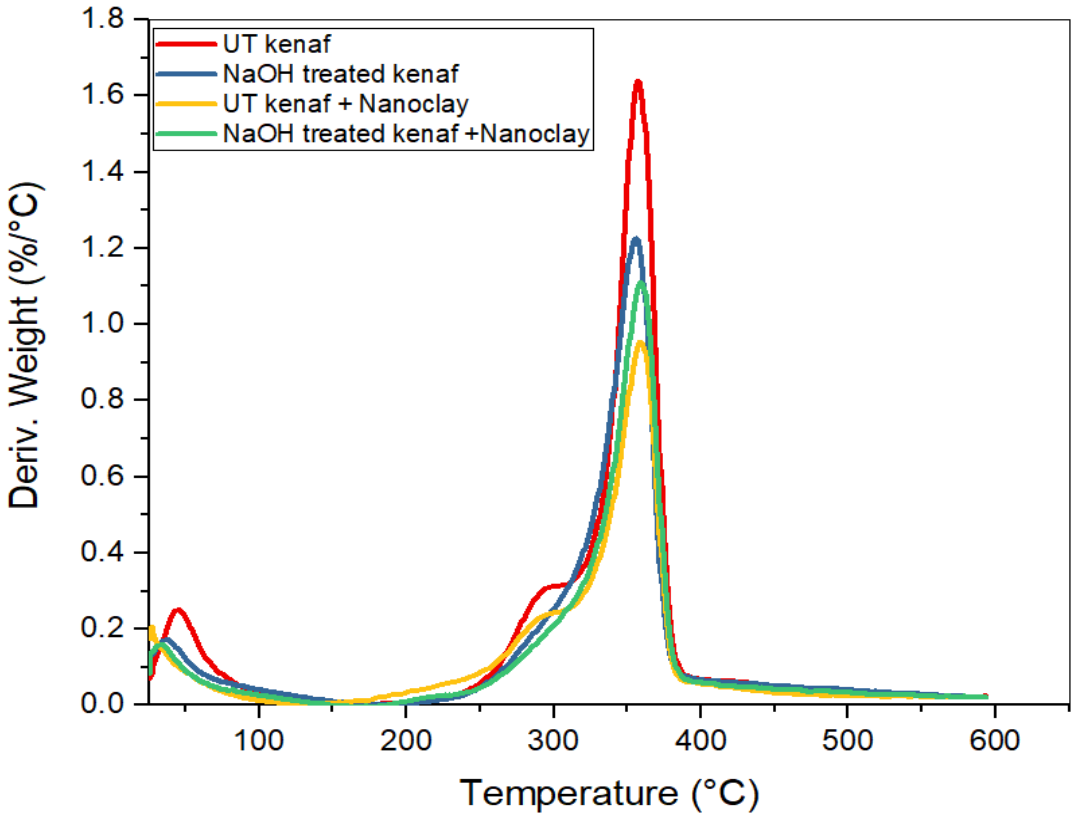

Figure 4.2 DTG thermogram for untreated and treated kenaf fibre only

Key: UT = Untreated

Figure 4.2 shows a peak for a component that decomposed between 250 ºC and 310 ºC for untreated kenaf fibre and untreated kenaf fibre infused with clay nanoparticles. This component was hemicellulose because the decomposition temperature range is typical of hemicellulose. However, hemicellulose was not present in both samples that had NaOH treatment. This indicates that the treatment with NaOH eliminated the hemicellulose component from the kenaf fibre by hydrolysis. The decomposition peak between 310 ºC to about 390 ºC represents decomposition of cellulose. This was the bulk decomposition because kenaf fibre is cellulosic in nature. The cellulose component was even present in the NaOH treated kenaf fibres indicating that the NaOH did not affect the cellulose component. Figure 4.2 also shows that the peak decomposition temperatures slightly shifted towards higher temperatures for the kenaf

fibres that received treatments. This shows that the peak decomposition temperature increased with the introduction of NaOH treatments and clay nanoparticle infusion. Literature reports that the removal of hemicellulose from natural cellulosic fibres improves their crystallinity level and improves mechanical properties like tensile strength and modulus [254, 257, 258, 271-275].

Table 4.1 shows a summary of the thermal decomposition process of untreated and treated kenaf fibres only.

Table 4.1 Thermal decomposition of untreated and treated kenaf fibres only

Sample	**Process temperature (°C)**			**Mass loss at 390 °C (wt.%)**	**Mass loss at 600 °C (wt.%)**	**Mass loss at 100 °C (wt.%)**
	Onset	Peak	End			
Untreated kenaf fibre	310	336	390	82	91	9
NaOH treated kenaf fibre	310	337	390	67	77	7
Untreated kenaf fibre infused with clay nanoparticles	310	339	390	58	64	5
NaOH treated kenaf fibre infused with clay nanoparticles	310	340	390	59	66	5

Table 4.1 shows that the peak degradation temperatures for the kenaf fibres increased with the introduction of the NaOH treatment and combined NaOH treatment and clay nanoparticle infusion. Treatment of kenaf fibre with NaOH only improved the peak decomposition temperature by 0.3%, infusion of untreated kenaf fibres with clay nanoparticles improved the peak decomposition temperature by 0.9% and combined treatment of kenaf fibre using NaOH and infusion with clay nanoparticles improved the peak decomposition temperature by 1.2%. Residual mass at 390 °C, that is after the decomposition of cellulose, was 18 wt%, 33 wt%, 42 wt% and 41 wt% for untreated kenaf fibre, NaOH treated kenaf fibre, untreated kenaf fibre infused with clay nanoparticles and NaOH treated kenaf fibre infused with clay nanoparticles, respectively. The mass loss at the end of the thermal decomposition process (at 600 °C) shows that treatment of kenaf fibres with NaOH reduced mass loss by 15%, infusion with clay nanoparticle reduced mass loss by 29.7% and combined treatment with NaOH and infusion with clay nanoparticles reduced mass loss by 27.5%. All these observations indicate that treatment of kenaf fibres with NaOH, infusion with clay nanoparticles and combined treatment with NaOH and clay nanoparticles all culminated in an elevation of thermal stability. In the case of treatment with NaOH, the improvement in thermal stability was due to improvement in

the crystallinity level of the kenaf fibres brought about by the hydrolysis of the hemicellulose by NaOH. In the case of untreated kenaf fibre infused with clay nanoparticles, improvement in thermal stability was brought about by the thermal barrier impact of the clay nanoparticles which cause a reduction in heat transfer efficiency within the morphological structure of the fibre. The clay nanoparticles diminish the rate of heat transfer to the fibres as well as retaining some of the heat thereby improving the thermal stability of the fibres. In the case of combined treatment, improvement in thermal stability was brought about by the combined effects of hemicellulose removal by NaOH and clay nanoparticles' thermal barrier impact.

Additionally, untreated kenaf fibre, NaOH treated kenaf fibre, untreated kenaf infused with clay nanoparticles and NaOH treated kenaf fibre infused with clay nanoparticles lost 9 wt%, 7wt%, 5wt% and 5wt%, respectively, below 100 ^{o}C. This shows that the treatments reduced the moisture regain of the kenaf fibre. In the case of NaOH treated kenaf fibre, a drop in the moisture regain was largely caused by the elimination of hemicellulose which is hydrophilic. In the case of clay nanoparticle infused kenaf fibres, reduction in the moisture regain was thought to be due to the water flow barrier property brought about by clay nanoparticles. Literature reports that clay nanoparticles act as barrier medium that hinder the flow of water into a material from all directions which results in a decreased equilibrium water content [273, 276, 277].

4.2.2 FTIR results

Figure 4.3 shows FTIR results for untreated and treated kenaf fibres only.

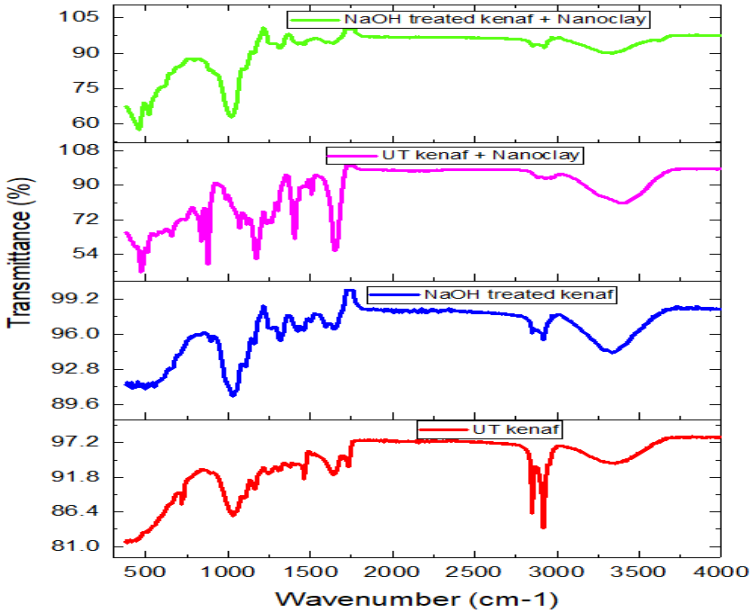

Figure 4.3 FTIR spectra for untreated and treated kenaf fibres only

The FTIR results in Figure 4.3 generally shows that the treatments done to the kenaf fibres altered the functional groups of the raw (untreated) kenaf fibre. Untreated kenaf fibre has a broad peak at 3350 cm^{-1} which represents the OH group found in raw (cellulosic) kenaf fibres. This is supported by literature [257, 272, 274, 275, 277-279]. This is a characteristic functional group for all natural cellulosic fibres. Figure 4.3 shows that treatment with NaOH did not significantly alter OH group as the peak position did not change. However, the peak intensity was slightly reduced indicating a decrease in water absorption ability after treatment with NaOH.

Peaks at 2918 cm^{-1} and 2849 cm^{-1} in the untreated kenaf fibre represent CH stretching vibration. Similar findings were reported in literature [274, 275, 277-279]. Figure 4.3 shows that the two peaks almost vanished after treatment with NaOH an indication that there was a change of bonds with the formation of new functional group. This could have been a reaction of the NaOH and the $–CH_2OH$ parts of the repeat unit for kenaf fibre forming $–CH_2ONa$. This also contributes to reduction in water absorption ability.

The peak observed at 1736 cm^{-1} in the untreated fibre is attributed to C=O group. This is carbonyl stretching for acetyl group in hemicellulose [257, 274, 275, 277, 278]. This peak disappeared when the kenaf fibre was treated with NaOH indicating that the hemicellulose was removed by the alkali treatment. Removal of hemicellulose has an effect of reducing water absorption ability.

Peak at 1650 cm^{-1} and 1463 cm^{-1} are for aromatic C-C bonds. Literature reported similar findings relating these peaks to carbonyl stretching and aldehyde group in lignin [277-279]. These peaks disappeared when NaOH treatment was performed on the kenaf fibres indicating the removal of lignin. Peaks observed around 1413 cm^{-1} and 1317 cm^{-1} are for CH_2 wagging in lignin. Rana et al. (1997) reported CH_2 wagging in lignin for jute fibre at 1320 cm^{-1} [279] whilst Nascimento et al. (2018) reported CH_2 wagging in lignin for mallow fibre at 1400 cm^{-1} [280].

Peaks observed at 1167 cm^{-1} and 1000 cm^{-1} in untreated kenaf fibre are attributed to C-O band as well as C-O-C stretching of cellulose fibre. Literature reports a strong C-O band around 1050 cm^{-1} due to the $C-O-CH_3$ group which confirms the existence of lignin in kenaf [277, 278]. Nascimento et al. (2018) assigned the peak at 1050 cm^{-1} to C-O stretching in cellulose, hemicellulose and lignin found in un-mercerised mallow fibres but got considerably attenuated after mercerisation [280]. In this work, peak 1167 cm^{-1} disappeared with the addition of NaOH indicating that it was the one attributed to the acetyl group in lignin and hence was removed by

treating the fibres with NaOH. Peak 1000 cm^{-1} remained unchanged after treatment with NaOH, indicating that it is the one related to the C-O-C bond of the skeletal glucopyranose ring vibration in agreement with literature. Peak observed at 719 cm^{-1} in untreated kenaf fibre is attributed CH stretching as well as OH group. Literature reports out of plane OH vibrations around 700 cm^{-1} as well as CH stretching [277, 278, 281]. This peak disappeared when the fibres were treated with NaOH indicating that OH group reacted with NaOH.

Treatment with nanoclay resulted in many functional groups in the untreated kenaf fibre disappearing. This was thought not to be due to a chemical reaction but masking effect of clay nanoparticle which prevented detection of the kenaf peaks. Clay nanoparticle peaks were the ones detected as the new functional groups that appeared are characteristic of clay nanoparticle FTIR pattern. However, after infusion with clay nanoparticles a strong band at 3350 cm^{-1} was observed. Chrzanowska et. al (2018) reported that the strengthening of the band at around 3350 cm^{-1} was due to the adsorbed water on the surface of the clay nanoparticles [282]. This was thought to be a similar case in this work. Also, peak 1000 cm^{-1} for the C-O-C bond of the glucopyranose ring skeletal peak was observed an indication that infusion with nanoclay did not alter the skeletal structure of the kenaf fibre.

Combined treatment with NaOH and nanoparticle infusion brought about combined effects to the kenaf fibres as shown in Figure 4.3. It can be seen that the FTIR pattern is a combination of the effects brought about by NaOH and nanoclay infusion. The intensity at 3350 cm^{-1} was different from that of fibres treated with NaOH alone and those infused with nanoclay alone. The peak intensity reduced when compared to the peak intensity observed when fibres were treated with clay nanoparticles alone indicating a reduction in water adsorption when combined treatment is used. Notably, the peak at 1000 cm^{-1} was more pronounced when combined treatment was done. This means the C-O-C bond of the glucopyranose ring skeletal structure was strengthened by combined treatment. This was thought to be due to the overlapping of Si-O stretching band in the clay nanoparticle filler and the C-O-C bridge stretching. A similar finding was reporting in literature where clay nanoparticles were used on chitosan [282]. The disappearance of peaks related to OH groups, hemicellulose and lignin peaks means they were removed by the NaOH and hence a reduction in water absorption was expected.

4.2.3 Results on SEM analysis

SEM results on morphological analysis of untreated and treated fibres only are shown in Figure 4.4. The magnification for the images shown in Figure 4.4 is 1000X.

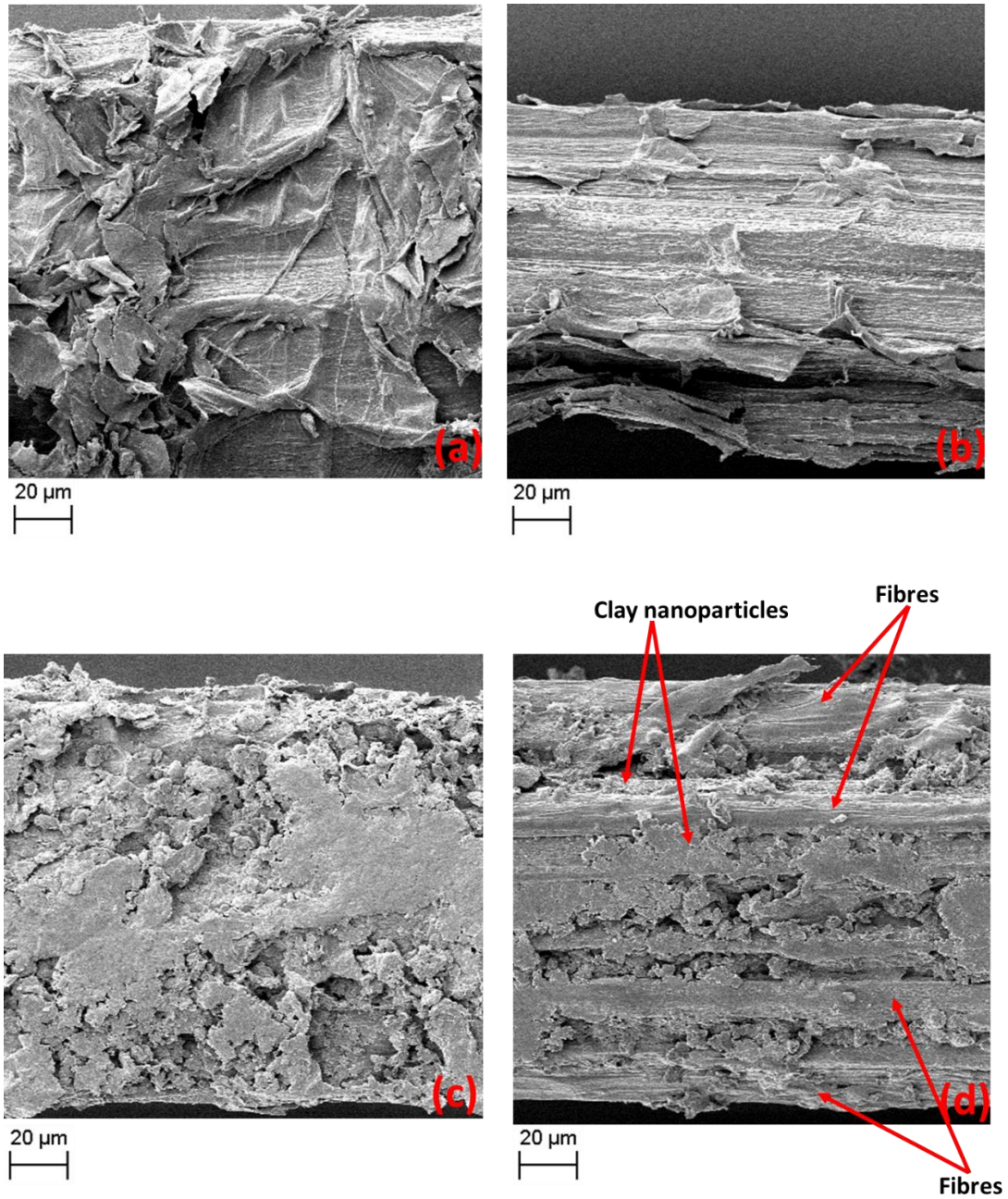

(a) Untreated kenaf, (b) NaOH treated kenaf, (c) Untreated kenaf + Nanoclay and (d) NaOH treated kenaf + Nanoclay

Figure 4.4 Morphological images of untreated and treated kenaf fibres only

Figure 4.4 (a) shows that the untreated kenaf fibre had a rough surface with some scales-like components being part of the fibre surface. Figure 4.4 (b) shows that treatment of the kenaf fibre with NaOH remove these scales-like components leaving the fibre a bit smooth and

reduced diameter. These observations were in agreement with some published work [254, 257, 258, 271-275]. These components removed (as supported by TGA and FTIR analyses) were hemicellulose and lignin. Figure 4.4 (c) shows that indeed the fibres had nanoclay and infusion of untreated fibre results in the clay nanoparticles covering the whole surface of the fibre. As can be seen in Figure 4.4 (c), the fibre striations could not be seen. Perhaps, this is one way the clay nanoparticles form a barrier medium around the fibre leading to high thermal stability and reduced water absorption as it will prevent water percolating into the fibre. Figure 4.4 (d) also shows the presence of clay nanoparticles as well as striations of the fibre. This shows that when clay nanoparticles are infused on NaOH treated kenaf fibres, more nanoparticles are able to move into the inner parts of the fibre. The ability of more nanoparticles to move into the inner parts could be due the absence of hemicellulose and lignin which provide a cementing materials for the fibre. Their absence allows easy penetration by substances, in this case, clay nanoparticles. Literature reported that removal of hemicellulose from natural cellulosic fibres leads to a rise in the crystallinity level of the natural cellulosic fibre

Figure 4.5 shows the cross-sectional images of untreated and treated kenaf fibres only. The magnification used for the analysis of the cross-section of the fibres was 1300X.

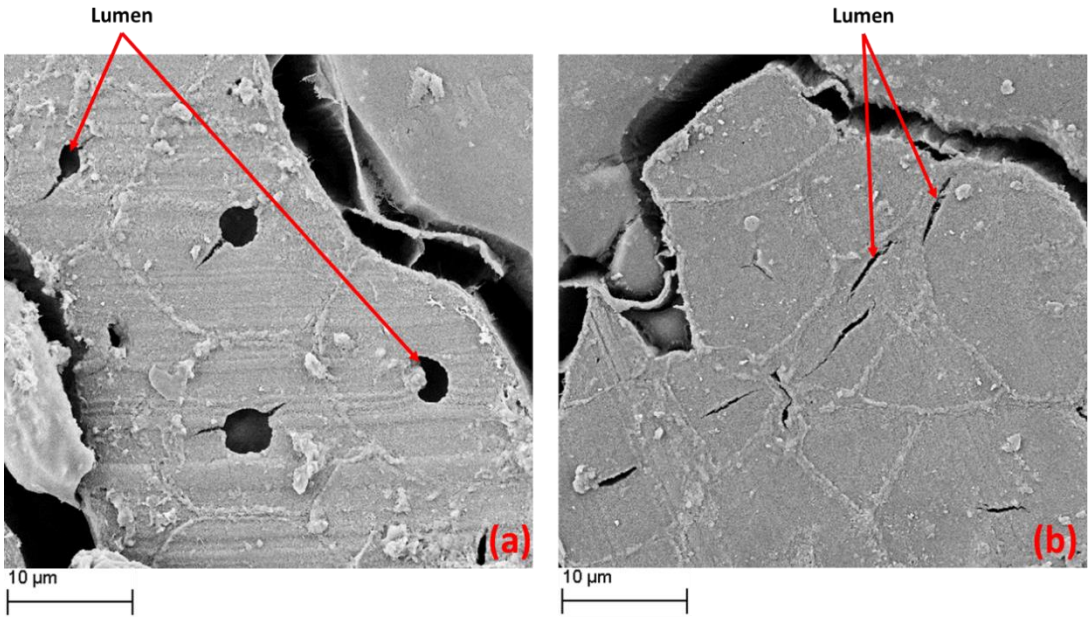

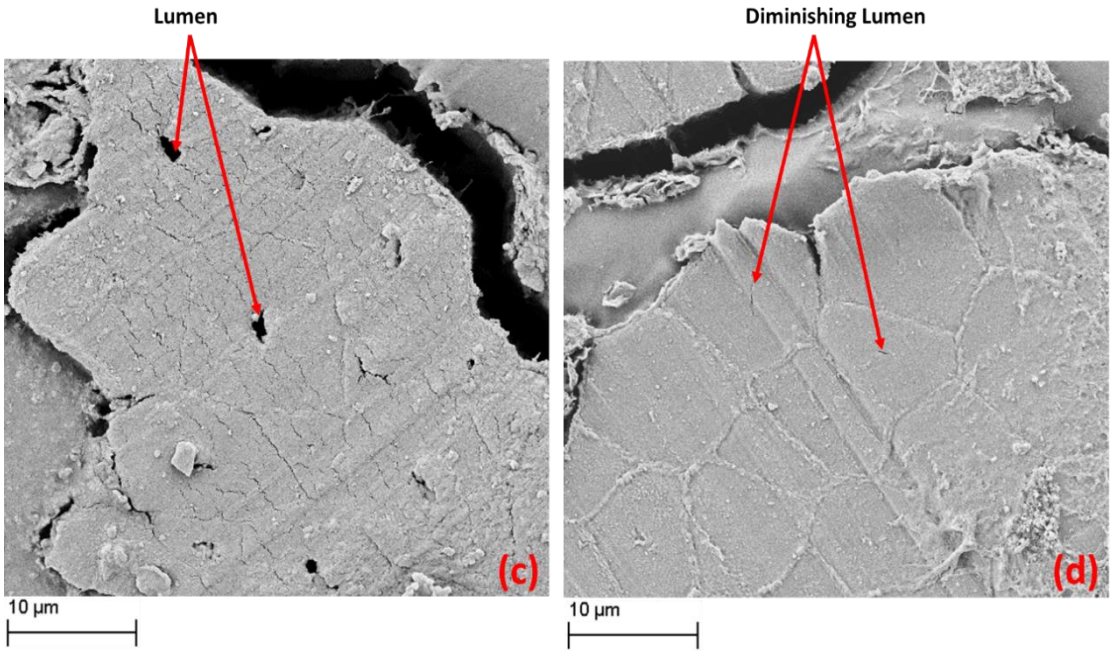

(a) Untreated kenaf, (b) NaOH treated kenaf, (c) Untreated kenaf + Nanoclay and (d) NaOH treated kenaf + Nanoclay

Figure 4.5 Cross-sectional images of untreated and treated kenaf fibres only

Figure 4.5 (a) shows untreated kenaf fibre has a large lumen which look roundish and semi-round. Treatment with NaOH results in the lumens significantly shrinking and changing the lumens shape to thin striations as shown in Figure 4.5 (b). Lumen changes have a big impact on the structure of the fibre and mechanical properties. Reduction in water absorption is expected since reduction in lumen size means reduction in the capillary action of the fibre. Infusing untreated kenaf fibres with clay nanoparticles also resulted in the distortion of the lumen shape and slight reduction in lumen size as shown in Figure 4.5 (c). However, the degree of distortion and reduction in size was far much lower than the one experienced with NaOH treatment. This distortion in shape and reduction in lumen size after infusion with clay nanoparticles could mean that some clay nanoparticles penetrated the fibres structure up to the lumen. These changes also result in fibre property changes. Combined treatment with NaOH and infusion with clay nanoparticles resulted in the disappearance of the lumen as shown in Figure 4.5 (d). This brings about major changes on the mechanical properties and performance of the fibres as well as the resultant materials.

4.2.4 EDX mapping and elemental composition

SEM-EDX elemental composition, distribution and mapping results for untreated and treated kenaf fibres only are shown on Table 4.2.

Table 4.2 Fibres Elemental composition, distribution and mapping

Specimen	**Major elements present (wt%) and Mapping** (1000X Magnification) 50µm			
	Carbon	**Oxygen**	**Silicon**	**Aluminum**
Untreated kenaf	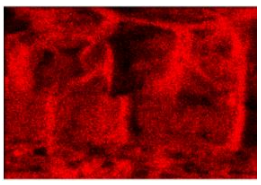 72.35 wt%	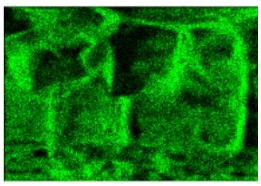 27.08 wt%	nil	nil
NaOH treated kenaf	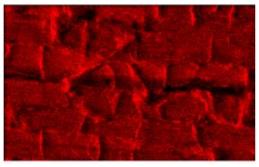 72.26 wt%	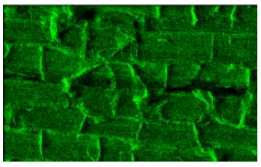 26.99 wt%	nil	nil
Untreated kenaf + Nanoclay	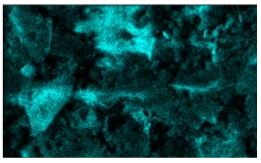 70.24 wt%	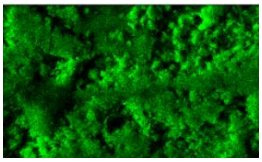 24.46 wt%	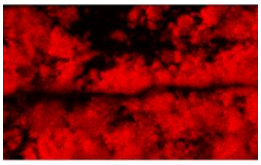 3.01 wt%	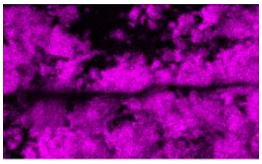 1.48 wt%
NaOH treated kenaf + Nanoclay	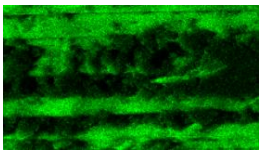 71.03 wt%	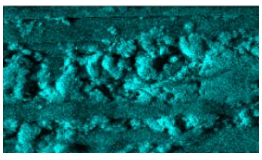 25.37 wt%	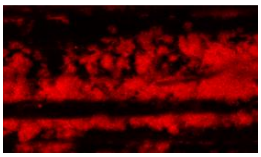 2.01 wt%	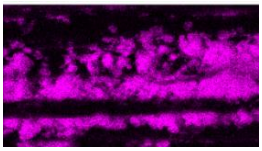 1.03 wt%

Table 4.2 shows that untreated kenaf fibre has carbon and oxygen as the dominating elements. This is because in addition to hydrogen (not detected by EDX), carbon and oxygen are the main elements found in natural cellulosic fibres such as kenaf. EDX analysis system cannot detect the hydrogen element and this is the reason for it not appearing on the EDX spectrum but it is one of the main elements found in plant fibres which are cellulosic in nature. Trace elements consisted of 0.58 wt% and in this work the detected trace elements included potassium (K) element, magnesium (Mg) element, chlorine (Cl) element, calcium (Ca) element, copper (Cu) and molybdenum (Mo). These are residual elements during plant growth and after the maturity of the natural plant kenaf fibre. The carbon and oxygen elements in the untreated kenaf fibre

were uniformly distributed as shown in Table 4.2. NaOH treated kenaf fibre also had carbon and oxygen as the major elements and uniformly distributed. The NaOH treated kenaf fibre had sodium (Na) as an additional trace element to those found under untreated kenaf fibre and the total quantity of the trace elements was 0.75 wt%. The additional Na element was from NaOH used during the alkali treatment. Si and Al elements detected in the kenaf fibres treated with clay nanoparticles were from the clay nanoparticles. This confirms that the clay nanoparticles were indeed infused into the fibres. The fibres that received combined NaOH treatment and clay nanoparticle infusion also had Si and Al which confirms the presence of clay nanoparticles.

4.3 Basic mechanical properties of the biocomposites

This section presents results and discussion of the basic mechanical properties established after a series of density (floatation) tests, tensile strength tests, flexural strength tests, TGA and DMA on the biocomposites. Some of the results are discussed in summary and more information about them is in the respective published journal papers referred to in the following sections.

4.3.1 Floatation test results

The hybrid composites fabricated in this research work were observed to have positive buoyancy, that is, they floated in water. This was as expected since the theoretical densities of all the specimens were less than the density of water (1 g/cm^3). The theoretical densities were 0.655, 0.669, 0.679 and 0.691 g/cm^3 for the biocomposites infused with 0, 3, 5 and 7 wt% clay nanoparticle content, respectively. This shows that the hybrid biocomposites fabricated in this work were really lightweight and could not sink in water. They resemble the lightweight the metal matrix composite reported by the New York University researchers in 2015 [243]. The experimental density for the neat kenaf/PLA biocomposite was found to be 0.638 g/cm^3 for both biocomposites made using kenaf fibres of 250 gsm and 500 gsm. The experimental density for kenaf/nanoclay/PLA hybrid biocomposites infused with 3, 5 and 7 wt% clay nanoparticle content was found to be 0.655, 0.666 and 0.677, respectively.

4.3.2 Tensile strength test results

Figure 4.6 shows the one of the biocomposite laminates under tensile loading and the nature of failure it sustained.

Figure 4.6 Biocomposite laminate under tensile strength testing

It can be seen in Figure 4.6 that the biocomposite specimen failure occurred in the middle position (middle of the gauge length) which was a sign of a good failure. Also, this was a sign that the fabrication of the biocomposites was done uniformly. Figure 4.7 shows the tensile strength results of the biocomposites.

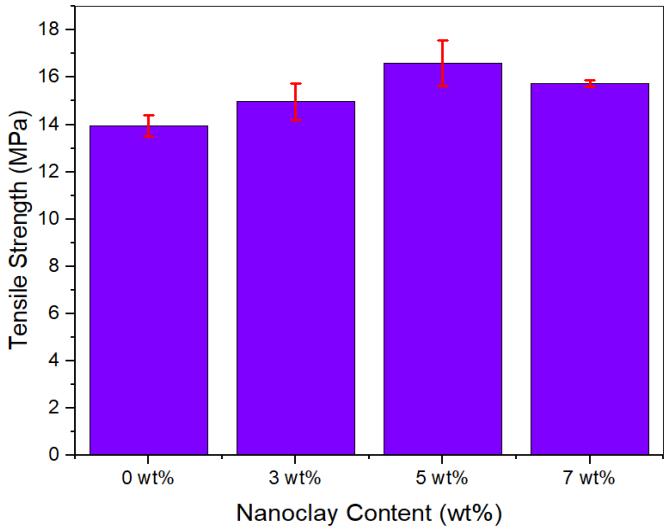

Figure 4.7 Tensile strength of the biocomposites

Figure 4.7 shows that the tensile strength of the biocomposites improved with increase in the clay nanoparticle content. Addition of 3, 5 and 7 wt% clay nanoparticle enhanced the tensile strength of the biocomposites by 7.4%, 19.1% and 12.9%, respectively. This shows that hybridisation with clay nanoparticles significantly improved the tensile strength. Tensile strength values obtained in this work were comparable to the tensile strength reported by other researchers who worked on other natural fibre-reinforced composites [136, 283-286]. Figure

4.8 shows the percentage (%) elongation of the different biocomposite samples at break (maximum tensile stress).

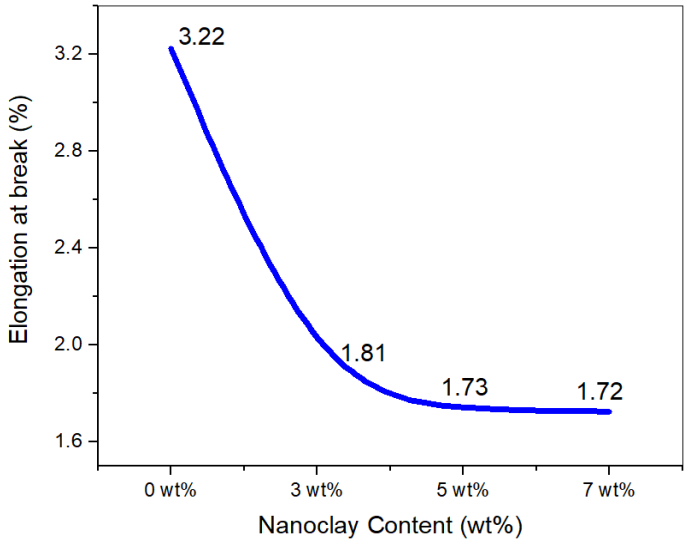

Figure 4.8 Percentage elongation of the biocomposites

Figure 4.8 shows that the elongation at break of the biocomposites was reduced with the addition of clay nanoparticles. This indicates increased stiffness of the biocomposites introduced by the clay nanoparticles. Addition of 3, 5 and 7 wt% clay nanoparticles reduced the % elongation by 43.8%, 46.3% and 46.4%, respectively. This shows that the clay nanoparticles significantly increased the stiffness of the biocomposites and hence the clay nanoparticle infused biocomposites were more difficult to strain than the neat biocomposites.

The Young's modulus values for the biocomposites are shown in Figure 4.9.

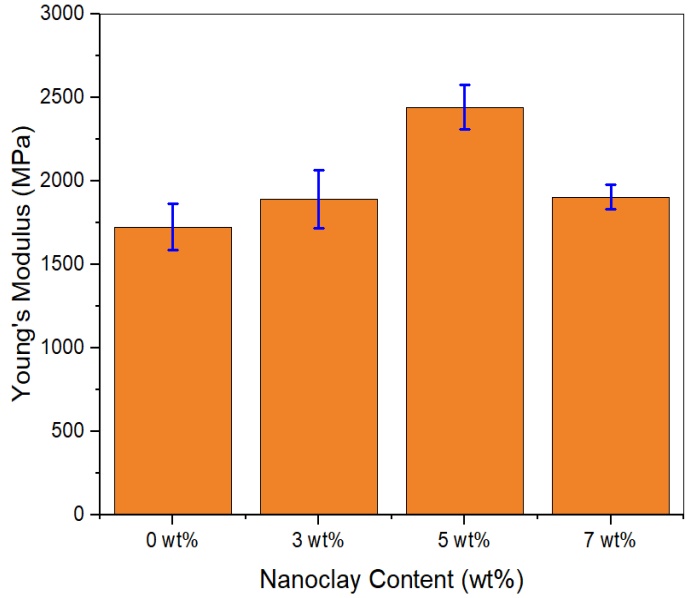

Figure 4.9 Young's modulus for the biocomposites

Figure 4.9 shows that addition of clay nanoparticles raised the Young's modulus of the biocomposites. This is agreement with changes in elongation shown in Figure 4.8. The increase in Young's modulus was 9.5%, 41.5% and 10.3% for 3, 5 and 7 wt% clay nanoparticle content, respectively. The results show that clay nanoparticles increase the stiffness of the biocomposites. A drop in Young's modulus after the 5 wt% clay content was due to clay agglomeration. The Young's modulus values obtained in this work where comparable to the Young's modulus of some biocomposites reported in literature [136, 140, 283-288].

4.3.3 Flexural strength results

Figure 4.10 shows the flexural strength results of the kenaf/nanoclay/PLA hybrid biocomposites obtained in this research work.

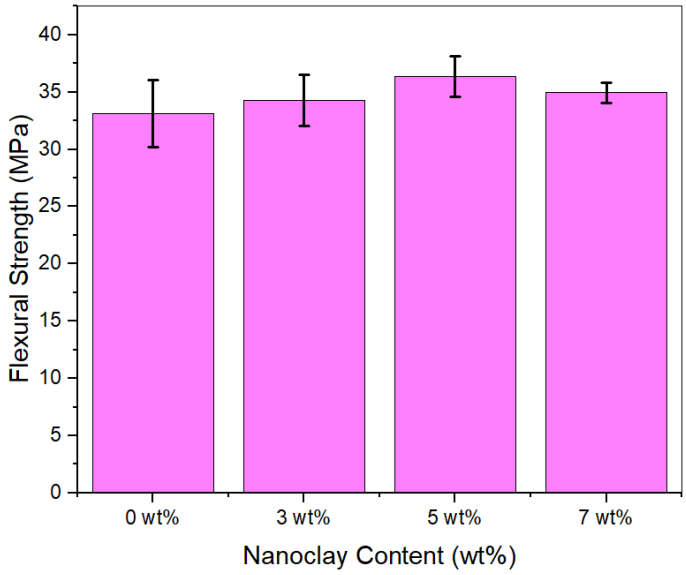

Figure 4.10 Flexural strength of the biocomposites

Figure 4.10 shows that the flexural strength of the kenaf/nanoclay/PLA hybrid biocomposites ranged from 33 to 35 MPa. These results were comparable to the flexural strength properties of 4mm thick PLA composites reinforced with cotton waste, flax fibres and maleic anhydride polypropylene (MAPP) reported by Bajracharya et al. (2017). [285]. The results are also comparable to other findings reported in literature [136, 283, 284, 286]. The increase in flexural strength was 3.5%, 9.8% and 5.4% for 3, 5 and 7 wt% clay nanoparticle content, respectively. The increase is attributed to the improvement in the mechanical properties brought about by the clay nanoparticles which improve the stress transfer mechanism. Reduction in flexural strength after 5 wt% was due to clay nanoparticle agglomeration which blocks or reduces the

stress transfer efficiency. Figure 4.11 shows the percentage change in the flexural strain at maximum flexural stress.

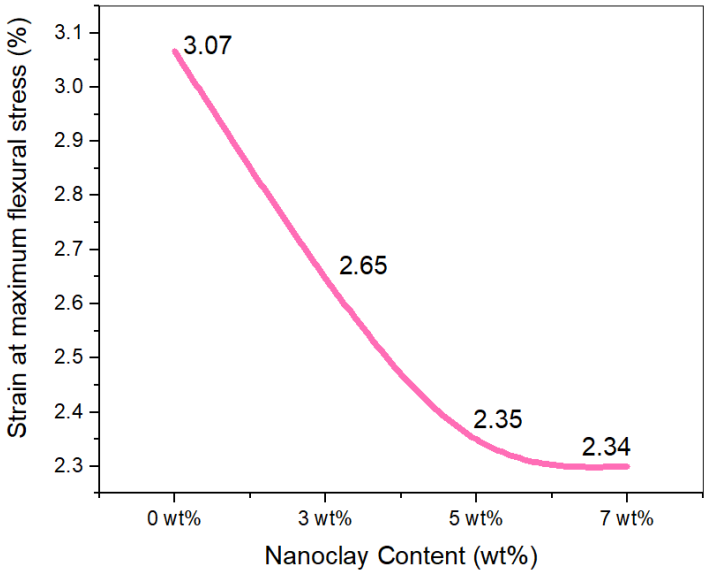

Figure 4.11 Percentage strain at maximum flexural stress

There was a gradual reduction in the strain at maximum flexural stress as shown in Figure 4.11. Addition of 3, 5 and 7 wt% reduced the strain at maximum flexural stress by 13.7%, 23.4% and 23.6%, respectively. Therefore, the clay nanoparticles improved the flexural stiffness of the kenaf/nanoclay/PLA biocomposites making them more difficult to strain under flexural loading than the neat kenaf/nanoclay/PLA biocomposites.

The flexural modulus results of the biocomposites are shown in Figure 4.12.

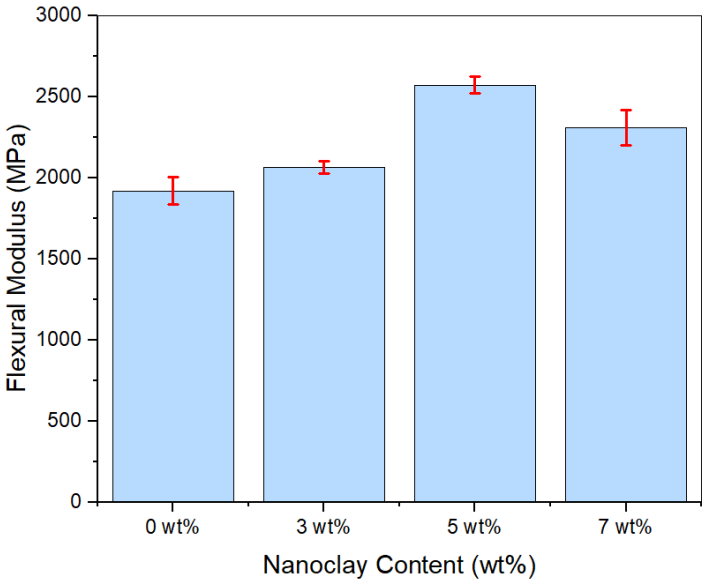

Figure 4.12 Flexural modulus for the biocomposites

Infusion of clay nanoparticles improved the flexural modulus of the kenaf/nanoclay/PLA biocomposites as shown in Figure 4.12. The results are comparable to some published results on flexural modulus of some biocomposites [136, 285, 288]. The improvement in the flexural modulus was 7.5%, 34% and 20.2% for clay nanoparticle loading of 3 wt%, 5 wt% and 7 wt%, respectively. Therefore, the clay nanoparticles improved the stiffness of the biocomposites. A drop in flexural modulus after 5 wt% nanoclay content loading was due to clay nanoparticle agglomeration.

In conclusion, the improvements in tensile strength, Young's modulus, flexural strength and flexural modulus and a reduction in strain at break were attributed to the:

- improvement in the kenaf fibre to PLA bonding which increased the kenaf fibre to PLA interfacial adhesion.
- reduction in the micro-voids which are known to weaken a material. The clay nanoparticles sealed the micro-voids thereby promoting strong adhesion between PLA and kenaf fibres.
- improvement in the crystallinity level brought about by NaOH and nanoclay treatment.
- improvement in the composite stiffness due to increased crystallinity. Increase in stiffness results in reduced strain at break.
- improvement in stress-transfer properties of the resultant hybrid biocomposite due to good interfacial adhesion and the presence of clay nanoparticle which also act as load transfer systems.

4.3.4 Results on the thermo-mechanical properties of the biocomposites

TGA and DMA results of the biocomposites have been presented and discussed in published journal papers titled, "Thermo-mechanical response of kenaf/PLA biocomposites to clay nanoparticles infusion" and "Effects of combined alkali treatment and clay nanoparticle infusion on thermo-mechanical response of kenaf/PLA biocomposites" published in the Materials Today: Proceedings Journal, Volume 38, Part 2, 2021, Pages 609-613 and the South African Journal of Science and Technology (2022), Volume 40 Issue 1, pages 137-141, respectively. The summary of these papers is presented in the next chapters.

4.4 Low velocity impact resistance of the biocomposites

The resistance of the kenaf/nanoclay/PLA hybrid biocomposites to low velocity impact loading was analysed based on the impact energy absorbed by the notched specimens and the impact strength calculated using both the ISO and ASTM as mentioned in chapter 3.

The low velocity impact energy absorbed by the kenaf/nanoclay/PLA hybrid biocomposites is shown in Figure 4.13.

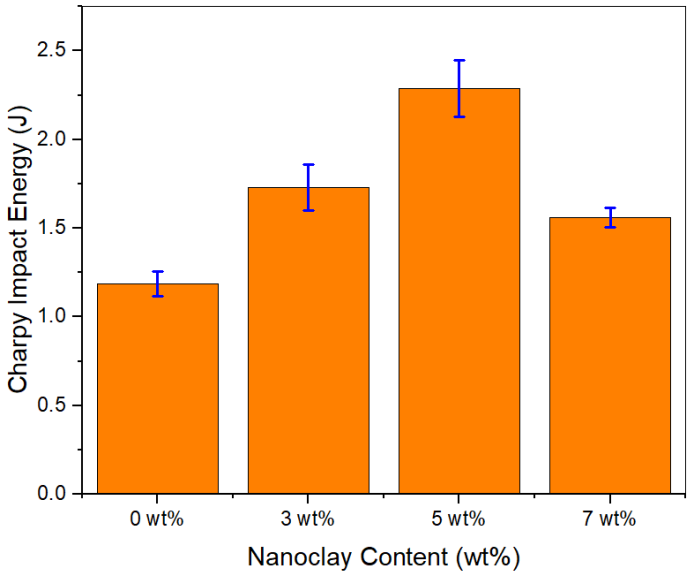

Figure 4.13 Charpy impact energy absorbed

Figure 4.13 shows that infusion of clay nanoparticles improved the energy absorption of the kenaf/nanoclay/PLA biocomposites. Infusion with 3 wt% clay nanoparticle content improved low velocity impact energy absorption by 45.7% whilst infusion with 5 wt% clay nanoparticle content improved the low velocity impact energy absorption by 92.9% and lastly, infusion with 7 wt% clay nanoparticle infusion improved the low velocity impact energy absorption by 31.4%. The improvement in the low velocity energy absorption capability was due to increase in the crystallinity level of the biocomposites and improved stress transfer capability for the hybrid biocomposites with clay nanoparticles. The crystallinity level for the neat kenaf/PLA hybrid biocomposite was 58.21% and addition of 3 wt%, 5 wt% and 7 wt% clay nanoparticles increased the crystallinity of the hybrid biocomposites by 12.5%, 18.3% and 18.1%, respectively. Hybrid biocomposites with 7 wt% clay nanoparticle content had a lower improvement than 5 wt% clay nanoparticle content due to agglomeration of clay nanoparticles at 7 wt%. The low velocity impact energy absorbed in this research work was comparable to the low velocity impact energy absorbed by kenaf/epoxy composites reported by Salman et al. (2015) who reported energy absorption ranging from 0.497 J to 0.895 J [289]. The results were also comparable to the energy absorbed by the glass fibre-reinforced epoxy composites with nano graphene reported by Erklig et al. (2017) who reported Charpy impact energy absorption ranging from 1.7 J (for the neat specimen) to 3.8 J for the composites with nano graphene [290].

The impact strength of the kenaf/nanoclay/PLA hybrid biocomposites determined using the ASTM standard is shown in Figure 4.14.

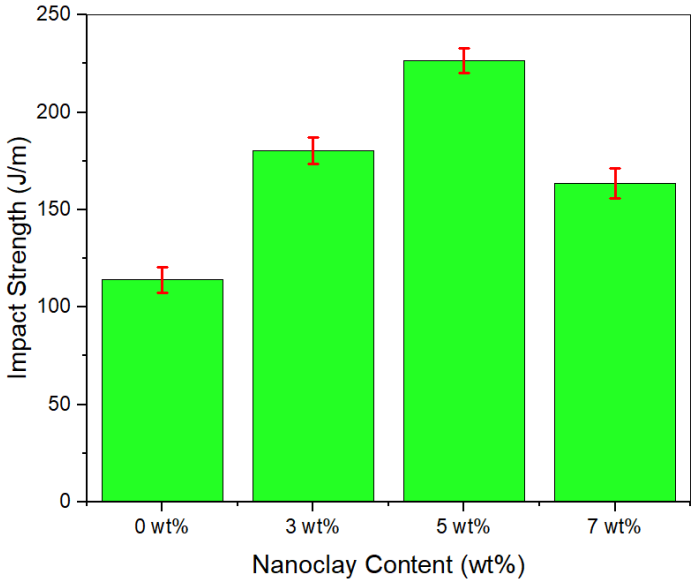

Figure 4.14 Impact strength according to ASTM standard

The low velocity impact strength of the biocomposites determined using the ASTM standard shows that the impact strength was ranging between 100 and 250 J/m. The hybrid biocomposites which had clay nanoparticles had a higher impact strength than the neat kenaf/PLA biocomposites. Addition of 3 wt% clay nanoparticle content resulted in 58.2% increase in impact strength, whilst addition of 5 wt% clay nanoparticle content resulted in 98.7% increase in impact strength and 7 wt% clay nanoparticle content resulted in 43.5% improvement in impact strength. The drop in improvement at the 7 wt% was due to clay agglomeration.

Figure 4.15 shows the impact strength of the kenaf/nanoclay/PLA hybrid biocomposites determined using the ISO 179 standard.

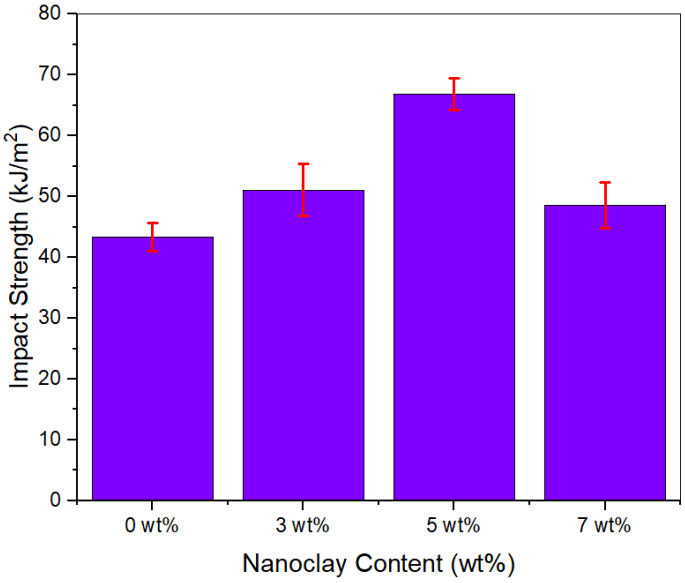

Figure 4.15 Impact strength according to ISO standard

Figure 4.15 shows that the low velocity impact strength of the biocomposites determined using the ISO standard ranged between 40 and 70 kJ/m^2. The hybrid biocomposites with clay nanoparticles had a higher impact strength than the neat kenaf/PLA biocomposites. Addition of 3 wt% clay nanoparticle content resulted in 17.7% increase in impact strength, whilst addition of 5 wt% clay nanoparticle content resulted in 54.1% increase in impact strength and 7 wt% clay nanoparticle content resulted in 11.9% increase in impact strength. The drop in impact resistance at 7 wt% clay nanoparticle content was due to agglomeration of the clay nanoparticles as observed on the SEM results.

The impact strength results obtained in this research work were comparable and in agreement with some of the published impact strength of biocomposites [239, 270, 280, 284, 287, 291-294]. The nanoparticles improve the impact properties of the biocomposites by improving the stress transfer efficiency of the biocomposites and by reducing the quantity of micro-voids in the composite material, improving the fibre to matrix bonding and improving other mechanical properties as discussed in the next chapters on published results.

4.5 Biocomposites' resistance to medium velocity impact

The results and discussion on the resistance of the biocomposites to medium velocity impact have been presented and discussed in the Journal of Applied Nanoscience (2021), volume 11, Issue 1, pages 441-443, in the paper titled, "The efficacy of nanoclay loading in the medium velocity impact resistance of kenaf/PLA biocomposites", by **Moyo Mufaro**, Kanny Krishnan and Velmurugan Raman and in Journal of Fibers and Polymers (2020), Volume 21, Issue 11,

pages 2642-2651, in the paper titled, “Performance of kenaf non-woven mat/PLA biocomposites under medium velocity impact”, by **Moyo Mufaro**, Kanny Krishnan and Velmurugan Raman. The next chapters present a summary of these papers.

4.6 Structure-property relationships

The structure-property relationships established using SEM, EDX, optical microscope and XRD were used in providing insights to the different observations made in this research. They provided scientific explanations to the mechanical properties, impact properties and other behaviour of the kenaf/nanoclay/PLA hybrid biocomposites observed in this research. The structure-property relationships were also presented and discussed in journal papers that have been published and a summary about the relationship is given in the next chapters.

4.7 Conclusion

This chapter presented and discussed the results that have not been published yet and a summary of the published results. Treatment with NaOH and clay nanoparticle improved the thermal stability and crystallinity of kenaf fibres because of the elimination of hemicellulose and lignin. Cross-sectional images revealed that NaOH alone attenuated the lumen size of the fibres and changed its shape whilst combined NaOH treatment followed by clay nanoparticle infusion almost completely diminished the fibre lumen and in some parts of the fibre the lumen completely vanished. These changes had a considerable influence on the mechanical properties of the resultant biocomposite materials. SEM and EDX mapping and elemental composition showed uniformly distributed elements even after infusion with clay nanoparticles. Incidences of clay nanoparticle agglomeration were, however, noticed at 7 wt% clay nanoparticle infusion and this adversely affects many mechanical properties.

The fabricated novel hybrid composites are very lightweight and have a positive buoyancy as they float in water. This shows that the hybrid biocomposites developed in this research are really potential sustainable and lightweight materials which could take the place of the non-sustainable conventional synthetic fibre-reinforced composites. Mechanical properties of the hybrid biocomposites improved with the addition of clay nanoparticles. Tensile strength and flexural strength increased by 19.1% and 9.8%, respectively, at 5 wt% clay nanoparticle loading. Young’s modulus and flexural modulus improved by 41.5% and 34%, respectively, at 5 wt% clay nanoparticle loading. The hybrid biocomposites’ thermal decomposition and dynamic mechanical properties improved with the addition of clay nanoparticles. However,

due to agglomeration effects, 7 wt% clay nanoparticle loading had lower basic mechanical properties than 5 wt% clay nanoparticle loading.

Impact properties kenaf/nanoclay/PLA hybrid biocomposites were also considerably improved by clay nanoparticles. Energy absorption at low velocity impact improved by 92.9% at 5 wt% clay nanoparticle loading. At 5 wt% clay nanoparticle loading. the low velocity impact strength determined using the ASTM increased by 98.7% and when determined using the ISO standard the low velocity impact strength increased by 54.1%. The resistance of the kenaf/nanoclay/PLA hybrid biocomposites to medium velocity impact was considerably improved by clay nanoparticle infusion. Detailed discussions on how the clay nanoparticles influenced the behaviour of kenaf/nanoclay/PLA hybrid biocomposites under medium velocity are presented in chapters 5 and 6. Like in the case of basic mechanical properties, impact properties were also adversely affected by clay nanoparticle agglomeration at 7 wt% clay nanoparticle loading.

The structure-property relationship showed that the combined treatment with NaOH and clay nanoparticles improved the microstructural properties of the kenaf/nanoclay/PLA hybrid biocomposites, reduced micro-voids, improved crystallinity, improved adhesion between the PLA and kenaf fibres and improved the stress transfer efficiency of the hybrid composites. The XRD analysis discussed in chapter 6 under published results showed there was intercalation and exfoliation of the clay nanoparticles. All these had a compounded effect of improving the basic mechanical properties and impact properties of the hybrid biocomposites.

Chapter 5 Medium velocity impact performance of kenaf/ PLA biocomposites

5.1 Introduction

This chapter is a summary of the journal paper titled "Performance of kenaf non-woven mat/PLA biocomposites under medium velocity impact", by **Moyo Mufaro**, Kanny Krishnan and Velmurugan Raman published in the Journal of Fibers and Polymers (2020), Volume 21, Issue 11, pages 2642-2651. The paper focused on characterising the performance of kenaf nonwoven fibre mat reinforced PLA biocomposites exposed to medium velocity impact loading conditions.

5.2 Objectives of the journal paper

The major objectives of this journal paper were to:

- fabricate layered kenaf/PLA biocomposites (without clay nanoparticles) that could resist projectile impact velocity in the medium velocity range.
- establish the perforation threshold of the biocomposites.
- determine the damaged areas for the biocomposites.
- determine the impact-induced damage mechanisms of the biocomposites.

5.3 Summary of the journal paper

Needle punched kenaf nonwoven fibre mats were used in the fabrication of single layered biocomposites and double layered biocomposites, respectively. Detailed discussion on the fabrication has been discussed in chapter 3 and also in the journal paper. Medium velocity impact testing was performed on a laboratory high speed gas gun as discussed in chapter 3 and in the journal paper. Impact velocities of 25 m/s, 35 m/s, 45 m/s, 65 m/s, 85 m/s and 100 m/s were used in this work. It was observed that increasing the nonwoven fibre mat aerial density improved the impact resistance. The reason being that an increase in fibre aerial density means there will be more constituent fibres in action against the projectile velocity. The perforation threshold for the biocomposites made kenaf nonwoven mats of aerial density 250 g/m^2 was found to be 26 m/s whilst for biocomposites made using kenaf nonwoven mats of aerial density 500 g/m^2 was established to be 37 m/s. This shows that doubling of kenaf fibre mat aerial density results in 42.3% improvement in the perforation threshold. These results were comparable to some of the glass fibre chopped strand mats or woven roving fabrics reinforced epoxy composites reported in literature [185]. Energy absorption behaviour was observed to improve with increase in impact velocity up to a certain critical impact velocity beyond which

the energy absorption capability started to drop progressively. The critical impact velocity was found to be 45 m/s for the biocomposites fabricated using kenaf nonwoven mats of aerial density 250 g/m^2 and 65 m/s for kenaf nonwoven mats of aerial density 500 g/m^2. The decline in energy absorption capability beyond the critical impact velocity is due to diminishing projectile-to-target specimens contact time resulting in parsimonious time for the target to satisfactorily undergo damage. Observations of similar nature were noted for some conventional fibre-reinforced polymer composites reported in literature [208, 212, 220].

Analysis of damage was done by grouping the damage into three zones as follows;

- Zone 1 representing damage behaviour below the perforation threshold limit and the critical impact velocity.
- Zone 2 representing the damage behaviour between the perforation threshold limit and the critical impact velocity.
- Zone 3 representing damage behaviour beyond the critical impact velocity.

Damage in zone 1 represented the damage behaviour when the projectile failed to penetrate (perforate) the biocomposites. Figure 5.1 shows images for zone 1 damages.

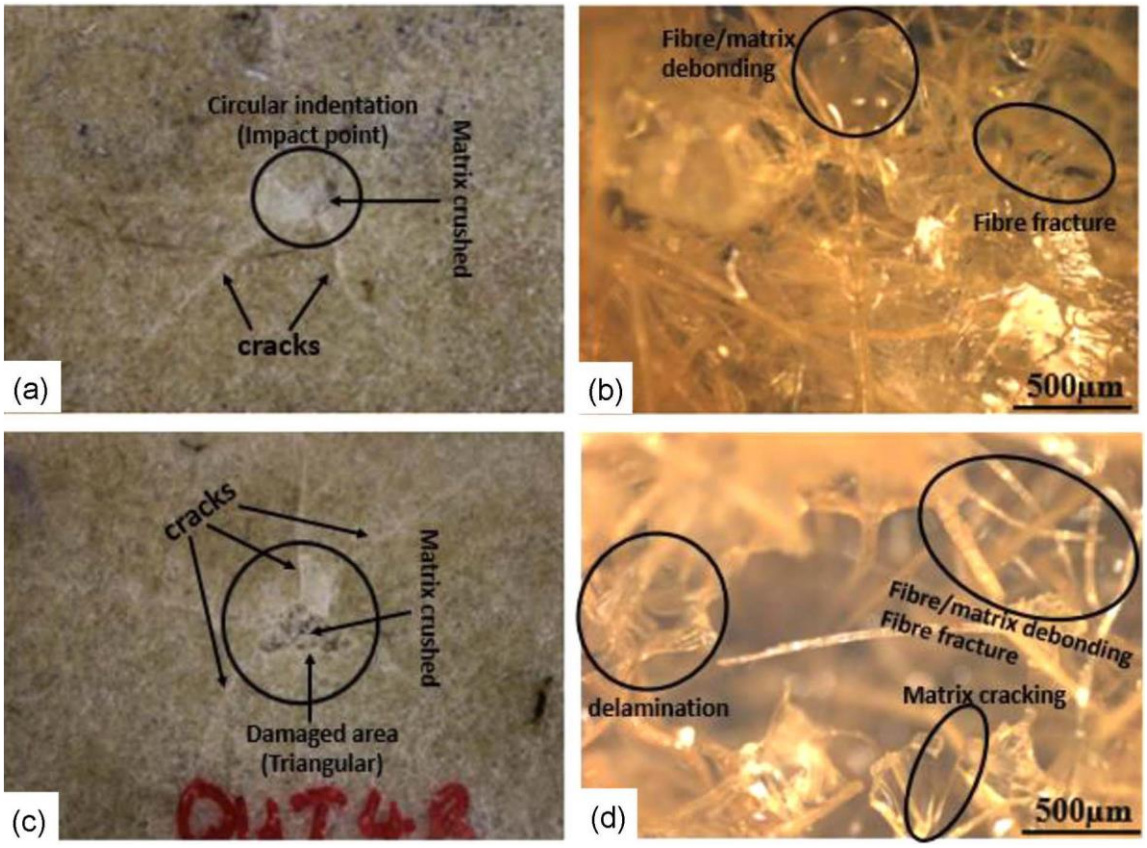

Figure 5.1 Zone 1 damages

Figure 5.1 (a) represents the impacted side image, (b) represents the impacted area microscopic image, (c) represents the back side image and (d) represents the back side microscopic image.

Damage in this zone was signified by circular indentations at the impacted spot and visible cracks as shown in Figure 5.1 (a). The back parts of the specimens were characterised by some cracks radiating from the centre part of the point impacted on the front side of the specimen. The main failure modes observed on the impacted biocomposite front side consisted of matrix crushing and cracking, fracture of fibres and fibre/matrix debonding as shown in Figure 5.1 (b). The leading failure modes on the back sides of the specimens consisted of matrix crushing and cracking, fractured fibre, delamination and fibre/matrix debonding as shown in Figure 5.1 (c) and (d).

Zone 2 represented damage response when the target specimens were completely penetrated by the projectile. The analysis in this zone focused on the back side of the biocomposite target specimen since the perforation geometry on the front side resembled the projectile size and shape. Figure 5.2 shows zone 2 damages.

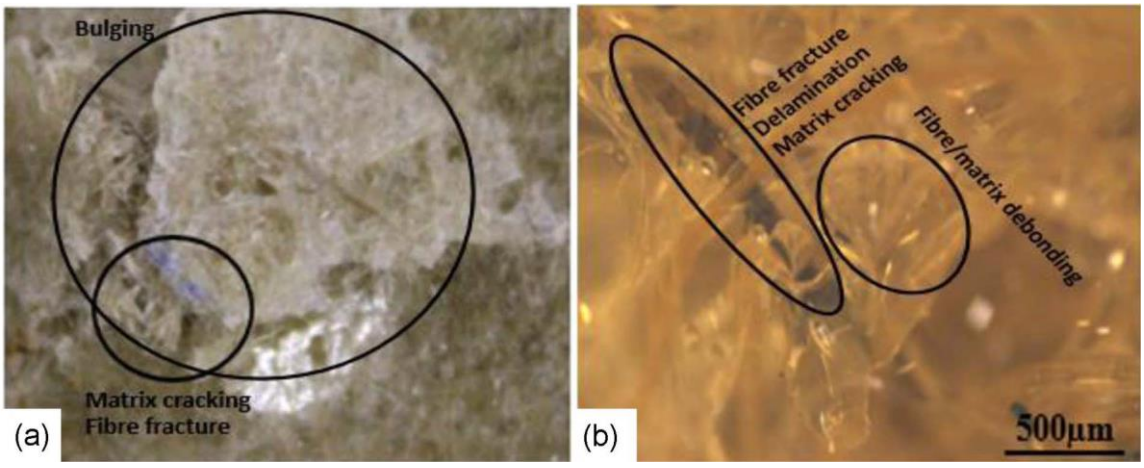

Figure 5.2 Zone 2 damages

Figure 5.2 (a) represents the back side image and (b) represents the back side microscopic image.

Major failure on the impacted side of the target specimens resulted from compression loading and shear stress. Analysis in this zone showed that the primary fibres and secondary fibres failed to contain the projectile velocity resulting in the target specimens being completely penetrated. There was cracking and bulging on the back side of the laminate. The bulges formed when the fibres and matrix got pushed to the back side when the projectile was wedging through the biocomposite thickness. During the moment of budging, shear plugging took place. Main mechanisms of damage observed in zone 2 included shear, crushing and cracking of the matrix,

fracturing of fibres, bulging (cone formation), fibre/matrix debonding, shear plugging and delamination as shown in Figure 5.2 (a) and (b).

In zone 3, the projectile completely penetrated the specimen like in zone 2 and the perforation geometry on the front side resembled the projectile size and shape. Therefore, like in zone 2, analysis of the damage behaviour of the biocomposites in zone 3 centred on the biocomposites' back sides. Figure 5.3 shows zone 3 damages.

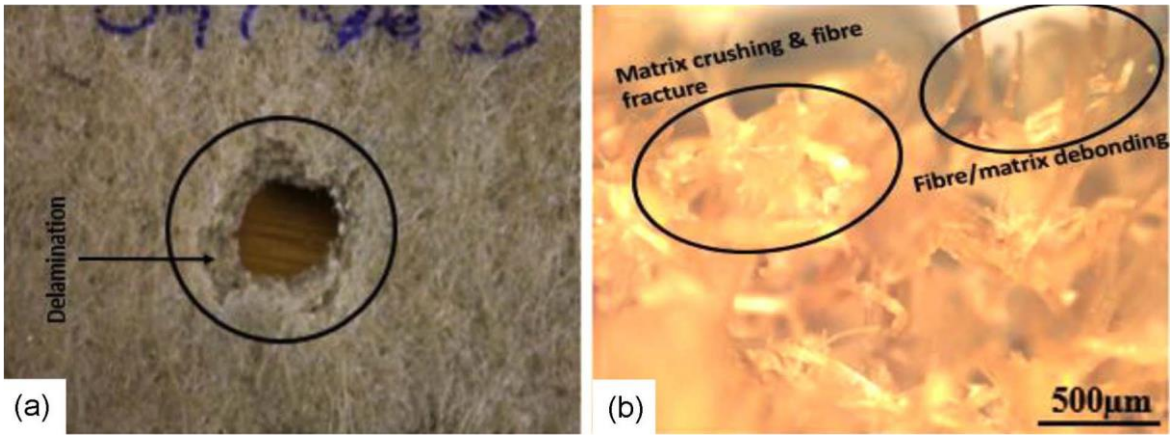

Figure 5.3 Zone 3 damages

Figure 5.3 (a) represents the back side image and (b) represents the back side microscopic image.

When the front sides were perforated, spallation occurred on the back side of the biocomposites for all the velocities in this zone. The damages observed in this zone shows that velocities beyond the critical impact velocity cause localised damage resulting in circular holes on the target biocomposite specimens as shown in Figure 5.3 (a). This occurred because the fibres were broken and then disconnected and ejected out of the biocomposite specimens. No incidences of bulging were observed in this zone like in zone 2. This was thought to be due to excessively high impact velocities resulting in short contact time for the biocomposite targets to experience satisfactory damage. In this zone, major failure mechanisms were matrix crushing, shear, fibre/matrix debonding, fibre fracture, delamination and interface debonding as shown in Figure 5.3 (a) and (b).

Largest damaged area was observed at the critical impact velocity after which the area damaged started to decrease progressively. The decrease in damaged area beyond the critical impact velocity was due to the impact velocities far much higher than the perforation threshold limit of the biocomposites which caused localised damage.

5.4 Conclusion

The perforation threshold limit for the kenaf nonwoven mat/PLA biocomposites was established to be about 26 m/s. This falls in the medium (intermediate) velocity impact range. Doubling the fibre content through doubling the aerial density increases the perforation threshold limit of the biocomposites with 42.3% to about 37 m/s. The doubling of fibre amount has an effect of doubling the capability of the biocomposites to contain the projectile energy. Comparison of the biocomposites' impact resistance at the perforation threshold limit showed that doubling of fibre amount improved the biocomposites' resistance to impact velocity by 27.6%. The biocomposites' resistance to damage when under medium velocity impact was also improved when the fibre content was increased. The improvements in impact behaviour properties were observed to increase up to the critical impact velocity level beyond which the properties started to progressively drop in value. The damage was observed to be localised at the velocities beyond the critical impact velocity. The damage mechanisms were noticed to be identical to those of conventional SFRPCs. The main mechanisms of damage observed were matrix crushing and cracking, fibre fracture, shear, debonding of fibre and matrix and interface debonding, delamination, bulging and shear plugging. Since the kenaf nonwoven mat PLA biocomposites' resistance to high speed projectiles was discovered to be in the medium velocity impact range, they can potentially protect against objects possessing medium velocity. Therefore, they could be ideal for replacing SFRPCs in cushioning against secondary blasts and debris.

Chapter 6 Impact performance of kenaf/nanoclay/PLA hybrid biocomposites

6.1 Introduction

This chapter is a summary of the journal paper titled "The efficacy of nanoclay loading in the medium velocity impact resistance of kenaf/PLA biocomposites", by **Moyo Mufaro**, Kanny Krishnan and Velmurugan Raman published in the Journal of Applied Nanoscience (2021), volume 11, Issue 1, pages 441-443. This paper focused on enhancing the performance of kenaf/PLA bionanocomposites by hybridising with clay nanoparticles.

6.2 Objectives of the journal paper

The major objectives of this journal paper were to:

- fabricate novel kenaf/nanoclay/PLA hybrid bionanocomposites that could resist medium velocity impact resistance.
- investigate the efficacy of different clay nanoparticle contents in enhancing the resistance of the bionanocomposites to medium velocity impact.
- establish the perforation threshold limit for hybrid bionanocomposites with different clay nanoparticle content.
- determine the optimum clay nanoparticle content.
- determine the interfacial bonding and microstructure characteristics of the hybrid bionanocomposites.

6.3 Summary on bionanocomposites' resistance to medium velocity impact

The PLA resin, clay nanoparticle dispersion and kenaf/nanoclay/PLA hybrid biocomposites were fabricated as discussed in chapter 3 and as presented in the journal paper. The clay nanoparticle contents were 0, 3, 5 and 7 wt%. The laboratory gas gun was used in testing the medium velocity impact resistance of the hybrid biocomposites. Impact velocities of 25 m/s, 35 m/s, 45 m/s, 65 m/s, 85 m/s and 100 m/s were used in this work.

The results showed that the capability of the hybrid biocomposites to reduce the exit velocity of the projectile increased with the addition of clay nanoparticles as shown in Figure 6.1.

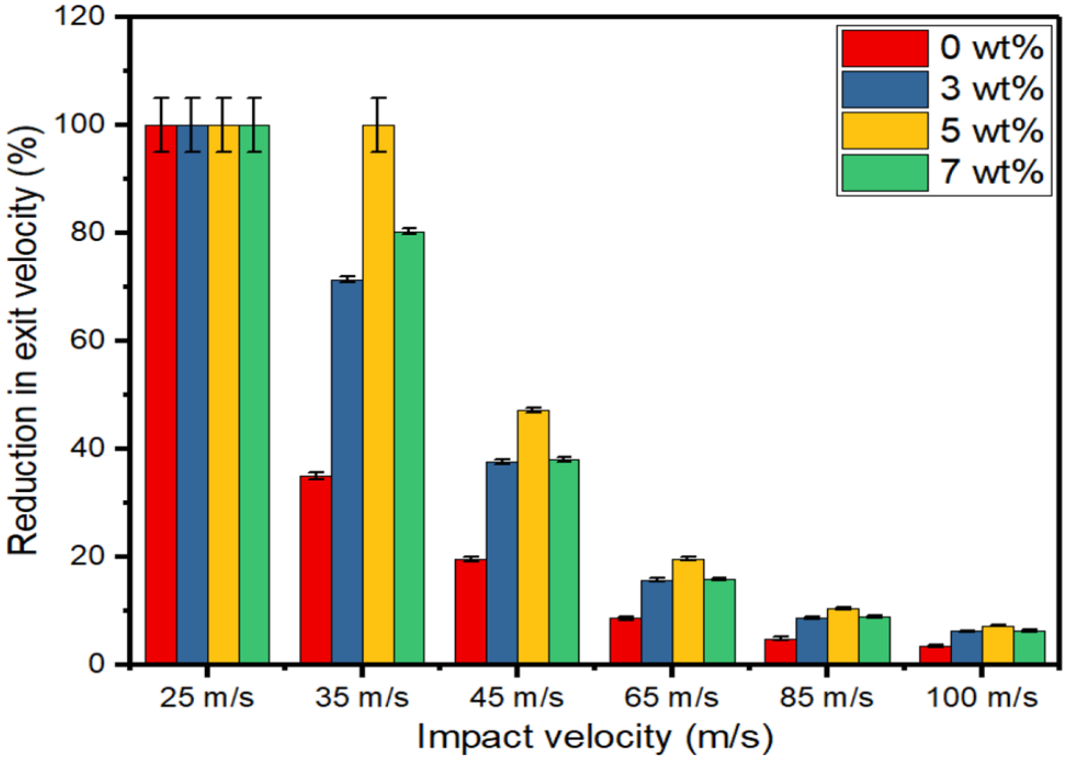

Figure 6.1 Effects of nanoclay on projectile exit velocity

However, as shown in Figure 6.1, a drop was noticed at 7 wt% clay nanoparticle content caused by the agglomeration effects of the clay nanoparticles.

Figure 6.2 shows the perforation threshold velocities for the biocomposites.

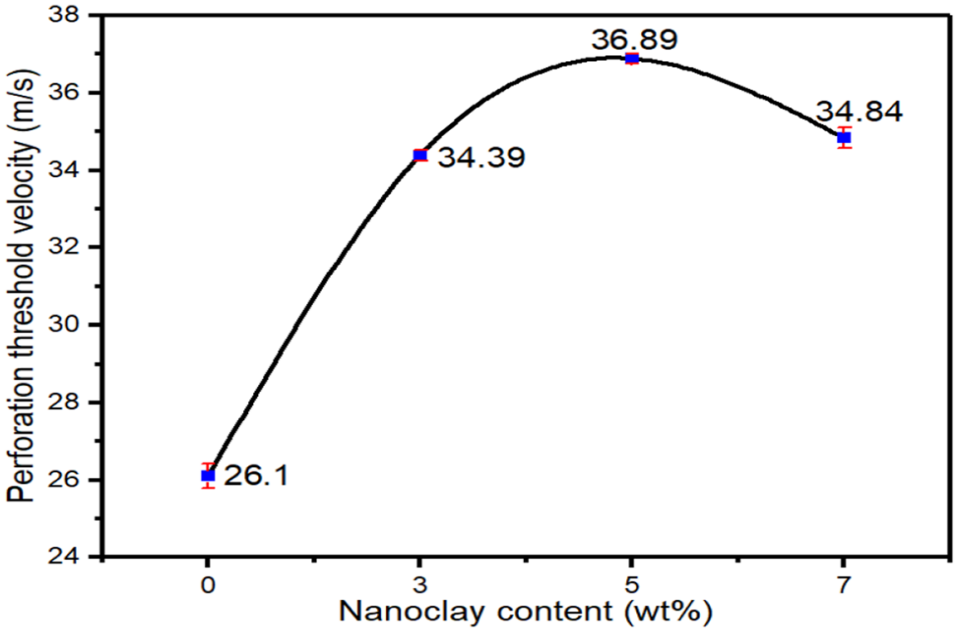

Figure 6.2 Perforation threshold velocities

Figure 6.2 shows that the perforation threshold velocities improved from 26 m/s for the neat biocomposite to 34 m/s for the hybrid biocomposite with 3 wt% clay nanoparticle content, 37 m/s for the hybrid biocomposite with 5 wt% clay nanoparticle content and 35 m/s for the hybrid biocomposite with 7 wt% clay nanoparticle content. This shows that addition of clay nanoparticles enhanced the perforation threshold limit of the hybrid bionanocomposites by 32.3, 41.9 and 33.8% for 3, 5 and 7 wt% clay nanoparticle loading, respectively. The critical impact velocity for hybrid biocomposites infused with 3 wt% and 7 wt% clay nanoparticle content was found to be 45 m/s and for hybrid bionanocomposites loaded with 5 wt% clay was found to be 65 m/s.

Figure 6.3 shows the effects of nanoclay on energy absorbed.

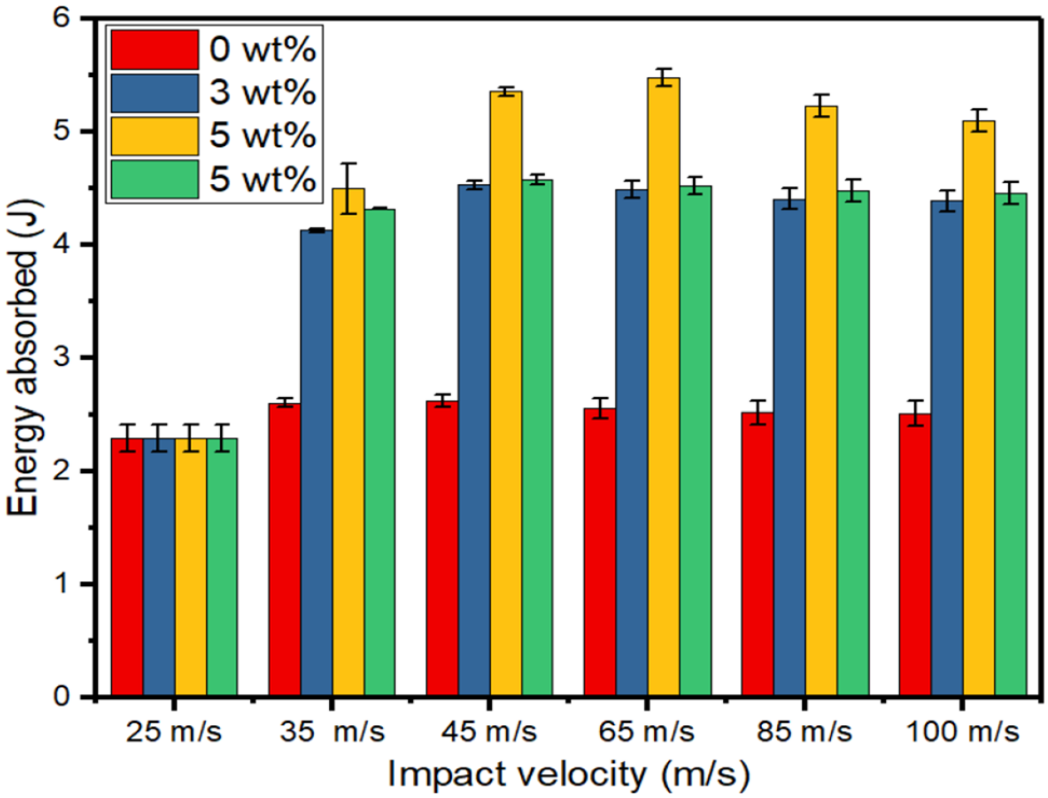

Figure 6.3 Effects of nanoclay on energy absorbed

The energy absorption abilities of the bionanocomposites was improved by 72.8%, 109%, and 74.5% for loading with clay nanoparticle of 3, 5 and 7 wt%, respectively. Figure 6.3 shows that that highest energy was absorbed at impact velocity of 45 m/s for biocomposites infused with 0, 3 and 7 wt% nanoclay content and 65 m/s for biocomposites infused with 5 wt% nanoclay content. The diminishing capacity to absorb energy at higher velocities was thought to be due

to significant reduction in the projectile-to-biocomposite contact time culminating in a parsimonious time for the biocomposites to amply absorb the projectile energy.

Figure 6.4 shows the damaged area experienced by the biocomposites at different impact velocities.

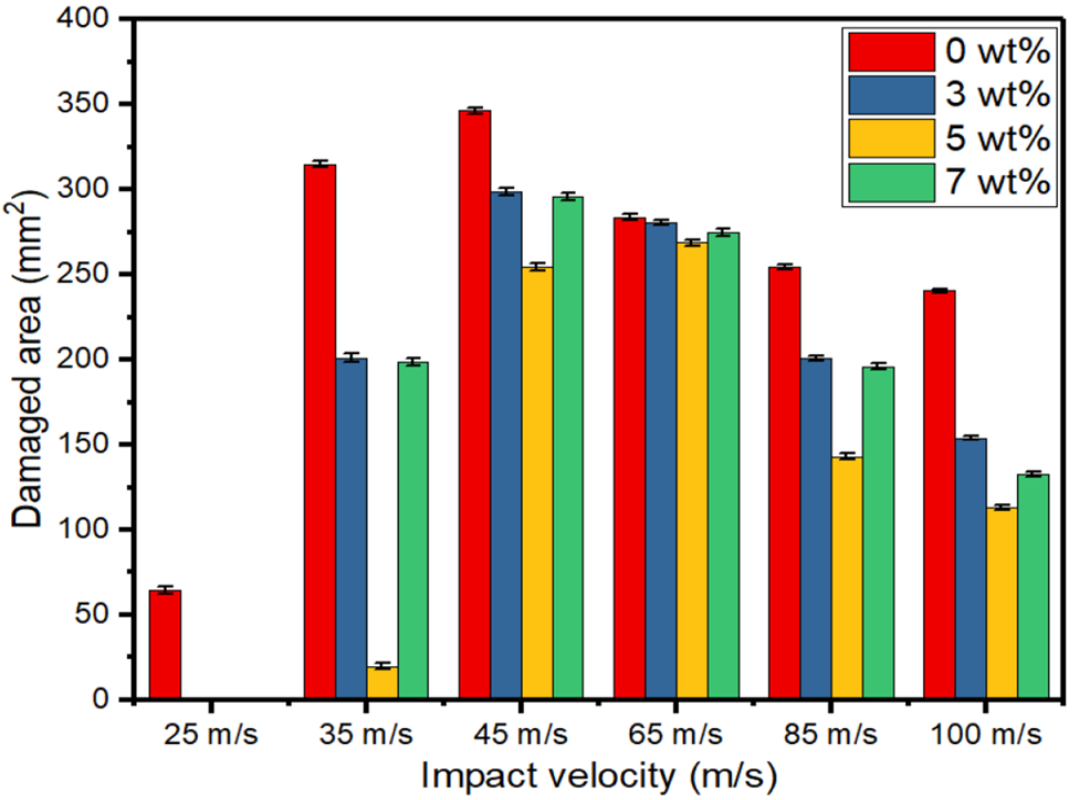

Figure 6.4 Damage resistance of the biocomposites

In terms of damage response, the damaged area reduced by 13.8%, 26.5% and 14.7% for the hybrid bionanocomposites loaded with 3 wt%, 5 wt% and 7 wt% clay nanoparticle content, respectively. As shown in Figure 6.4, damaged area on biocomposites relatively enlarged as impact velocity was raised up to a level marginally above the threshold velocity beyond which damaged area began to shrink. This implies that greatest damage is experienced at the velocity marginally above the threshold velocity. Therefore, the clay nanoparticles enhanced the bionanocomposites' resistance to damage. The damage beyond the critical impact velocity became localised. This observation was consistent with published literature [189, 193].

6.4 Summary on microstructural analysis of the hybrid biocomposites

The analysis of microstructural properties of the kenaf/nanoclay/PLA hybrid bionanocomposites was used in providing explanations to the various mechanical properties

and impact characteristics observed in this research work. Table 6.1 shows SEM–EDX mapping results, elemental composition and distribution of the biocomposites.

Table 6.1 Biocomposites SEM–EDX mapping, elemental composition and distribution

Specimen	Major Elements	**Maps** (Magnification: 1500X) 1mm Carbon	Oxygen	Silicon	Aluminum
0 wt%	C O	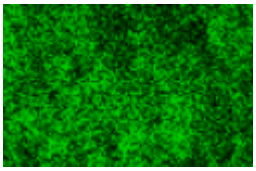	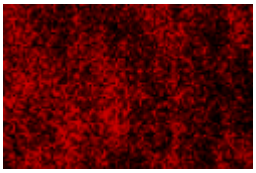	nil	nil
3 wt%	C O Si Al	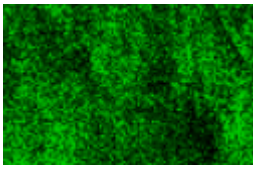	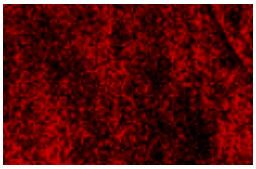	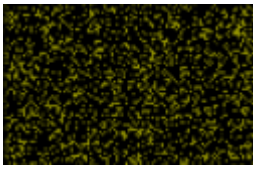	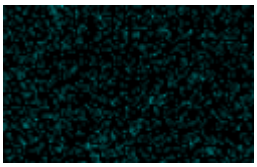
5 wt%	C O Si Al	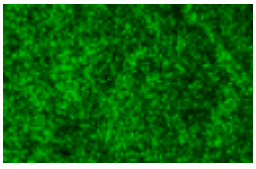	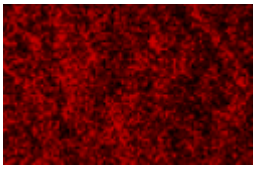	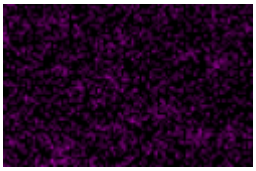	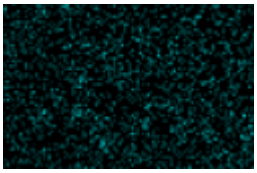
7 wt%	C O Si Al	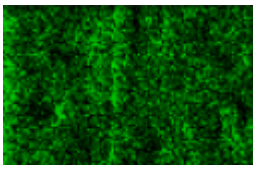	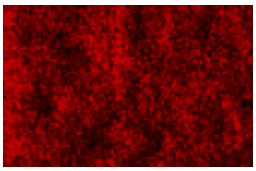	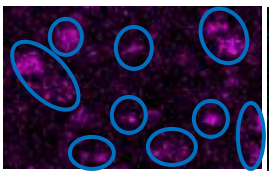	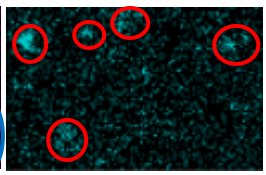

The SEM results showed a homogenous smooth surface morphology of the biocomposites, before infusion and after infusion with clay nanoparticles. This meant that there was effective interfacial bonding among PLA, kenaf fibres and clay nanoparticles. Also, the EDX results on Table 6.1 show carbon and oxygen as the major elements in the neat kenaf/PLA biocomposites. In addition to carbon and oxygen elements, silicon and aluminium elements were detected in all the kenaf/PLA biocomposites infused with clay nanoparticles. The silicon and aluminium elements were from the MMT nanoclays. The elemental maps show that all the elements were uniformly distributed in all cases. Uniform distribution of the silicon and aluminium elements in the nanoclay-infused biocomposites shows good dispersion of the nanoclays. However, incidences of nanoparticle agglomeration were observed at 7 wt% nanoclay content. The mapping shows that the silica nanoparticles were more agglomerated than the alumina nanoparticles. This was thought to be due to the inherently larger quantity of silica nanoparticles than alumina nanoparticles in the MMT clay nanoparticles used in this study.

Microstructural differences were observed under cross-sectional view as shown in Table 6.2.

Table 6.2 Microstructural properties of the biocomposites

Sample	**Microstructure** (Magnification: 1000X)	
	Surface 1mm	**Cross-sectional** 1mm
0 wt%	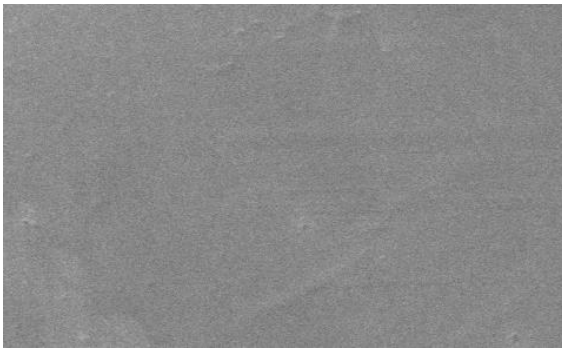	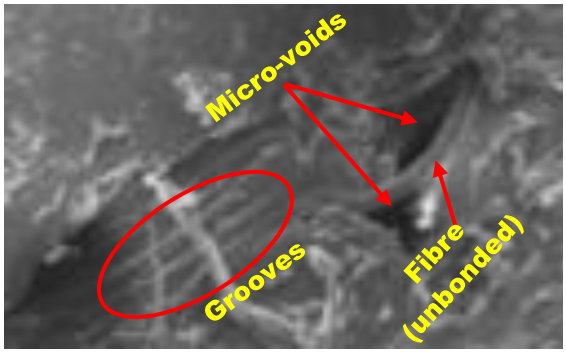
3 wt%	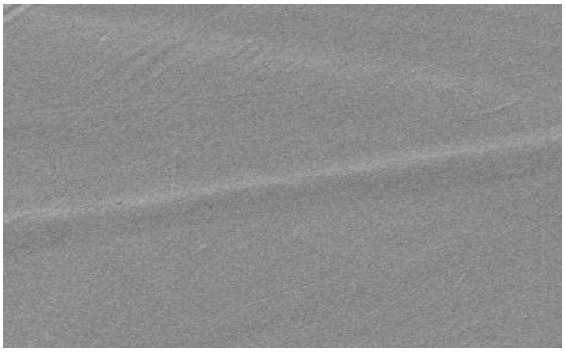	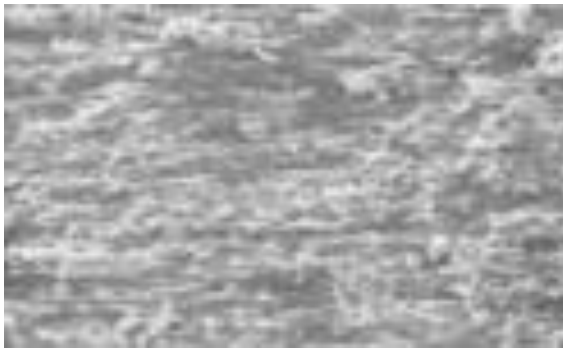
5 wt%	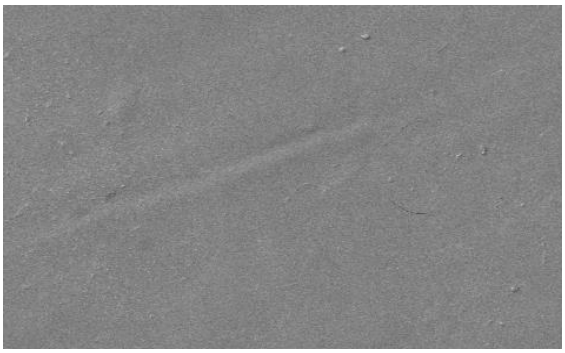	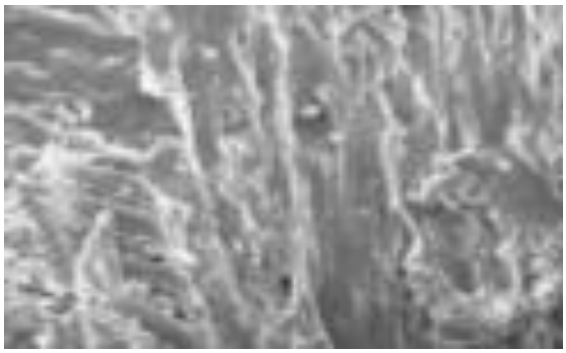
7 wt%	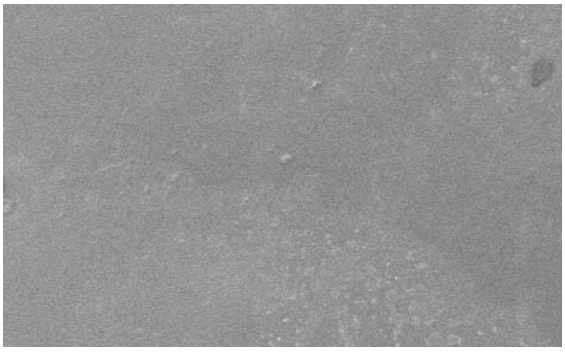	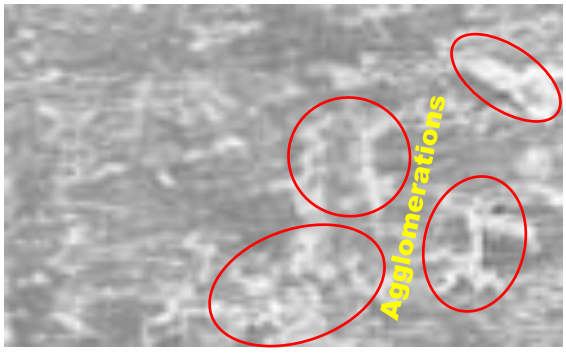

Table 6.2 shows that the control kenaf/PLA biocomposites' cross-section had some areas with micro-voids, completely unbonded and partially fibres and grooved sections. These were a reflection of poor or insufficient PLA to kenaf fibre adhesion. As a result, the mechanical properties of the control kenaf/PLA biocomposites were adversely affected because of insufficient filler to matrix bonding. The micro-voids were thought to be due to air entrapped during the stage of composite fabrication. Kenaf fibres in the sections with micro-voids were insufficiently wetted by the PLA matrix causing partial bonding and fibre portions not bonded at all as observed under SEM cross-section structure. The grooves showed striations of fibres insufficiently wetted or bonded by the PLA matrix. Table 6.2 shows that the cross-sectional structures at 3 wt% and 5 wt% clay nanoparticle content showed micro-voids free homogeneous structures. This shows that the clay nanoparticles sealed the sections with micro-voids and promoted very strong bonding between the kenaf fibres with the PLA resin. It was thought that as the clay nanoparticles move to occupy the sections with micro-voids, they also transport the PLA resin. This phenomenon can be validated using the kenaf fibre infused with clay nanoparticles SEM results discussed in chapter 4. The results showed a significant decrease in the kenaf fibre lumen structure which suggested that the clay nanoparticles were carried by the medium from the fibre surface to the lumen. When the clay nanoparticles eventually occupy the micro-void parts, some of the PLA resin carried by the nanoparticles wets the surrounding kenaf fibres. This promotes adequate wetting of the kenaf fibres so that all fibres in the area get wetted. This has a great effect of significantly improving the bonding between the PLA resin and the kenaf fibres resulting in the improvement of the hybrid bionanocomposites' properties. Though there were no micro-voids at the 7 wt% clay nanoparticle content, the microstructure showed some clustering of clay nanoparticles which was a sign of clay nanoparticle agglomeration as shown in Table 6.2. Insufficient wetting of clay nanoparticles and kenaf fibres occurs when there is agglomeration resulting in poor bonding between the PLA matrix and reinforcing kenaf fibre and nanoclay. Therefore, the kenaf fibre to PLA resin adhesion was reduced with a subsequent impact of reducing the mechanical and impact properties of the hybrid biocomposites.

Figure 6.5 shows XRD spectra of the neat and nanoclay-infused kenaf/PLA biocomposites.

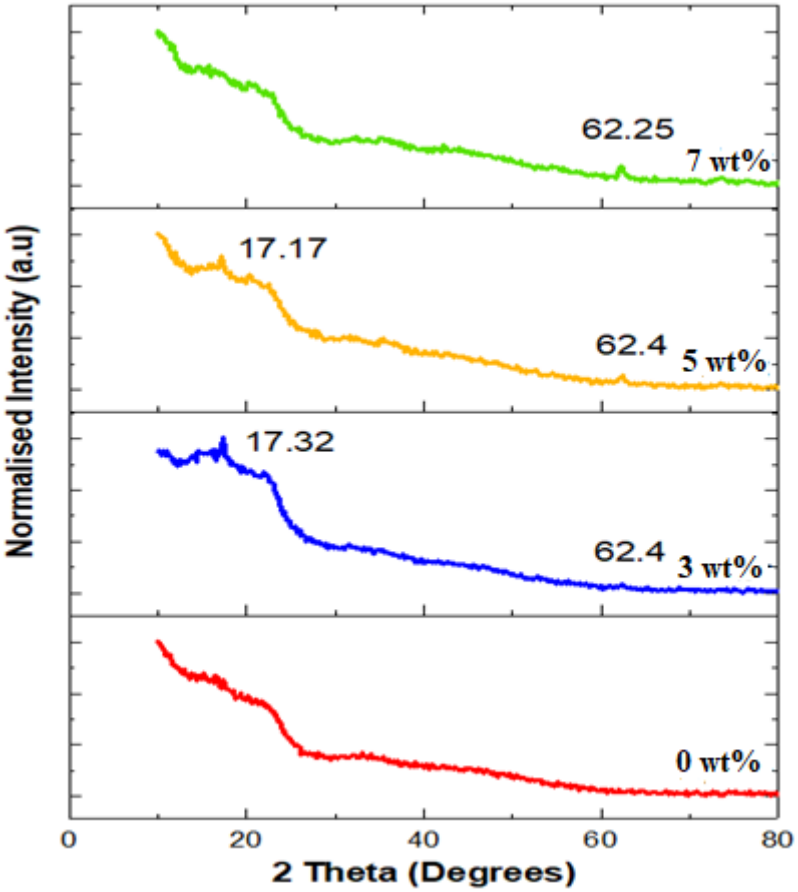

Figure 6.5 XRD pattern of the biocomposites

Figure 6.5 shows that there were no major crystalline peaks for the control kenaf/PLA biocomposites (0 wt% nanoclay content) indicating the highly amorphous nature of the kenaf/PLA biocomposites. This was attributed to the intrinsically amorphous nature of both kenaf fibres and PLA. The unavailability of characteristic peaks for PLA matrix and kenaf on the neat biocomposites is a demonstration that the characteristic peaks of PLA and kenaf fibres were disrupted during the process of forming the biocomposites. This means a good interaction between the kenaf and PLA resin leading to good interface bonding between the two. The hybrid bionanocomposites infused with clay nanoparticles had diffraction peaks showing that the addition of clay nanoparticles enhanced the crystallinity of the bionanocomposites when they get deposited into the phase structure of the hybrid bionanocomposites. The observed peaks were not characteristic of the peaks of pure MMT clay nanoparticle indicating that the layered structure of the clay nanoparticles was disrupted by the PLA resin causing a disappearance of the Bragg peak of the clay nanoparticles. This means that there was exfoliation. Literature also reported similar findings where the disappearance of peaks was attributed to separation of clay nanoparticle layers and exfoliation whilst the unavailability of

characteristic peaks for clay nanoparticles meant intercalation of the clay nanoparticles during the polymerisation process of the PLA resin [235]. The identity of the peaks affiliated with amorphous silica (SiO2) nanoparticles and silica-alumina structure from the clay nanoparticles was supported by literature [295-299]. The inter-gallery spacing between the clay nanoparticles and the respective hybrid bionanocomposites increased to 15.1 Å from 11.7 Å inter-gallery spacing of pure MMT clay nanoparticles. This meant intercalation of the PLA molecules into the inter-gallery clay nanoparticles as they percolate into the platelets of the clay nanoparticles resulting in the expansion of their basal plane spacing. This leads to the formation of an intercalated morphological structure and good interface bonding between the PLA matrix (resin) and the fillers. The XRD patterns obtained in this work are comparable to the XRD patterns for clay nanoparticle infused GFRPCs reported by Mohan et al. (2015) [229].

There were minimal variations in the peak angles and the inter-gallery spacing for observed peaks. This meant the extent of intercalation was not different for all the hybrid bionanocomposites infused with clay nanoparticles supported by the relatively similar intercalation figures. These observations meant the degree of penetration of the PLA molecules into the inter-gallery of the clay nanoparticle platelets did not change with the variation in the clay nanoparticle content. This was attributed to the constant quantity of PLA matrix applied during the bionanocomposites fabrication with only the quantity of clay nanoparticle content being varied. However, the peak intensity values increased with increase in the clay nanoparticle content indicating improved order, crystallisation level and arrangement. The crystallinity index determined from the XRD results showed an improved crystallinity index of the hybrid bionanocomposites with the addition of clay nanoparticles. The crystallinity improved from about 58% to 69%. Addition of 3 wt%, 5 wt% and 7 wt% clay nanoparticle loading content enhanced the crystallinity of the hybrid bionanocomposites by 12.5%, 15.5% and 15.3%, respectively. A slight drop in crystallinity at 7 wt% clay nanoparticle content compared to that acquired using 5 wt% clay nanoparticle loading content was due to clay nanoparticle agglomeration.

6.5 Summary on crack width

Crack width analysis was done to ascertain the impact of clay nanoparticles on kenaf/PLA biocomposites and kenaf/nanoclay/PLA hybrid bionanocomposites. The results showed a progressive decrease in crack width as the clay nanoparticle content increased. The neat

kenaf/PLA biocomposites (0 wt% clay content) sustained longer cracks than the kenaf/nanoclay/PLA hybrid biocomposites. Addition of 3 wt%, 5 wt% and 7 wt% clay nanoparticle content improved resistance to crack width propagation by 9.5%, 27.7% and 28.9%, respectively. This indicates that the clay nanoparticles play a role of load transfer thereby preventing the propagation of cracks. This can suggest that clay nanoparticles reduce crack propagation during low velocity and high velocity impact loading conditions. The nature of damages observed in this work in the medium velocity impact is in agreement with this notion. Also, there are some published studies which reported that nanoparticles prevented crack growth and delamination [104, 187, 192].

6.6 Conclusion

Novel hybrid bionanocomposites with improved impact properties were developed. Infusion with clay nanoparticles considerably improved the resistance of the hybrid bionanocomposites as exhibited by improvement in many of the parameters used in defining resistance to impact loading. Optimum improvements were achieved with 5 wt% clay nanoparticle content. The perforation threshold limit was enhanced by 41.9%, energy absorption ability was improved by 109%, damage resistance improved by 26.5% and resistance to crack propagation increased by 28.9%. The positive effects were a result of improved crystallinity, microstructural characteristics, improved bonding efficiency among the materials used to fabricate the bionanocomposites, enhanced stress transfer nanoclay network structure, exfoliation and intercalation of clay nanoparticles. The study revealed that inclusion of clay nanoparticles enhances the impact resistance of kenaf/PLA bionanocomposites in the medium velocity impact range. This means the bionanocomposites have a potential to protect against objects in the medium velocity range. Therefore, they could be ideal alternatives to the non-biodegradable conventional composites in protecting against secondary blasts or debris.

Chapter 7 Thermo-mechanical properties of the biocomposites

7.1 Introduction

This chapter summarises the thermo-mechanical properties of the kenaf/nanoclay/PLA hybrid biocomposites published in Materials Today: Proceedings Journal (2020), Volume 38, Part 2, 2021, Pages 609-613, in the paper titled, "Thermo-mechanical response of kenaf/PLA biocomposites to clay nanoparticles infusion", by **Moyo Mufaro**, Kanny Krishnan, Mohan T.P. The other publication is in the South African Journal of Science and Technology (2022), Volume 40 Issue 1, pages 137-141, in the paper titled, "Effects of combined alkali treatment and clay nanoparticle infusion on thermo-mechanical response of kenaf/PLA biocomposites", by **Moyo Mufaro**, Kanny Krishnan, Mohan T.P. The papers focus on the effects of alkalization treatment, clay nanoparticle infusion and combined NaOH and nanoclay infusion on the thermal and mechanical properties of kenaf/PLA bionanocomposites.

7.2 Summary on the effects of treatments on thermal decomposition

The TGA results showed that the biocomposites made using NaOH treated kenaf fibres and clay nanoparticle-doped PLA matrix exhibited more residual mass than the biocomposites made using untreated kenaf fibres as shown in Figure 7.1.

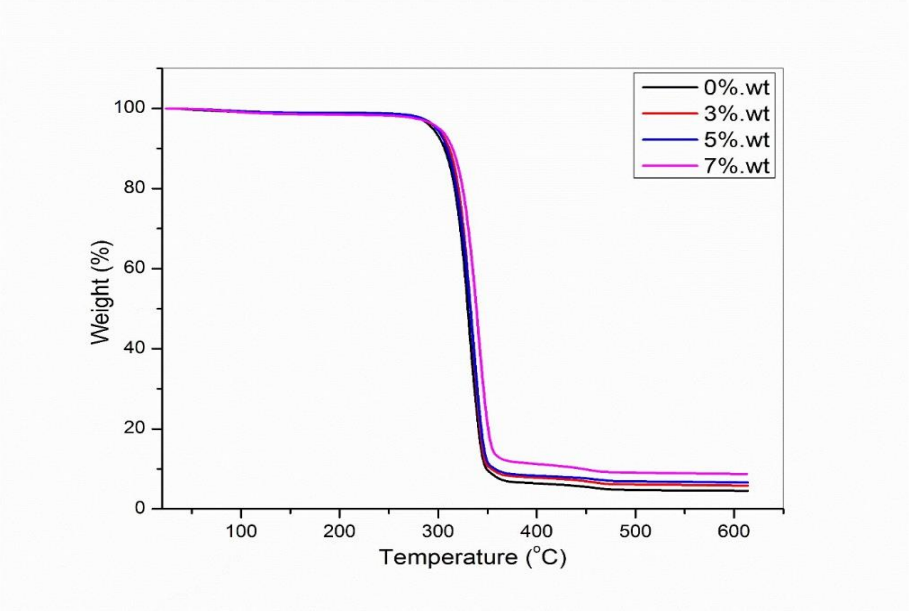

Figure 7.1 TGA of the biocomposites

Figure 7.1 shows all the biocomposites' initial mass loss at 100 ºC followed by a single stage decomposition and remaining inorganic components after the major decomposition. Mass loss

around 100 ^{o}C indicates loss of moisture and volatiles from the biocomposites. Figure 7.1 shows that at 600 ^{o}C the residual mass improved with increase in clay nanoparticle loading.

Figure 7.2 shows the DTG thermogram for the biocomposites.

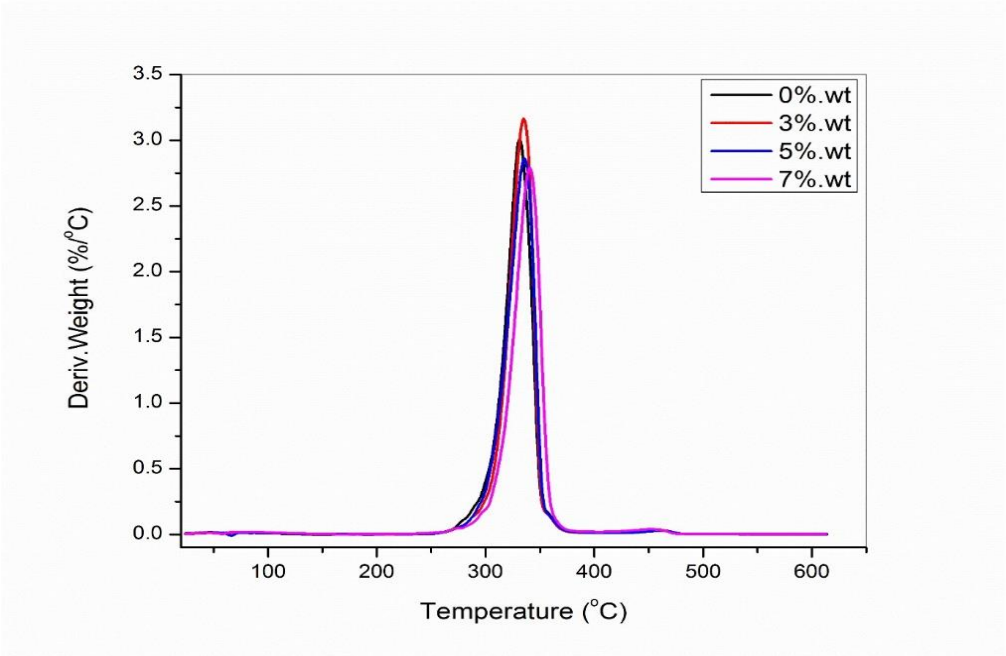

Figure 7.2 DTG Thermogram for the biocomposites

Figure 7.2 shows that the peak thermal decomposition temperatures of the biocomposites fabricated using treated kenaf fibres moved to elevated temperatures which indicates an improvement in the thermal stability.

The onset and peak thermal decomposition temperatures increased when combined treatment using NaOH and nanoclay was used. Treatment with NaOH alone resulted in 0.4% increase in the onset thermal decomposition temperature. Table 7.1 shows a summary of the stages involved in the thermal decomposition process of biocomposites infused with clay nanoparticles alone.

Table 7.1 Temperatures and mass loss for thermal decomposition of the biocomposites

Nanoclay Content	**Process temperature (°C)**			**Mass Loss (wt.%) @ 377°C**	**Mass Loss (wt.%) @ 600°C**
	Onset	**Peak**	**End**		
0 wt%	267	331	377	93.26	95.43
3 wt%	269	335	377	91.82	94.12
5 wt%	270	336	377	91.32	93.35
7 wt%	274	341	377	88.22	91.23

Table 7.1 shows that infusion of the biocomposites with clay nanoparticles alone of 3, 5, and 7 wt% content increased the onset thermal decomposition temperature by 0.75, 1.12 and 2.62%, respectively. In the case of combined NaOH treatment with 5 wt% and 7 wt% clay nanoparticle content, the improvement in onset decomposition temperatures was 0.7% and 1.5%, respectively. Treatment with NaOH alone resulted in 2.7% increase in the peak thermal decomposition temperature whilst infusion of the biocomposites with clay nanoparticles alone of 3, 5, and 7 %wt content increased the peak decomposition temperature of the bionanocomposites by 1.21%, 1.51% and 3.02%, respectively. The peak decomposition temperature for combined NaOH treatment with 5 wt% and 7 wt% clay nanoparticle loading increased by 1.8% and 2.1%, respectively. Treatment with NaOH alone resulted in 0.3% improvement in residual mass at 377 ^{o}C whilst infusion of the bionanocomposites with clay nanoparticles alone of content 3, 5, and 7 %wt improved the residual mass at 377 ^{o}C by 1.5%, 2.1% and 5.4%, respectively. In the case of combined NaOH treatment with 5 wt% and 7 wt% clay nanoparticle content, the residual mass at 377 ^{o}C improved by 3.3% and 5.4%, respectively. The results show that the treatments enhanced the thermal stability of the hybrid bionanocomposites. In the case of clay nanoparticle infusion alone, it was observed that there were minimal thermal decomposition variations between the bionanocomposites infused with clay nanoparticle content of 3 wt% and 5 wt%. As a result, when comparing with the combined treatment, only 5 wt% and 7 wt% were used.

The results demonstrated that the improvements in the thermal decomposition behaviour brought about by combined treatments were better than single method treatments. Comparing with some published studies in literature, acetylation treatment culminated in mass loss of above 95% [300] whilst in this research work, combined treatment curtailed mass loss to 91%. The improvement in the thermal stability of the biocomposites was attributed to improved crystallinity index brought about by the NaOH treatment and clay nanoparticles' thermal barrier impact. As mentioned in chapter 4, the removal of the hemicellulose component done by treatment with NaOH enhances fibre crystallinity. On the other hand, the clay nanoparticles' thermal barrier impact diminishes the heat transfer efficiency of the kenaf/PLA bionanocomposite system thereby reducing the rate at which heat transfers to the kenaf fibres and the PLA. This has an impact on delayed onset thermal decomposition temperature which raises the peak thermal decomposition temperature. This is in agreement with some published studies [99]. There were no noticeable changes on the end thermal decomposition temperature of the kenaf/PLA bionanocomposites.

7.3 Summary on the effects of treatments on storage modulus of the biocomposites

Treatments altered the storage and loss modulus as well as the damping (tandelta) properties of the bionanocomposites. Treatment with NaOH alone improved the storage modulus of the biocomposites by 2% and this was attributed to the better crystallinity in the treated kenaf fibres than that of the untreated kenaf fibres. Figure 7.3 shows the storage modulus of the biocomposites with clay nanoparticles only.

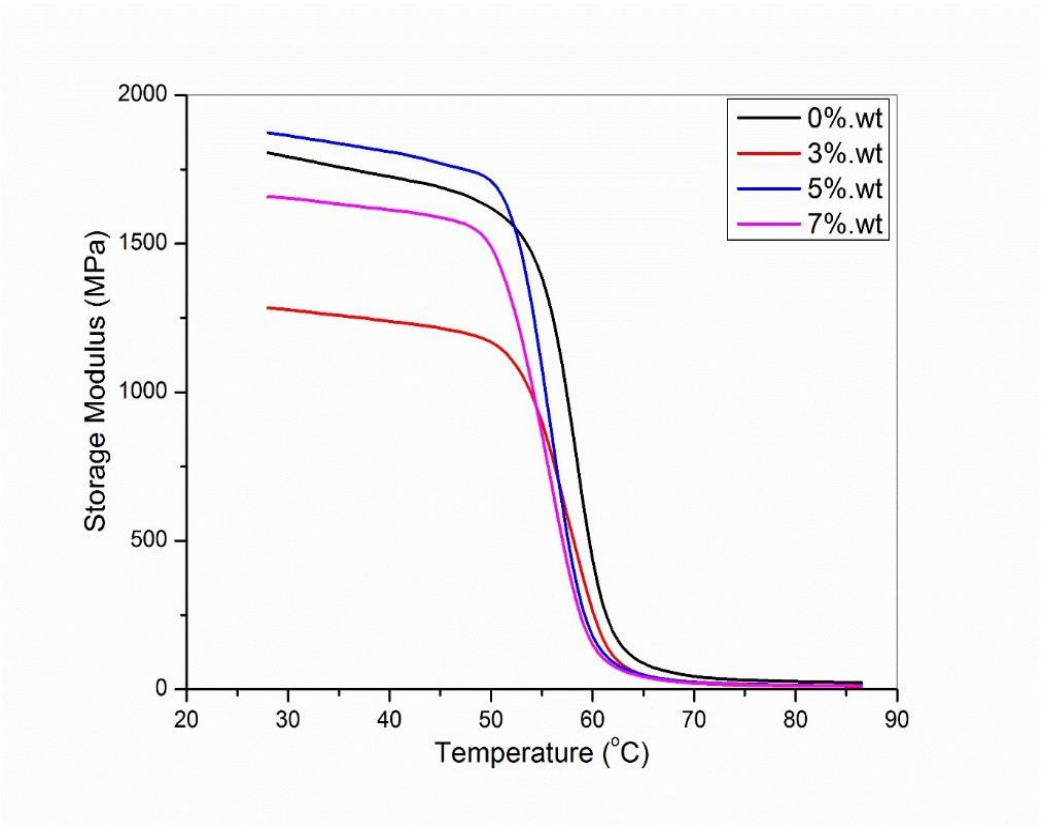

Figure 7.3 Storage modulus of the biocomposites

In the case of the biocomposites infused with clay nanoparticles alone, an initial decrease in storage modulus was observed when 3 wt% clay nanoparticle content were added. A similar observation was made on nanoparticle infused hybrid shape memory composites made using epoxy matrix [301]. The other explanation given in literature is about the relaxation affiliated with the glass to rubber transition of amorphous polymer [302]. Similar observation was observed in composite hydrogels [303]. At 5 wt% clay nanoparticle loading, the storage modulus increased by 3.7% and this was caused by clay nanoparticles that infused themselves into the kenaf fibre bionanocomposite phase structure introducing some crystallinity. A drop of 8.2% in storage modulus for biocomposites with 7 wt% clay nanoparticle was caused by clay nanoparticle agglomeration. Agglomeration results in stress concentration areas which

cause premature localised failure. This leads to reduced molecular friction and hence a drop in the storage modulus. A massive decline in the storage modulus for all the specimens was observed to occur at around 55 ^{o}C due to glass transition. In the case of combined NaOH treatment and clay nanoparticle infusion, an improvement in the storage modulus of about 0.3% was noticed for combined NaOH treatment with 5 wt% clay nanoparticle content. This was influenced by the increased fibre crystallinity which was effected by the NaOH treatment and the nanoparticles increased molecular friction which causes an increase in the storage modulus. Combined NaOH treatment with 7 wt% clay nanoparticle content culminated in 0.8% decline in the storage modulus and this was due to clay nanoparticle agglomeration which reduces molecular friction.

7.4 Summary on the effects of treatments on loss modulus of the biocomposites

In the case of biocomposites made using untreated kenaf fibres but infused with clay nanoparticles alone, the loss modulus increased from 148.8 MPa at 3 wt% clay nanoparticle content to 199.9 MPa at 5 wt% clay nanoparticle and at 7 wt% it dropped to 147.2 MPa as shown in Figure 7.4.

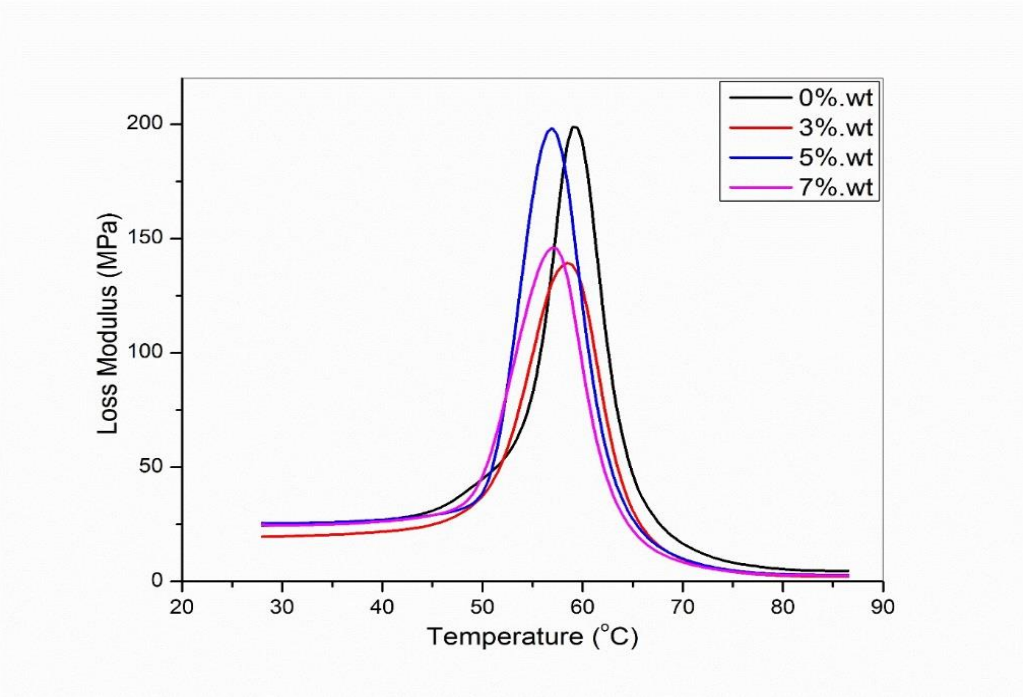

Figure 7.4 Loss modulus of the biocomposites

The increase in the loss modulus at 5 wt% was caused by increased restriction against PLA polymer chain molecular motion brought about by the clay nanoparticles. The reduction at 7 wt% was due to clay nanoparticle agglomeration effects observed above the optimal clay

nanoparticle content. However, it was noticed that the loss modulus of biocomposites with clay nanoparticles only had lower loss modulus values than the neat biocomposite except for the 5 wt% clay nanoparticle which had loss modulus that was 0.6% higher than the neat biocomposite. This trend was thought to be due to the insignificant effect of the clay nanoparticles on restricting amorphous PLA polymer molecular chain reinforced with highly amorphous untreated kenaf fibres. The bulk of the clay nanoparticles would be deposited in the fibre micelles thereby having little effect on PLA polymer chain motions. This problem was addressed by using NaOH treatment and combined NaOH treatment and clay nanoparticle infusion.

Treatment with NaOH only resulted in 20% increase in loss modulus. Combined treatment with NaOH and clay nanoparticles improved the loss modulus values by 60% and 51% for the biocomposites given combined NaOH treatment and infused with 5 wt% and 7 wt% clay nanoparticles, respectively. The improvements were due to the use of kenaf fibres with increased crystallinity brought about by NaOH treatment and increased restriction against chain molecular motion of PLA polymer brought about by the clay nanoparticles. In this case, the clay nanoparticles interact more with the PLA polymer than the fibre since the fibre were void of the amorphous hemicellulose and lignin. Agglomeration effects also caused a drop in the loss modulus at 7 wt%. The glass transition temperatures (Tg) were observed to shift to lower temperatures because of the increase in the crystallinity level of the bionanocomposites and clay nanoparticle infusion. It is important to mention here that the peak modulus values correspond to the Tg. The Tg for the neat biocomposites fabricated using untreated kenaf fibre was 59.3 ^{o}C and the Tg for the biocomposites fabricated using NaOH treated kenaf fibre was 56.3 ^{o}C. The bionanocomposites made using untreated kenaf fibres and infused with 3 wt%, 5 wt% and 7 wt% clay nanoparticle had Tg of 58.8 ^{o}C, 57.4% and 57.3%, respectively. The bionanocomposites made using combined NaOH treatment and clay nanoparticle infusion of 5 wt% and 7 wt% had Tg of 57.3 ^{o}C and 56.6 ^{o}C, respectively.

7.5 Summary on the effects of treatments on damping

The tandelta transition peaks for all the biocomposites given a single treatment and the biocomposites given a combined treatment showed that there was good compatibility between the clay nanoparticles and the PLA matrix. There was a gradual decrease in the tandelta values when the clay nanoparticle content was increased from 3 wt% to higher clay nanoparticle contents of 5 wt% and 7 wt% as shown in Figure 7.5.

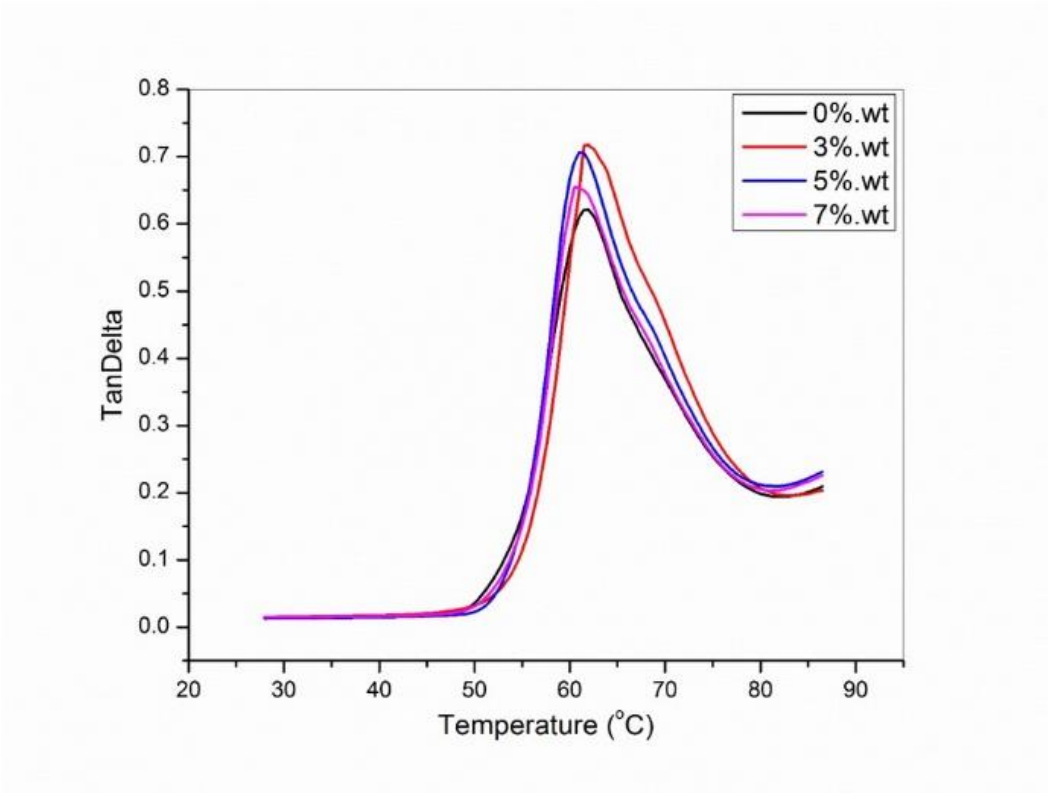

Figure 7.5 Effects of nanoclay on damping

At 5 wt% clay nanoparticle content, tandelta value decreased by 1.5% when compared to the tandelta value obtained at 3 wt% clay nanoparticle content. At 7 wt% clay nanoparticle content, tandelta value decreased by 8.8% when compared to the tandelta value obtained at 3 wt% clay nanoparticle content. This trend was due to increase in the restrictions against the PLA polymer chain motion as the clay nanoparticle content was increased. It was observed that when clay nanoparticle infusion was done to biocomposites fabricated using untreated kenaf fibres, the tandelta values were higher than the tandelta values for the neat kenaf/PLA biocomposites. This trend was different from some nanocomposites and other composites materials reported in literature which showed a reduction in the tandelta values when nanoparticles were added [304]. However, there is also published literature which report increased tandelta values as clay nanoparticles were added [230]. Treatment with NaOH only did not significantly change the tandelta value but the peak broadened which shows that the biocomposites made using NaOH treated kenaf fibres had better damping that the neat biocomposites fabricated using untreated kenaf fibres. This was due to better interaction between the PLA matrix and the NaOH treated kenaf fibres which were hemicellulose free. Combined NaOH treatment and clay nanoparticle infusion at 5 wt% and 7 wt% increased the tandelta values of the hybrid biocomposites by 25% and 18.3%, respectively. The increase was due to improved interaction of the PLA biopolymer,

kenaf fibres and the clay nanoparticles which was reflected by shifting of the damping peaks to higher temperatures for the hybrid biocomposites that had combined treatment. However, combined treatment with 7 wt% clay nanoparticles had a lower tandelta value that combined treatment with 5 wt% clay nanoparticles and this is attributed to clay nanoparticle agglomeration effects which adversely affected the interaction of the PLA biopolymer, kenaf fibres and clay nanoparticles. This adverse effect brought about by agglomeration was reflected by a shift of the combined treatment with 7 wt% clay nanoparticle damping peak to a lower temperature than that of the combined treatment with 5 wt% clay nanoparticle damping peak. These observed trend agrees with observations made in other studies which reported that addition of clay nanoparticles into composites increased tandelta values [230, 305]. However, some studies reported a reduction in tandelta with the addition of nanoparticles for some nanocomposites and other composite materials [233, 306].

Like in the case of the peak modulus temperature, the peak tandelta temperature is taken as the Tg for the material. The Tg for the neat kenaf/PLA biocomposites fabricated using untreated kenaf fibres was found to be 62.4 ^{o}C and the Tg for the neat kenaf/PLA biocomposites fabricated using NaOH treated kenaf fibres was found to be 59.8 ^{o}C. This shows that NaOH treatment reduced the Tg of the biocomposites by 4.2% and this was attributed to the increase in the crystallinity caused by the removal of hemicellulose from the kenaf fibres. The Tg was 61.5 ^{o}C, 61 ^{o}C and 60.5 ^{o}C for the hybrid biocomposites fabricated using untreated kenaf fibre but infused with clay nanoparticles of 3 wt%, 5 wt% and 7 wt%, respectively. This shows a slight decrease in Tg caused by the infusion of clay nanoparticles into the phase structure of the biocomposites as confirmed by the XRD analysis. The infusion with clay nanoparticles changed the PLA biopolymer chain molecular motions and the free volume which change the Tg of the biocomposites. Some studies focusing on glass fibre composites and adhesives infused with nanoparticles revealed that nanoparticles can increase the free volumes, for instance, by forcing the chains apart which causes a decrease in Tg [307-309]. The other possibility was given as due to the influence of nanoparticles on the curing reactions and prevention of crosslinking of the polymer chains [308]. In the case of combined treatment, Tg was 60.3 ^{o}C and 59.7 ^{o}C for combined NaOH treatment and clay nanoparticle infusion of 5 wt% and 7 wt%, respectively. These changes were due to improved crystallinity brought about by the NaOH and changes to the PLA polymer chain molecular motions caused by the clay nanoparticles. The Tg values acquired using the tandelta method are higher than the Tg values acquired using the loss modulus method. Literature also reported the same [266, 310].

7.6 Conclusion

Treatments improved thermal stability and thermomechanical properties of the hybrid bionanocomposites. Combined alkali treatment and clay nanoparticle infusion resulted in better improvement of the thermo-mechanical properties than the improvements effected by treatment using a single method, that is, NaOH treatment alone or infusion with clay nanoparticles alone. This shows that a treatment combination with NaOH and clay nanoparticle infusion does not have conflicted efforts but complimentary efforts on the properties of the hybrid bionanocomposites. The improvements were due to increase in the kenaf fibre crystallinity index caused by treatment with NaOH and clay nanoparticles' effects on thermal barrier property characteristic and molecular friction. Optimum improvements were from a combination of NaOH treatment and 5 wt% clay nanoparticle infusion. A drop in properties for the combination of NaOH treatment and 7 wt% clay nanoparticle infusion was largely due to clay nanoparticle agglomeration.

Chapter 8

8.0 Conclusions and Recommendations

8.1 Introduction

This chapter presents the overall conclusions gleaned from this research work of enhancing the properties of kenaf/nanoclay/PLA hybrid biocomposites and the recommendations. A novel hybrid biocomposite that is lightweight and with positive buoyancy was developed in this research work and its properties enhanced by clay nanoparticle infusion. The next sections present detailed conclusions about the novel kenaf/nanoclay/PLA hybrid bionanocomposites and recommendations. Clay nanoparticle loadings of 0 wt%, 3 wt%, 5 wt% and 7 wt% were used in this work. 5 wt% clay nanoparticle loading was the optimum and hence the conclusions discussed in the next sections focus on 5 wt% clay nanoparticle loading.

8.2 Conclusions

This research work resulted in the development of novel, sustainable, lightweight and floating kenaf/nanoclay/PLA hybrid bionanocomposite materials. The bionanocomposite materials made had enhanced basic mechanical properties and impact properties making them suitable for use in some high-performance applications replacing the conventional synthetic fibre-reinforced composites. The hybrid bionanocomposites made in this research work have an average density of 0.638 g/cm^3 for the neat kenaf/PLA bionanocomposites (without clay nanoparticles) and an average density of 0.666 g/cm^3 for the kenaf/nanoclay/PLA hybrid bionanocomposites with clay nanoparticles. This clearly shows that the kenaf/nanoclay/PLA hybrid bionanocomposites developed are lightweight and they float in water since their density is lower than that of water. In addition, these kenaf/nanoclay/PLA hybrid bionanocomposites are sustainable because they are made using biomaterials, that is, PLA biopolymer and kenaf biofibre.

It is concluded that combined NaOH treatment and clay nanoparticle infusion causes property changes to the kenaf/nanoclay/PLA hybrid bionanocomposites which result in the improvement of microstructure, crystallinity, kenaf fibre to PLA matrix adhesion, load bearing capacity and stress transfer efficiency. XRD results showed that there was intercalation and exfoliation of the clay nanoparticles. These improvements ultimately resulted in the enhancement of various properties of the kenaf/nanoclay/PLA hybrid bionanocomposites as summarised in the next paragraphs.

The basic mechanical properties, specifically tensile and flexural properties, thermal properties and thermomechanical properties of the kenaf/nanoclay/PLA hybrid bionanocomposites considerably improved with clay nanoparticle addition. 5 wt% clay nanoparticle infusion improved the tensile strength and Young's modulus of the hybrid bionanocomposites by 19.1% and 41.5%, respectively. Flexural strength and flexural modulus of the hybrid bionanocomposites improved by 9.8% and 34%, respectively after addition of 5 wt% clay nanoparticle content. Clay nanoparticles improved the thermal decomposition stability and dynamic mechanical properties of the kenaf/nanoclay/PLA hybrid bionanocomposites.

Impact properties of the kenaf/nanoclay/PLA hybrid bionanocomposites were considerably improved by the clay nanoparticles. The capability of the hybrid bionanocomposites to absorb energy when under low velocity impact loading improved by 92.9%. The low velocity impact strength of the kenaf/nanoclay/PLA hybrid bionanocomposites improved by 98.7% when determined using the ASTM standard (J/m) and when determined using the ISO standard (kJ/m^2), the impact strength increased by 54.1%. The performance behaviour of the kenaf/nanoclay/PLA hybrid bionanocomposites to medium velocity impact loading was assessed using different parameters. The perforation threshold limit of the neat novel kenaf/PLA biocomposites was established to be 26 m/s and addition of 5 wt% clay nanoparticle extended it by 42.3% to 37 m/s. The energy absorption capability and resistance to damage when under medium velocity impact loading improved by 109% and 26.5%, respectively, at 5 wt% clay nanoparticle loading. These results show that the clay nanoparticles considerably enhanced the impact resistance of the kenaf/nanoclay/PLA hybrid bionanocomposites. Prominent damage mechanisms for the kenaf/nanoclay/PLA hybrid bionanocomposites were matrix crushing and cracking, fibre fracturing, debonding at the interface and between fibre and matrix, delamination, bulging and shear plugging. The mechanisms of damage had resemblance to those of conventional SFRPCs. The study shows that addition of clay nanoparticles enhanced the impact properties of the kenaf/nanoclay/PLA hybrid bionanocomposites. The study revealed that inclusion of clay nanoparticles enhances the impact resistance of kenaf/PLA bionanocomposites in the medium velocity impact range. This means the bionanocomposites have a potential to protect against objects in the medium velocity range. Therefore, they could be ideal alternatives to the non-biodegradable conventional composites in protecting against secondary blasts or debris. In addition, the kenaf/nanoclay/PLA hybrid bionanocomposites are also suitable for applications where lightweight is required, for instance, in the transport sector for lightweight mass transit systems

and unmanned aerial vehicles (UAV), that is, drone technology. The kenaf/nanoclay/PLA hybrid bionanocomposites developed in this work would also positively contribute to the attainment of Sustainable Development Goals (SDG's) and hence are potentially part of materials for the future.

8.3 Recommendations

Some properties were not analysed due to resource limitations, time constraints and also because they were not part of the scope of this work. The following are some of the recommendations:

- further research on suitable hydrophobic surface treatments or finishes for the biocomposites so that they can be applied in areas with moisture or water thereby making them suitable for flotation or buoyancy applications like in amphibian vehicles.
- further analysis of some properties such as thermal conductivity, water absorption, fire resistance (burn rate), resistance to some environmental conditions.
- continued studies focusing on enhancing the resistance of the kenaf/nanoclay/PLA hybrid biocomposites from the currently established medium velocity impact range to high velocity impact resistance range. Other techniques of enhancing the impact properties such as use of shear thickening fluids can also be tried on biocomposites. Literature has reported significant improvement of impact resistance by composites impregnated with shear thickening fluids [311-313].
- study on how to accelerate post-use biodegradation of the kenaf/nanoclay/PLA hybrid biocomposites.
- modelling and simulation on processing and expected performance of the kenaf/nanoclay/PLA hybrid biocomposites to reduce the design and manufacturing costs of the biocomposites.
- prototype development, testing and validation for mass transit systems such as high-speed trains and amphibian vehicle.

References

[1] S. N. A. Safri, M. T. H. Sultan, M. Jawaid, and K. Jayakrishna, "Impact behaviour of hybrid composites for structural applications: A review," Composites Part B: Engineering, vol. 133, pp. 112-121, 2018/01/15/ 2018.

[2] L. Mohammed, M. N. M. Ansari, G. Pua, M. Jawaid, and M. S. Islam, "A Review on Natural Fiber Reinforced Polymer Composite and Its Applications," International Journal of Polymer Science, vol. 2015, p. 243947, 2015/10/01 2015.

[3] K. Begum and M. Islam, "Natural fiber as a substitute to synthetic fiber in polymer composites: A review," Research Journal of Engineering Sciences, vol. 2, pp. 46-53, 01/01 2013.

[4] M. Syduzzaman, M. A. Al Faruque, K. Bilisik, and M. Naebe, "Plant-Based Natural Fibre Reinforced Composites: A Review on Fabrication, Properties and Applications," Coatings, vol. 10, no. 10, p. 973, 2020.

[5] M. Li et al., "Recent advancements of plant-based natural fiber–reinforced composites and their applications," Composites Part B: Engineering, vol. 200, p. 108254, 2020/11/01/ 2020.

[6] S. Prashanth, K. M. Subbaya, K. S. Nithin, and S. Sachhidananda, "Fiber Reinforced Composites - A Review," Journal of Material Science & Engineering, vol. 06, 01/01 2017.

[7] O. Zabihi et al., "A Sustainable Approach to the Low-Cost Recycling of Waste Glass Fibres Composites towards Circular Economy," Sustainability, vol. 12, no. 641, pp. 1-10, 2020.

[8] G. S. Karuppannan and T. Kärki, "A review on the recycling of waste carbon fibre/glass fibre-reinforced composites: fibre recovery, properties and life-cycle analysis," SN Applied Sciences, vol. 2, no. 3, p. 433, 2020/02/18 2020.

[9] S. R. Naqvi, H. M. Prabhakara, E. A. Bramer, W. Dierkes, R. Akkerman, and G. Brem, "A critical review on recycling of end-of-life carbon fibre/glass fibre reinforced composites waste using pyrolysis towards a circular economy," Resources, Conservation and Recycling, vol. 136, pp. 118-129, 2018/09/01/ 2018.

[10] P. A. V. Dong, C. Azzaro-Pantel, and A.-L. Cadene, "Economie and environmental assessment of recovery and disposai pathways for CFRP waste management," Resources, Conservation and Recycling, vol. 133, pp. 63-75, 2018.

[11] S. M. C. Alves, F. S. da Silva, M. V. Donadon, R. R. Garcia, and E. J. Corat, "Process and characterization of reclaimed carbon fiber composites by pyrolysis and oxidation, assisted by thermal plasma to avoid pollutants emissions," Journal of Composite Materials, vol. 52, no. 10, pp. 1379-1398, 2018/05/01 2017.

[12] N. A. Shuaib and P. T. Mativenga, "Carbon footprint analysis of fibre reinforced composite recycling processes," Procedia Manufacturing, vol. 7, no. 2016, pp. 183-190, 2016.

[13] N. A. Shuaib, P. T. Mativenga, J. Kazie, and S. Job, "Resource efficiency and composite waste in UK supply chain," Procedia CIRP, vol. 29, no. 2015, pp. 662-667, 2015.

[14] G. Oliveux, L. O. Dandy, and G. A. Leeke, "Current status of recycling of fibre reinforcedpolymers: Review of technologies, reuse andresulting properties," Progress in Materials Science, vol. 72, no. 2015, pp. 61-99, 2015.

[15] P. A. V. Dong, C. Azzaro-Pantel, M. Boix, L. Jacquemin, and S. Domenech, "Modelling of Environmental Impacts and Economic Benefits of Fibre Reinforced Polymers Composite Recycling Pathways," Computer Aided Chemical Engineering, vol. 37, pp. 2009-2014, 2015.

[16] T. Väisänen, O. Das, and L. Tomppo, "A review on new bio-based constituents for natural fiber-polymer composites," Journal of Cleaner Production, vol. 149, pp. 582-596, 2017/04/15/ 2017.

[17] K. L. Pickering, M. G. A. Efendy, and T. M. Le, "A review of recent developments in natural fibre composites and their mechanical performance," Composites Part A: Applied Science and Manufacturing, vol. 83, pp. 98-112, 2016/04/01/ 2016.

[18] J. Cruz and R. Fangueiro, "Surface Modification of Natural Fibers: A Review," Procedia Engineering, vol. 155, pp. 285-288, 2016/01/01/ 2016.

[19] N. Saba, M. T. Paridah, and M. Jawaid, "Mechanical properties of kenaf fibre reinforced polymer composite: A review," Construction and Building Materials, vol. 76, pp. 87-96, 2015/02/01/ 2015.

[20] M. R. Sanjay, P. Madhu, M. Jawaid, P. Senthamaraikannan, S. Senthil, and S. Pradeep, "Characterization and properties of natural fiber polymer composites: A comprehensive review," Journal of Cleaner Production, vol. 172, pp. 566-581, 2018/01/20/ 2018.

[21] W. Liu et al., "Properties of natural fiber-reinforced biobased thermoset biocomposites: Effects of fiber type and resin composition," Composites Part B: Engineering, vol. 171, pp. 87-95, 2019/08/15/ 2019.

[22] Y. Wu, C. Xia, L. Cai, A. C. Garcia, and S. Q. Shi, "Development of natural fiber-reinforced composite with comparable mechanical properties and reduced energy consumption and environmental impacts for replacing automotive glass-fiber sheet molding compound," Journal of Cleaner Production, vol. 184, pp. 92-100, 2018/05/20/ 2018.

[23] S. B. Roy, S. C. Shit, R. A. Sengupta, and P. R. Shukla, "A Review on Bio-Composites: Fabrication, Properties and Applications," International Journal of Innovative Research in Science, Engineering and Technology, vol. 03, no. 10, pp. 16814-16824, 2014.

[24] V. T. Rathod, J. S. Kumar, and A. Jain, "Polymer and ceramic nanocomposites for aerospace applications," Applied Nanoscience, vol. 7, no. 8, pp. 519-548, 2017/11/01 2017.

[25] M. Md, M. Madhavi, and F. M. Ahsanullah, "Study on effects of E-glass fiber hybrid composites enhanced with multi-walled carbon nanotubes under tensile load using full factorial design of experiments," Applied Nanoscience, vol. 7, no. 6, pp. 283-289, 2017/08/01 2017.

[26] R. Siakeng, M. Jawaid, H. Ariffin, S. M. Sapuan, M. Asim, and N. Saba, "Natural fiber reinforced polylactic acid composites: A review," Polymer Composites, vol. 40, no. 2, pp. 446-463, 2018.

[27] D. K. Rajak, D. D. Pagar, P. L. Menezes, and E. Linul, "Fiber-Reinforced Polymer Composites: Manufacturing, Properties, and Applications," Polymers, vol. 11, no. 10, p. 1667, 2019.

[28] A. Lotfi, H. Li, D. V. Dao, and G. Prusty, "Natural fiber–reinforced composites: A review on material, manufacturing, and machinability," Journal of Thermoplastic Composite Materials, p. 0892705719844546, 2019.

[29] H. Yaghoobi and A. Fereidoon, "Preparation and characterization of short kenaf fiber-based biocomposites reinforced with multi-walled carbon nanotubes," Composites Part B: Engineering, vol. 162, pp. 314-322, 2019/04/01/ 2019.

[30] N. Kumar and D. Das, "Fibrous biocomposites from nettle (Girardinia diversifolia) and poly(lactic acid) fibers for automotive dashboard panel application," Composites Part B: Engineering, vol. 130, pp. 54-63, 2017/12/01/ 2017.

[31] X.-S. Yi, S. Du, and L. Zhang, Eds. Composite Materials Engineering, Volume 1: Fundamentals of Composite Materials, 1 ed. 2018, p. 786.

[32] E. J. Barbero, Introduction to Composite Materials Design, 3 ed. London: CRC Press, 2017.

[33] B. Harris, Engineering Composite Materials. London: The Institute of Materials, 1999.

[34] D. Gay, S. V. Hoa, and S. W. Tsai, Composite Materials: Design and Applications. London: CRC Press, 2003, p. 523.

[35] A. R. Bunsell and J. Renard, Fundamentals of Fibre Reinforced Composite Materials, Cantor B, Goringe M. J, Ma E (ed). United Kingdom: IOP Publishing Ltd, 2005, p. 401.

[36] P. K. Bajpai and I. Singh, Eds. Reinforced Polymer Composites: Processing, Characterization and Post Life Cycle Assessment. Germany: Wiley-VCH Verlag GmbH & Co. KGaA, Boschstr, 2019, p. 278.

[37] P. K. Mallick, Fiber-Reinforced Composites: Materials Manufacturing and Design, 3 ed. London: CRC Press, 2007, p. 616.

[38] M. J. Mochane et al., "Recent progress on natural fiber hybrid composites for advanced applications: A review," eXPRESS Polymer Letters, vol. 13, no. 2, pp. 159–198, 2019.

[39] A. Atmakuri, A. Palevicius, A. Vilkauskas, and G. Janusas, "Review of Hybrid Fiber Based Composites with Nano Particles-Material Properties and Applications," (in eng), Polymers, vol. 12, no. 9, p. 2088, 2020.

[40] M.-p. Ho et al., "Critical factors on manufacturing processes of natural fibre composites," Composites Part B: Engineering, vol. 43, no. 8, pp. 3549-3562, 2012/12/01/ 2012.

[41] K. G. Satyanarayana, G. G. C. Arizaga, and F. Wypych, "Biodegradable composites based on lignocellulosic fibers—An overview," Progress in Polymer Science, vol. 34, no. 9, pp. 982-1021, 9// 2009.

[42] O. Faruk, A. K. Bledzki, H.-P. Fink, and M. Sain, "Biocomposites reinforced with natural fibers: 2000–2010," Progress in Polymer Science, vol. 37, no. 11, pp. 1552-1596, 11// 2012.

[43] A. Gholampour and T. Ozbakkaloglu, "A review of natural fiber composites: properties,modification and processing techniques,characterization, applications," Journal of Materials Science 2019.

[44] M. J. John and S. Thomas, "Biofibres and biocomposites," Carbohydrate Polymers, vol. 71, no. 3, pp. 343-364, 2/8/ 2008.

[45] M. Rahman and M. R. Hasan, "Synthetic Biopolymers," in Functional Biopolymers. Polymers and Polymeric Composites: A Reference Series. , S. H. Jafar Mazumder M., Al-Ahmed A., Ed. Cham, Switzerland: Springer, 2019, pp. 1–43.

[46] G. T. G. Yashas, M. R. Sanjay, S. K. Bhat, P. Madhu, P. Senthamaraikannan, and B. Yogesha, "Polymer matrix-natural fiber composites: An overview," Cogent Engineering, vol. 5, no. 1, p. 1446667, 2018/01/01 2018.

[47] K. Jha, R. Kataria, J. Verma, and S. Pradhan, "Potential biodegradable matrices and fiber treatment for green composites: A review," AIMS Materials Science, vol. 6, no. 1, pp. 119–138, 2019.

[48] J. K. Bhatia, B. S. Kaith, and S. Kalia, "Recent Developments in Surface Modification of Natural Fibers for Their Use in Biocomposites," in Biodegradable Green Composites, S. Kalia, Ed.: John Wiley & Sons, 2016, pp. 80-117.

[49] M. Mohy Eldin, A. Omer, and T. Tamer, "A Review on Hyaluronan Biopolymer: Properties and Pharmaceutical Applications," 2014.

[50] Q. Li, Y. Niu, P. Xing, and C. Wang, "Bioactive polysaccharides from natural resources including Chinese medicinal herbs on tissue repair," (in eng), Chinese medicine, vol. 13, pp. 7-7, 2018.

[51] O. J. Shesan, A. C. Stephen, A. G. Chioma, R. Neerish, and S. E. Rotimi, "Fiber-Matrix Relationship for Composites Preparation," in Renewable and Sustainable Composites, A. B. Pereira and F. A. O. Fernandes, Eds. London: IntechOpen, 2019.

[52] H. Idrees, S. Z. J. Zaidi, A. Sabir, R. U. Khan, X. Zhang, and S.-u. Hassan, "A Review of Biodegradable Natural Polymer-BasedNanoparticles for Drug Delivery Applications," Nanomaterials, vol. 10, no. 1970, pp. 1-22, 2020.

[53] V. K. Thakur and M. K. Thakur, "Processing and characterization of natural cellulose fibers/thermoset polymer composites," Carbohydrate Polymers, vol. 109, pp. 102-117, 2014/08/30/ 2014.

[54] S. Z. Rogovina, E. V. Prut, and A. A. Berlin, "Composite Materials Based on Synthetic Polymers Reinforced with Natural Fibers," Polymer Science, Series A, vol. 61, no. 4, pp. 417-438, 2019/07/01 2019.

[55] H. A. Mohamed, Y. Assem, R. Said, and A. M. El-Masry, "Synthesis of polyesteramides: poly(ethylene adipate amide) and poly(ethylene succinate amide) and their application as corrosion inhibitors in paint formulations," Journal of Coatings Technology and Research, vol. 15, no. 5, pp. 967-981, 2018/09/01 2018.

[56] B. M. Upton and A. M. Kasko, "Biodegradable Aromatic–Aliphatic Poly(ester–amides) from Monolignol-Based Ester Dimers," ACS Sustainable Chemistry & Engineering, vol. 6, no. 3, pp. 3659-3668, 2018/03/05 2018.

[57] C. Girard et al., "Synthesis and characterization of poly(ester amide amide)s of different alkylene chain lengths," Polymer Bulletin, vol. 76, no. 1, pp. 495-509, 2019/01/01 2019.

[58] L. T. Sin and B. S. Tueen, Polylactic Acid: A practical guide for the processing, manufacturing and applications of PLA (Polylactic Acid (Second Edition)). William Andrew Publishing, 2019, pp. 347-363.

[59] M. Murariu and P. Dubois, "PLA composites: From production to properties," Advanced Drug Delivery Reviews, vol. 107, no. 2016, pp. 17-46, 2016/12/15/ 2016.

[60] W. Baltus et al., "Market study on: Bio-based Polymers in the World Capacities, Production and Applications: Status Quo and Trends towards 2020," nova-Institut GmbH, Germany, 2013.

[61] F. Aeschelmann and M. Carus, "Bio-based Building Blocks and Polymers in the World: Capacities, Production and Applications: Status Quo and Trends towards 2020," nova-Institut GmbH, Germany, 2015, [Online]. Available: www.bio-based.eu/markets.

[62] E. Rudnik, "Chapter 3 - Properties and applications," in Compostable Polymer Materials (Second Edition), E. Rudnik, Ed. Boston: Elsevier, 2019, pp. 49-98.

[63] NatureWorks, "Ingeo™ Biopolymer 10361D Technical Data Sheet," NatureWorks, USA.

[64] S. Farah, D. G. Anderson, and R. Langer, "Physical and mechanical properties of PLA, and their functions in widespread applications — A comprehensive review," Advanced Drug Delivery Reviews, vol. 107, no. 2016, pp. 367-392, 2016/12/15/ 2016.

[65] E. Castro-Aguirre, F. Iñiguez-Franco, H. Samsudin, X. Fang, and R. Auras, "Poly(lactic acid)—Mass production, processing, industrial applications, and end of life," Advanced Drug Delivery Reviews, vol. 107, no. 2016, pp. 333-366, 2016/12/15/ 2016.

[66] H.-y. Cheung, M.-p. Ho, K.-t. Lau, F. Cardona, and D. Hui, "Natural fibre-reinforced composites for bioengineering and environmental engineering applications," Composites Part B: Engineering, vol. 40, no. 7, pp. 655-663, 10// 2009.

[67] K.-t. Lau, P.-y. Hung, M.-H. Zhu, and D. Hui, "Properties of natural fibre composites for structural engineering applications," Composites Part B: Engineering, vol. 136, pp. 222-233, 2018/03/01/ 2018.

[68] M. Asim et al., "A Review on Pineapple Leaves Fibre and Its Composites," International Journal of Polymer Science, vol. 2015, p. 950567, 2015/10/19 2015.

[69] P. Antov, V. Savov, and N. Neykov, "Utilization of agricultural waste and wood industry residues in the production of natural fiber - reinforced composite materials," vol. International Journal – Wood, Design & Technology, vol.6, 03/23 2017.

[70] R. Dunne, D. Desai, R. Sadiku, and J. Jayaramudu, "A review of natural fibres, theirsustainability and automotive applications," Journal of Reinforced Plastics and Composites, vol. 35, no. 13, pp. 1041–1050, 2016.

[71] O. Adekomaya, T. Jamiru, R. Sadiku, and Z. Huan, "A review on the sustainability of natural fiber in matrix reinforcement – A practical perspective," Journal of Reinforced Plastics and Composites, vol. 35, no. 1, pp. 3-7, 2016.

[72] A. K. Mohanty, M. Misra, and L. T. Drzal, "Surface modifications of natural fibers and performance of the resulting biocomposites: An overview," Composite Interfaces, vol. 8, no. 5, pp. 313-343, 2001/01/01 2001.

[73] K. M. F. Hasan, P. G. Horváth, and T. Alpár, "Potential Natural Fiber PolymericNanobiocomposites: A Review," Polymers, vol. 12, no. 1072, pp. 1-25, 2020.

[74] M. Sood and G. Dwivedi, "Effect of fiber treatment on flexural properties of natural fiber reinforced composites: A review," Egyptian Journal of Petroleum, vol. 27, no. 4, pp. 775-783, 2018/12/01/ 2018.

[75] P. Sahu and M. Gupta, "A review on the properties of natural fibres and its bio-composites: Effect of alkali treatment," Proceedings of the Institution of Mechanical Engineers, Part L: Journal of Materials: Design and Applications, vol. 234, no. 1, pp. 198-217, 2020.

[76] T. D. Tavares, J. C. Antunes, F. Ferreira, and H. P. Felgueiras, "Biofunctionalization of Natural Fiber-ReinforcedBiocomposites for Biomedical Applications," Biomolecules, vol. 10, no. 148, pp. 1-44, 2020.

[77] W. Webo, M. Maringa, and L. Masu, "The Combined Effect of Mercerisation, Silane Treatment and Acid Hydrolysis on the Mechanical Properties of Sisal Fibre/Epoxy Resin Composites," MRS Advances, vol. 5, no. 23-24, pp. 1225-1233, 2020.

[78] O. Adekomaya and T. Majozi, "Sustainability of surface treatment of natural fibre in composite formation: challenges of environment-friendly option," The International Journal of Advanced Manufacturing Technology, vol. 105, no. 7, pp. 3183-3195, 2019/12/01 2019.

[79] Mukesh and S. S. Godara, "Effect of chemical modification of fiber surface on natural fiber composites: A review," Materials Today: Proceedings, vol. 18, pp. 3428-3434, 2019/01/01/ 2019.

[80] R. Latif, S. Wakeel, N. Zaman Khan, A. Noor Siddiquee, S. Lal Verma, and Z. Akhtar Khan, "Surface treatments of plant fibers and their effects on mechanical properties of fiber-reinforced composites: A review," Journal of Reinforced Plastics and Composites, vol. 38, no. 1, pp. 15-30, 2019/01/01 2018.

[81] M. Zwawi, "A Review on Natural Fiber Bio-Composites, SurfaceModifications and Applications," Molecules, vol. 26, no. 404, pp. 1-28, 2021.

[82] Thakur Manju. Kumari, Rana Ashvinder. Kumar, Liping Yang, Singha Amar. Singh, Thakur Vijay. Kumar, " Surface Modification of Biopolymers: An Overview", in Surface modification of biopolymers, V. K. Thakur and A. r. S. Singha, Eds. Hoboken, New Jersey: John Wiley & Sons, Inc., 2015, pp. 1-19.

[83] R. Ahmad, R. Hamid, and S. A. Osman, "Physical and Chemical Modifications of Plant Fibres for Reinforcement in Cementitious Composites," Advances in Civil Engineering, vol. 2019, p. 5185806, 2019/03/12 2019.

[84] G. Koronis, A. Silva, and M. Fontul, "Green composites: A review of adequate materials for automotive applications," Composites Part B: Engineering, vol. 44, no. 1, pp. 120-127, 1// 2013.

[85] H. n. P.S, K. B.N, T. N, N. Ab Shukor, and P. M. Tahir, "Anatomical Structures and Fiber Morphology of New Kenaf Varieties," Asian Journal of Scientific Research, vol. 2, 03/01 2009.

[86] S. a. Giwa Ibrahim et al., "Kenaf (Hibiscus cannabinus L.) Seed and its Potential Food Applications: A Review," Journal of Food Science, vol. 84, no. 8, pp. 2015-2023, 2019.

[87] A. Kakoty, W. S. N. Sangma, A. R. Phukan, and B. B. Kalita, "Extraction of kenaf fiber and its physico-chemical properties for various end uses," International Journal of Chemical Studies, vol. 7, no. 3, pp. 2617-2620, 2019.

[88] M. M. Islam et al., "Performance of some jute & allied fiber varieties in the southern part of Bangladesh," 2018, Jute; Kenaf; Mesta; Allied fiber; Southern part; Bangladesh. vol. 6, no. 1, p. 5, 2018-04-17 2018.

[89] E. Ogunbode, J. Yatim, M. Ishak, R. Masoud, and R. Meisam, "Potentials of kenaf fibre in bio-composite production: A review," Jurnal Teknologi, vol. 77, 11/17 2015.

[90] C. A. Akinrotimi and P. I. Okocha, "Evaluations of Genetic Divergence in Kenaf (Hibiscus Cannabinus L.) Genotypes Using Agro-Morphological Characteristics," Journal of Plant Sciences and Agricultural Research, vol. 2, no. 2:12, 2018.

[91] J. Ryu et al., "Morphological characteristics, chemical and genetic diversity of kenaf (Hibiscus cannabinus L.) genotypes," Journal of Plant Biotechnology, vol. 44, pp. 416-430, 12/31 2017.

[92] H. P. S. Khalil, Abdul. , I. A. F. Yusra, A. H. Bhat, and M. Jawaid, "Cell wall ultrastructure, anatomy, lignin distribution, and chemical composition of Malaysian cultivated kenaf fiber," Industrial Crops and Products, vol. 31, pp. 113-121, 05/13 2010.

[93] G. Faruq, M. A. Alamgir, M. Rahman, S. Bhassu, and R. M, "Evaluation of genetic variability of kenaf (Hibiscus cannabinus L.) From different geographic origins using morpho-agronomic traits and multivariate analysis," Australian Journal of Crop Science, vol. 5, pp. 1882-1890, 12/01 2011.

[94] "Kenaf fibres and composites," in Kenaf Fibers and Composites, S. M. Sapuan, J. Sahari , M. R. Ishak, and M. L. Sanyang, Eds. Boca Raton: Taylor & Francis Group, 2018, p. 244.

[95] N. Saba, P. M. Tahir, M. Jawaid, K. Abdan, and N. Ibrahim, "Potential Utilization of Kenaf Biomass in Different Applications," 2015.

[96] A. Ali and A. Andriyana, "Properties of multifunctional composite materials based on nanomaterials: a review," RSC Advances, 10.1039/C9RA10594H vol. 10, no. 28, pp. 16390-16403, 2020.

[97] D. K. Rajak, D. D. Pagar, P. L. Menezes, and E. Linul, "Fiber-Reinforced Polymer Composites: Manufacturing, Properties, and Applications," Polymers, vol. 11, no. 1667, pp. 1-37, 2019.

[98] Experimental impact study on unidirectional glass-carbon hybrid composite laminates, 2016, p. 721. [Online]. Available: https://www.degruyter.com/view/j/secm.2016.23.issue-6/secm-2013-0063/secm-2013-0063.xml. Accessed: 2019-06-05t22:20:08.551+02:00.

[99] T. D. Ngo, Q. T. Nguyen, T. P. Nguyen, and P. Tran, "Effect of Nanoclay on Thermomechanical Properties of Epoxy/Glass Fibre Composites," Arab J Sci Eng, vol. 41, no. 251–1261, 2016.

[100] S. N. A. B. Safri, M. T. H. Sultan, and M. Jawaid, "Damage analysis of glass fiber reinforced composites," in Durability and Life Prediction in Bio-, Fibre-Reinforced, and Hybrid Composites, M. Jawaid, M. Thariq, and N. Saba, Eds. First ed. Cambridge, United Kingdom: Woodhead Publishing Ltd, 2018, pp. 133-147.

[101] E. B and G. S, "Effect of nanoclay and nanoscale TiO2 on carbon/glass fibrereinforced polymer composites," Materials Research Express, vol. 7, no. 7, p. 075303, 2020/07/16 2020.

[102] V. S. Gálvez, F. Gálvez, D. Cendón, and L. Sánchez, "High-speed Impact Performance of Carbon/Epoxy Composites at Very Low Temperatures," Procedia Engineering, vol. 167, pp. 116-119, 2016/01/01/ 2016.

[103] Improved impact response of hygrothermally conditioned carbon/epoxy woven composites, 2016, p. 699. [Online]. Available: https://www.degruyter.com/view/j/secm.2016.23.issue-6/secm-2014-0105/secm-2014-0105.xml. Accessed: 2019-06-05t22:31:03.115+02:00.

[104] H. Rahmani, R. Eslami-Farsani, and H. Ebrahimnezhad-Khaljiri, "High Velocity Impact Response of Aluminum- Carbon Fibers-Epoxy Laminated Composites Toughened by Nano Silica and Zirconia," Fibers and Polymers, vol. 21, no. 1, pp. 170-178, 2020/01/01 2020.

[105] M. Pagnoncelli et al., "Mechanical and ballistic analysis of aramid/vinyl ester composites," Journal of Composite Materials, vol. 52, no. 3, pp. 289-299, 2018.

[106] M. Sauer and M. Kühnel, "Market developments, trends, outlook and challenges," Germany, 2017.

[107] S. Mazumdar, D. Pichler, M. Benevento, W. Seneviratine, R. Liang, and E. Witten, "2020 State of the Industry Report: Composite Manufacturing," 2020, [Online]. Available: http://compositesmanufacturingmagazine.com/2020/01/2020-state-of-the-industry-report/, Accessed on: 02/02/2021.

[108] T. K. Das, P. Ghosh, and N. C. Das, "Preparation, development, outcomes, and application versatility of carbon fiber-based polymer composites: a review," Advanced Composites and Hybrid Materials, vol. 2, no. 2, pp. 214-233, 2019/06/01 2019.

[109] M. F. Khurshid, M. Hengstermann, M. M. B. Hasan, A. Abdkader, and C. Cherif, "Recent developments in the processing of waste carbon fibre for thermoplastic composites – A review," Journal of Composite Materials, vol. 54, no. 14, pp. 1925-1944, 2020/06/01 2019.

[110] E. Pakdel, S. Kashi, R. Varley, and X. Wang, "Recent progress in recycling carbon fibre reinforced composites and dry carbon fibre wastes," Resources, Conservation and Recycling, vol. 166, p. 105340, 2021/03/01/ 2021.

[111] S.-S. Yao, F.-L. Jin, K. Y. Rhee, D. Hui, and S.-J. Park, "Recent advances in carbon-fiber-reinforced thermoplastic composites: A review," Composites Part B: Engineering, vol. 142, pp. 241-250, 2018/06/01/ 2018.

[112] R. A. Witik, R. Teuscher, V. Michaud, C. Ludwig, and J.-A. E. Månson, "Carbon fibre reinforced composite waste: An environmental assessment of recycling, energy recovery and landfilling," Composites Part A: Applied Science and Manufacturing, vol. 49, pp. 89-99, 2013/06/01/ 2013.

[113] L. Lin and A. K. Schlarb, "Recycled carbon fibers as reinforcements for hybrid PEEK composites with excellent friction and wear performance," Wear, vol. 432-433, p. 202928, 2019/08/15/ 2019.

[114] V. Vara Prasad and S. Talupula, "A Review on Reinforcement of Basalt and Aramid (Kevlar 129) fibers," Materials Today: Proceedings, vol. 5, no. 2, Part 1, pp. 5993-5998, 2018/01/01/ 2018.

[115] J. Zhang, V. S. Chevali, H. Wang, and C.-H. Wang, "Current status of carbon fibre and carbon fibre composites recycling," Composites Part B: Engineering, vol. 193, p. 108053, 2020/07/15/ 2020.

[116] D. He, V. K. Soo, H. C. Kim, P. Compston, and M. Doolan, "Comparative life cycle energy analysis of carbon fibre pre-processing, processing and post-processing recycling methods," Resources, Conservation and Recycling, vol. 158, p. 104794, 2020/07/01/ 2020.

[117] E. Clark, M. Bleszynski, F. Valdez, and M. Kumosa, "Recycling carbon and glass fiber polymer matrix composite waste into cementitious materials," Resources, Conservation and Recycling, vol. 155, p. 104659, 2020/04/01/ 2020.

[118] A. Lefeuvre, S. Garnier, L. Jacquemin, B. Pillain, and G. Sonnemann, "Anticipating in-use stocks of carbon fibre reinforced polymers and related waste generated by the wind power sector until 2050," Resources, Conservation and Recycling, vol. 141, pp. 30-39, 2019/02/01/ 2019.

[119] F. Meng, J. McKechnie, and S. J. Pickering, "An assessment of financial viability of recycled carbon fibre in automotive applications," Composites Part A: Applied Science and Manufacturing, vol. 109, pp. 207-220, 2018/06/01/ 2018.

[120] G. Marsh, "Next step for automotive materials," Materials Today - MATER TODAY, vol. 6, pp. 36-43, 04/01 2003.

[121] E. Council, "Directive 2000/53/EC of the European Parliament and of the Council on end-of-life vehicles," Offical Journal of the Europian Communities, vol. 43, no. L269, pp. 34-43, 2000.

[122] A. D. La Rosa, D. R. Banatao, S. J. Pastine, A. Latteri, and G. Cicala, "Recycling treatment of carbon fibre/epoxy composites: Materials recovery and characterization and environmental impacts through life cycle assessment," Composites Part B: Engineering, vol. 104, pp. 17-25, 2016/11/01/ 2016.

[123] L. Delvere, M. Iltina, M. Shanbayev, A. Abildayeva, S. Kuzhamberdieva, and D. Blumberga, "Evaluation of polymer matrix composite waste recycling methods," Environmental and Climate Technologies, vol. 23, no. 1, pp. 168–187, 2019.

[124] Y. F. Khalil, "Comparative environmental and human health evaluations of thermolysis and solvolysis recycling technologies of carbon fiber reinforced polymer waste," Waste Management, vol. 76, pp. 767-778, 2018/06/01/ 2018.

[125] M. L. Longana, N. Ong, H. Yu, and K. D. Potter, "Multiple closed loop recycling of carbon fibre composites with the HiPerDiF (High Performance Discontinuous Fibre) method," Composite Structures, vol. 153, pp. 271-277, 2016/10/01/ 2016.

[126] D. R. Vieira, R. K. Vieira, and M. Chang Chain, "Strategy and management for the recycling of carbon fiber-reinforced polymers (CFRPs) in the aircraft industry: a critical review," International Journal of Sustainable Development & World Ecology, vol. 24, no. 3, pp. 214-223, 2017/05/04 2017.

[127] F. L. King, A. Arul Jeya Kumar, and S. Vijayaragahavan, "Mechanical characterization of polylactic acid reinforced bagasse/basalt hybrid fiber composites," Journal of Composite Materials, vol. 53, no. 1, pp. 33-43, 2019.

[128] M. Moyo, K. Kanny, and R. Velmurugan, "Performance of kenaf non-woven mat/PLA biocomposites under medium velocity impact," Fibers and Polymers, vol. 21, no. 11, pp. 2642-2651.

[129] B. Asaithambi, G. Ganesan, and S. Ananda Kumar, "Bio-composites: Development and mechanical characterization of banana/sisal fibre reinforced poly lactic acid (PLA) hybrid composites," Fibers and Polymers, journal article vol. 15, no. 4, pp. 847-854, April 01 2014.

[130] K. Oksman, M. Skrifvars, and J. F. Selin, "Natural fibres as reinforcement in polylactic acid (PLA) composites," Composites Science and Technology, vol. 63, no. 9, pp. 1317-1324, 2003/07/01/ 2003.

[131] E. Omrani, P. L. Menezes, and P. K. Rohatgi, "State of the art on tribological behavior of polymer matrix composites reinforced with natural fibers in the green materials world," Engineering Science and Technology, an International Journal, vol. 19, no. 2, pp. 717-736, 2016/06/01/ 2016.

[132] M. Maghsoudi-Ganjeh, L. Lin, X. Wang, and X. Zeng, "Bioinspired design of hybrid composite materials," International Journal of Smart and Nano Materials, vol. 10, no. 1, pp. 90-105, 2019/01/02 2019.

[133] N. Subramani, J. G. Murali, P. Suresh, and V. V. A. Sankar, "Review on Hybrid Composite Materialsand its Applications," International Research Journal of Engineering and Technology (IRJET), vol. 4, no. 2, pp. 1921-1925, 2017.

[134] Y. M. Kanitkar, A. P. Kulkarni, and K. S. Wangikar, "Characterization of Glass Hybrid composite: A Review," Materials Today: Proceedings, vol. 4, no. 9, pp. 9627-9630, 2017/01/01/ 2017.

[135] B. Mitra, "Environment Friendly Composite Materials: Biocomposites and Green Composites," Defence Science Journal, vol. 64, no. 3, pp. 244-261, 2014.

[136] M. Z. R. Khan, S. K. Srivastava, and M. K. Gupta, "Tensile and flexural properties of natural fiber reinforced polymer composites: A review," Journal of Reinforced Plastics and Composites, vol. 37, no. 24, pp. 1435-1455, 2018/12/01 2018.

[137] P. Peças, H. Carvalho, H. Salman, and M. Leite, "Natural Fibre Composites and Their Applications: A Review," Journal of Composites Science, vol. 2, no. 4, p. 66, 2018.

[138] S. Witayakran, W. Smitthipong, R. Wangpradid, R. Chollakup, and P. Clouston, "Natural Fiber Composites: Review of Recent Automotive Trends," in Reference Module in Materials Science and Materials Engineering, 2017, pp. 1-9.

[139] G. S. Mann, L. P. Singh, P. Kumar, and S. Singh, "Green composites: A review of processing technologies and recent applications," Journal of Thermoplastic Composite Materials, vol. 33, no. 8, pp. 1145-1171, 2020.

[140] M. Mihai and M.-T. Ton-That, "Novel bio-nanocomposite hybrids made from polylactide/nanoclay nanocomposites and short flax fibers," Thermoplastic Composite Materials, vol. 32, no. 1, pp. 3-28, 2019.

[141] A. B. Nair and R. Joseph, "Eco-friendly bio-composites using natural rubber (NR) matrices and natural fiber reinforcements," 2014.

[142] B. D. Agarwal, L. J. Broutman, and K. Chandrashekhara, Analysis and Performance of Fiber Composites, 4th ed. New Delhi: John Wiley & Sons, 2017, p. 576.

[143] A. Toldy, P. Niedermann, Z. Rapi, and B. Szolnoki, "Flame retardancy of glucofuranoside based bioepoxy and carbon fibre reinforced composites made thereof," Polymer Degradation and Stability, vol. 142, pp. 62-68, 2017/08/01/ 2017.

[144] F. V. Ferreira, L. S. Cividanes, R. F. Gouveia, and L. M. F. Lona, "An overview on properties and applications of poly(butylene adipate-co-terephthalate)–PBAT based composites," Polymer Engineering & Science, vol. 59, no. s2, pp. E7-E15, 2017.

[145] M. M. A. Nassar, R. Arunachalam, and K. I. Alzebdeh, "Machinability of natural fiber reinforced composites: a review," The International Journal of Advanced Manufacturing Technology, vol. 88, no. 9, pp. 2985-3004, 2017/02/01 2017.

[146] L. Ciccarelli et al., "Sustainable composites: Processing of coir fibres and application in hybrid-fibre composites," Journal of Composite Materials, vol. 54, no. 15, pp. 1947-1960, 2020/06/01 2019.

[147] D. Pico and W. Steinmann, "Synthetic Fibres for Composite Applications," in Fibrous and Textile Materials for Composite Applications. Berlin/Heidelberg, Germany: Springer, 2016.

[148] M. S. Huda, L. Drzal, D. Ray, A. Mohanty, and M. Mishra, "Natural-fiber composites in the automotive sector," in Properties and Performance of Natural-Fibre Composites. Amsterdam, The Netherlands: Elsevier:, 2008.

[149] M. M. Davoodi, S. M. Sapuan, D. Ahmad, A. Aidy, A. Khalina, and M. Jonoobi, "Concept selection of car bumper beam with developed hybrid bio-composite material," Materials and Design, vol. 32, no. 10, pp. 4857-4865, 2011.

[150] A. K. Sinha, H. K. Narang, and S. Bhattacharya, "Mechanical properties of natural fibre polymer composites," Journal of Polymer Engineering, vol. 37, no. 9, pp. 879-895, 2017.

[151] O. Akampumuza, P. Wambua, A. Ahmed, l. Wei, and X.-H. Qin, "A review of the applications of bio composites in the automotive industry," Polymer Composites, 11/01 2016.

[152] A. K. Mohanty, M. Misra, and L. T. Drzal, Eds. Natural Fibers, Biopolymers, and Biocomposites 1st ed. Boca Raton: CRC Press, 2005.

[153] N. Graupner, A. S. Herrmann, and J. Müssig, "Natural and man-made cellulose fibre-reinforced poly(lactic acid) (PLA) composites: An overview about mechanical characteristics and application areas," Composites Part A: Applied Science and Manufacturing, vol. 40, no. 6, pp. 810-821, 2009/07/01/ 2009.

[154] A. Khan, S. M. Rangappa, M. Jawaid, S. Siengchin, and A. M. Asiri, Eds. Hybrid Fiber Composites: Materials, Manufacturing, Process Engineering. Weinheim, Germany: Wiley-VCH, 2020.

[155] B. Ravishankar, S. K. Nayak, and M. A. Kader, "Hybrid composites for automotive applications – A review," Journal of Reinforced Plastics and Composites, vol. 38, no. 18, pp. 835-845, 2019/09/01 2019.

[156] T. Moli, M. Sultan, M. Gobalakrishnan, and G. Muthaiyah, "Ballistic impact response of laminated hybrid composite materials 10," 2018.

[157] Y. Swolfs, I. Verpoest, and L. Gorbatikh, "Recent advances in fibre-hybrid composites: materials selection, opportunities and applications," International Materials Reviews, vol. 64, no. 4, pp. 181-215, 2019/05/19 2019.

[158] U. K. Vaidya, "Impact Response of Laminated and Sandwich Composites," in Impact Engineering of Composite Structures, S. Abrate, Ed., S. Abrate, Ed. Brimingham: Springer-Verlag Wien, 2011, pp. 97-191.

[159] J. Naveen, K. Jayakrishna, M. T. B. Hameed Sultan, and S. M. M. Amir, "Ballistic Performance of Natural Fiber Based Soft and Hard Body Armour- A Mini Review," (in English), Frontiers in Materials, Mini Review vol. 7, 2020-December-09 2020.

[160] A. T. Souza et al., "Ballistic Properties and Izod Impact Resistance of Novel Epoxy Composites Reinforced with Caranan Fiber (Mauritiella armata)," (in eng), Polymers (Basel), vol. 14, no. 16, Aug 17 2022.

[161] S. N. A. Safri, M. T. H. Sultan, N. Yidris, and F. Mustapha, "Low Velocity and High Velocity Impact Test on Composite Materials – A review," International Journal Of Engineering And Science, vol. 3, no. 9, pp. 50-60, 2014.

[162] Low velocity impact behaviour of glass fabric/epoxy honeycomb core sandwich composites, 2015, p. 525. [Online]. Available: https://www.degruyter.com/view/j/secm.2015.22.issue-5/secm-2013-0069/secm-2013-0069.xml. Accessed: 2019-06-05t22:31:56.481+02:00.

[163] M. Taşyürek and M. Kara, "Low-velocity impact response of pre-stressed glass fiber/nanotube filled epoxy composite tubes," Journal of Composite Materials, vol. 55, no. 7, pp. 915-926, 2021/03/01 2020.

[164] R. Reghunath, M. Lakshmanan, and K. M. Min, "Low velocity impact analysis on glass fiber reinforced composites with varied volume fractions," 2015: IOP Conference Series: Materials Science and Engineering.

[165] F. A. Shishevan, H. Akbulut, and M. A. Mohtadi-Bonab, "Low Velocity Impact Behavior of Basalt Fiber-Reinforced Polymer Composites," Journal of Materials Engineering and Performance, vol. 26, no. 6, pp. 2890-2900, 2017.

[166] A. J. Turner, M. A. Rifaie, A. Mian, and R. Srinivasan, "Low-Velocity Impact Behavior of Sandwich Structureswith Additively Manufactured Polymer Lattice Cores," Journal of Materials Engineering and Performance, vol. 27, no. 5, pp. 2505-2512, 2018.

[167] K. I. Ismail, M. T. H. Sultan, A. U. M. Shah, M. Jawaid, and S. N. A. Safri, "Low velocity impact and compression after impact properties of hybrid bio-composites modified with multi-walled carbon nanotubes," Composites Part B: Engineering, vol. 163, pp. 455-463, 2019/04/15/ 2019.

[168] A. S. AlOmari, K. S. Al-Athel, A. F. M. Arif, and F. A. Al-Sulaiman, "Experimental and Computational Analysis ofLow-Velocity Impact on Carbon-, Glass- andMixed-Fiber Composite Plates," Journal of Composite Science (J. Compos. Sci.), vol. 4, no. 148, pp. 1-19, 2020.

[169] S. Nayak, R. K. Nayak, and I. Panigrahi, "Improvement of Low-Velocity Impact and Abrasive Wear Resistance of Carbon/Glass Fiber-Reinforced Polymer Hybrid Composites," Transactions of the Indian Institute of Metals, 2021/06/18 2021.

[170] P. N. B. Reis, A. M. Amaro, M. A. Neto, and J. S. Cirne, "Effect of Hostile Solutions on Composites Laminates Subjected to Low and High Velocity Impact Loads," Fibers and Polymers, journal article vol. 20, no. 1, pp. 158-164, January 01 2019.

[171] H. Liu et al., "Effects of Impactor Geometry on the Low-Velocity Impact Behaviour of Fibre-Reinforced Composites: An Experimental and Theoretical Investigation," Applied Composite Materials, vol. 27, no. 5, pp. 533-553, 2020/10/01 2020.

[172] Y. Shi, C. Pinna, and C. Soutis, "5 - Low-velocity impact of composite laminates: Damage evolution," in Dynamic Deformation, Damage and Fracture in Composite Materials and Structures, V. V. Silberschmidt, Ed.: Woodhead Publishing, 2016, pp. 117-146.

[173] J. Leng et al., "Analysis of Low-Velocity Impact Resistance of Carbon Fiber Reinforced Polymer Composites Based on the Content of Incorporated Graphite Fluoride," (in eng), Materials (Basel, Switzerland), vol. 13, no. 1, p. 187, 2020.

[174] R. Olsson and C. Paget, "Response and damage due to medium velocityimpact on composites," Aeronautics Division, FFA, SE-172 90 Stockholm, Sweden, 2001.

[175] O. Dorival et al., "Experimental results of medium velocity impact tests for reinforced foam core braided composite structures," Journal of Sandwich Structures & Materials, vol. 20, no. 1, pp. 106-129, 2018/01/01 2016.

[176] A. Trellu et al., "Combined loadings after medium velocity impact on large CFRP laminate plates: Tests and enhanced computation/testing dialogue," Composites Science and Technology, vol. 196, p. 108194, 2020/08/18/ 2020.

[177] H. Wang, K. R. Ramakrishnan, and K. Shankar, "Experimental study of the medium velocity impact response of sandwich panels with different cores," Materials & Design, vol. 99, no. C, pp. 68-82, 2016.

[178] A. Kolopp, S. Rivallant, and C. Bouvet, "Experimental study of sandwich structures as armour against medium-velocity impacts," International Journal of Impact Engineering, vol. 61, pp. 24-35, 2013/11/01/ 2013.

[179] STANAG 2920 PPS (Edition 2) - Ballistic Test Method for Personal Armour Materials and Combat Clothing, 2003.

[180] Standard for V50 Ballistic Test for Armor, 1987

[181] Standard for Ballistic Resistance of Body Armor NIJ Standard-0101.06, 2008.

[182] Summary of Newly Ratified NATO Standard AEP 2920, Ed. A, V1, 2016.

[183] Standard for Bullet and Stab Proof Vests, 2019.

[184] International standards for personal armor.

[185] M. G. Babu, R. Velmurugan, and N. K. Gupta, "Energy absorption and ballistic limit of targets struck by heavy projectile," Latin American Journal of Solids and Structures, vol. 3, pp. 21-39, 2006.

[186] G. Faur-Csukat, "A Study on the Ballistic Performance of Composites," Macromolecular Symposia, vol. 239, no. 1, pp. 217-226, 2006.

[187] N. Domun et al., "Ballistic impact behaviour of glass fibre reinforced polymer composite with 1D/2D nanomodified epoxy matrices," Composites Part B: Engineering, vol. 167, pp. 497-506, 2019/06/15/ 2019.

[188] L. Verma, J. Andrew, S. M. Sivakumar, G. Balaganesan, S. Vedantam, and H. N. Dhakal, "Ballistic Impact Behaviour of Glass/Epoxy Composite Laminates Embedded with Shape Memory Alloy (SMA) Wires," (in eng), Molecules (Basel, Switzerland), vol. 26, no. 1, p. 138, 2020.

[189] A. VanderKlok et al., "An experimental investigation into the high velocity impact responses of S2-glass/SC15 epoxy composite panels with a gas gun," International Journal of Impact Engineering, vol. 111, pp. 244-254, 2018/01/01/ 2018.

[190] S. Dolati, A. Fereidoon, and A. R. Sabet, "Damage Assessment in Glass Fiber-Epoxy Matrix Composite under High Velocity Impact of Ice," Journal of Ultrafine Grained and Nanostructured Materials, vol. 46, no. 1, pp. 47-54, 2013.

[191] C. Ulven, U. K. Vaidya, and M. V. Hosur, "Effect of projectile shape during ballistic perforation of VARTM carbon/epoxy composite panels," Composite Structures, vol. 61, no. 1, pp. 143-150, 2003/07/01/ 2003.

[192] X. Liu, W. Gu, Q. Liu, X. Lai, and L. Liu, "Damage of hygrothermally conditioned carbon epoxy composites under high-velocity impact," Materials, vol. 11, pp. 1-16, 2018.

[193] P. Hazell, G. J. Appleby-Thomas, and G. Kister, "Impact, penetration, and perforation of a bonded carbon-fibre-reinforced plastic composite panel by a high-velocity steel sphere: An experimental study," Journal of Strain Analysis for Engineering Design, vol. 45, no. 6, pp. 439-450, 2010.

[194] B. L. Buitrago, S. K. García-Castillo, and E. Barbero, "Influence of shear plugging in the energy absorbed by thin carbon-fibre laminates subjected to high-velocity impacts," Composites Part B: Engineering, vol. 49, pp. 86-92, 2013/06/01/ 2013.

[195] L. Sorrentino, C. Bellini, A. Corrado, W. Polini, and R. Aricò, "Ballistic Performance Evaluation of Composite Laminates in Kevlar 29," Procedia Engineering, vol. 88, pp. 255-262, 2014/01/01/ 2015.

[196] A. K. Bandaru, V. V. Chavan, S. Ahmad, R. Alagirusamy, and N. Bhatnagar, "Ballistic impact response of Kevlar® reinforced thermoplastic composite armors," International Journal of Impact Engineering, vol. 89, pp. 1-13, 2016/03/01/ 2016.

[197] S. N. Monteiro et al., "Novel ballistic ramie fabric composite competing with Kevlar™ fabric in multilayered armor," Materials & Design, vol. 96, pp. 263-269, 2016/04/15/ 2016.

[198] S. D. Salman, Z. Leman, M. T. H. Sultan, M. R. Ishak, and F. Cardona, "Ballistic Impact Resistance of Plain Woven Kenaf/Aramid Reinforced Polyvinyl Butyral Laminated Hybrid Composite," Bioresorces, Kenaf fibres; PVB film; Kevlar fibres; Ballistic properties; Helmet vol. 11, no. 3, p. 14, 2016-07-14 2016.

[199] A. K. Bandaru, S. Ahmad, and N. Bhatnagar, "Ballistic performance of hybrid thermoplastic composite armors reinforced with Kevlar and basalt fabrics," Composites Part A: Applied Science and Manufacturing, vol. 97, pp. 151-165, 2017/06/01/ 2017.

[200] A. Khodadadi, G. Liaghat, S. Vahid, A. R. Sabet, and H. Hadavinia, "Ballistic performance of Kevlar fabric impregnated with nanosilica/PEG shear thickening fluid," Composites Part B: Engineering, vol. 162, pp. 643-652, 2019/04/01/ 2019.

[201] S. G. Nunes, W. F. de Amorim, A. Manes, and S. C. Amico, "The effect of thickness on vacuum infusion processing of aramid/epoxy composites for ballistic application," Journal of Composite Materials, vol. 53, no. 3, pp. 383-391, 2019.

[202] A. Khodadadi et al., "High velocity impact behavior of Kevlar/rubber and Kevlar/epoxy composites: A comparative study," Composite Structures, vol. 216, pp. 159-167, 2019/05/15/ 2019.

[203] A. A. Ramadhan, A. A. R. Talib, M. A. S. Rafie, and R. Zahari, "High velocity impact response of Kevlar-29/epoxy and 6061-T6 aluminum laminated panels," Materials & Design, vol. 43, pp. 307-321, 2013/01/01/ 2013.

[204] G. Balaganesan, R. Velmurugan, M. Srinivasan, N. K. Gupta, and K. Kanny, "Energy absorption and ballistic limit of nanocomposite laminates subjected to impact loading," International Journal of Impact Engineering, vol. 74, pp. 57-66, 2014/12/01/ 2014.

[205] M. H. Pol, G. Liaghat, E. Zamani, and A. Ordys, "Investigation of the ballistic impact behavior of 2D woven glass/epoxy/nanoclay nanocomposites," Journal of Composite Materials, vol. 49, no. 12, pp. 1449-1460, 2015.

[206] E. E. Haro, A. G. Odeshi, and J. A. Szpunar, "The energy absorption behavior of hybrid composite laminates containing nano-fillers under ballistic impact," International Journal of Impact Engineering, vol. 96, pp. 11-22, 2016/10/01/ 2016.

[207] P. Murugan, K. Naresh, K. Shankar, R. Velmurugan, and G. Balaganesan, "High velocity impact damage investigation of Carbon/epoxy/clay nanocomposites using 3D Computed Tomography," in AMPCO-2017, Italy, 2018, vol. 5, no. 9: Elsevier Ltd, pp. 16946-16955.

[208] E. Kazemi-Khasragh, F. Bahari-Sambran, M. Hossein Siadati, and R. Eslami-Farsani, "High Velocity Impact Response of Basalt Fibers/Epoxy Composites Containing Graphene Nanoplatelets," Fibers and Polymers, journal article vol. 19, no. 11, pp. 2388-2393, November 01 2018.

[209] K. S. Pandya, J. R. Pothnis, G. Ravikumar, and N. K. Naik, "Ballistic impact behavior of hybrid composites," Materials & Design, vol. 44, pp. 128-135, 2013/02/01/ 2013.

[210] R. Yahaya, S. M. Sapuan, M. Jawaid, Z. Leman, and E. S. Zainudin, "Measurement of ballistic impact properties of woven kenaf–aramid hybrid composites," Measurement, vol. 77, pp. 335-343, 2016/01/01/ 2016.

[211] R. Yahaya, S. M. Sapuan, M. Jawaid, Z. Leman, and E. S. Zainudin, "Investigating ballistic impact properties of woven kenaf-aramid hybrid composites," Fibers and Polymers, journal article vol. 17, no. 2, pp. 275-281, February 01 2016.

[212] S. Jambari, M. Y. Yahya, M. R. Abdullah, and M. Jawaid, "Woven Kenaf/Kevlar Hybrid Yarn as potential fiber reinforced for anti-ballistic composite material," Fibers and Polymers, journal article vol. 18, no. 3, pp. 563-568, March 01 2017.

[213] J. Tirillò et al., "High velocity impact behaviour of hybrid basalt-carbon/epoxy composites," Composite Structures, vol. 168, pp. 305-312, 2017/05/15/ 2017.

[214] M. Grujicic, B. Pandurangan, D. C. Angstadt, K. L. Koudela, and B. A. Cheeseman, "Ballistic-performance optimization of a hybrid carbon-nanotube/E-glass reinforced poly-vinyl-ester-epoxy-matrix composite armor," Journal of Materials Science, journal article vol. 42, no. 14, pp. 5347-5359, July 01 2007.

[215] Y. Zhang, Z. Kerr, B. Jarvis, and R. J. Volant, "High-velocity impact behaviour of a new hybrid fibre-reinforced cementitious composite," Advances in Structural Engineering, vol. 21, no. 4, pp. 589-597, 2018.

[216] P. Wambua, B. Vangrimde, S. Lomov, and I. Verpoest, "The response of natural fibre composites to ballistic impact by fragment simulating projectiles," Composite Structures, vol. 77, pp. 232-240, 2007.

[217] G. García del Pino et al., "Hybrid Polyester Composites Reinforced with Curauá Fibres and Nanoclays," Fibers and Polymers, vol. 21, no. 2, pp. 399-406, 2020/02/01 2020.

[218] S. Salman, Z. Leman, M. Ishak, and F. Cardona, "Effect of kenaf fibers on trauma penetration depth and ballistic impact resistance for laminated composites," vol. 87, pp. 2051-2065, 2017.

[219] S. Quintero, A. Porras, C. Hernandez, and A. Maranon, "The response of manicaria saccifera natural fabric reinforced PLA composites to impact fragment simulating projectiles," in Advances in Natural Fibre Composites: Raw Materials, Processing and Analysis, R. Fangueiro and S. Rana, Eds. Switzerland: Springer International, 2018, pp. 89-98.

[220] F. S. d. Luz, F. d. C. Garcia Filho, M. S. Oliveira, L. F. C. Nascimento, and S. N. Monteiro, "Composites with Natural Fibers and Conventional Materials Applied in a Hard Armor: A Comparison," Polymers, vol. 12, no. 9, p. 1920, 2020.

[221] S. S. Chee, M. Jawaid, O. Y. Alothman, and H. Fouad, "Effects of Nanoclay on Mechanical and Dynamic Mechanical Properties of Bamboo/Kenaf Reinforced Epoxy Hybrid Composites," Polymers, vol. 13, no. 3, p. 395, 2021.

[222] M. Jawaid, A. e. K. Qaiss, and R. Bouhfid, Eds. "Nanoclay Reinforced Polymer Composites: Natural Fibre/Nanoclay Hybrid Composites." Singapore: Springer Nature, 2016.

[223] A. S. Rana, M. K. Vamshi, K. Naresh, R. Velmurugan, and R. Sarathi, "Effect of nanoclay on mechanical, thermal and morphological properties of silicone rubber and EPDM/silicone rubber hybrid composites," Advances in Materials and Processing Technologies, vol. 7, no. 1, pp. 109-116, 2021/01/02 2021.

[224] M. H. Mat Yazik, M. T. H. Sultan, A. U. M. Shah, M. Jawaid, and N. Mazlan, "Effect of nanoclay content on the thermal, mechanical and shape memory properties of epoxy nanocomposites," Polymer Bulletin, vol. 77, no. 11, pp. 5913-5931, 2020/11/01 2020.

[225] M. Bulut, Ö. Y. Bozkurt, A. Erkliğ, H. Yaykaşlı, and Ö. Özbek, "Mechanical and Dynamic Properties of Basalt Fiber-Reinforced Composites with Nanoclay Particles," Arabian Journal for Science and Engineering, vol. 45, no. 2, pp. 1017-1033, 2020/02/01 2020.

[226] B. Mylsamy, S. K. Palaniappan, S. Pavayee Subramani, S. K. Pal, and K. Aruchamy, "Impact of nanoclay on mechanical and structural properties of treated Coccinia indica fibre reinforced epoxy composites," Journal of Materials Research and Technology, vol. 8, no. 6, pp. 6021-6028, 2019/11/01/ 2019.

[227] M. Pushparaja, G. Balaganesan, R. Velmurugan, and N. K. Gupta, "Energy Absorption Characteristics of Carbon /Epoxy Nano Filler Dispersed Composites Subjected to Localized Impact Loading," Procedia Engineering, vol. 173, pp. 175-181, 2017/01/01/ 2017.

[228] V. Sridharan, T. Raja, and N. Muthukrishnan, "Study of the Effect of Matrix, Fibre Treatment and Graphene on Delamination by Drilling Jute/Epoxy Nanohybrid Composite," Arabian Journal for Science and Engineering, vol. 41, no. 5, pp. 1883-1894, 2016/05/01 2016.

[229] T. P. Mohan, R. Velmurugan, and K. Kanny, "Damping characteristics of nanoclay filled hybrid laminates during medium velocity impact," Composites Part B: Engineering, vol. 82, pp. 178-189, 2015/12/01/ 2015.

[230] T. P. Mohan and K. Kanny, "Nanoclay infused banana fiber and its effects on mechanical and thermal properties of composites," Journal of Composite Materials, vol. 50, no. 9, pp. 1261-1276, 2016/04/01 2015.

[231] S. Arulmurugan and N. Venkateshwaran, "Effect of nanoclay addition and chemical treatment on static and dynamic mechanical analysis of jute fibre composites," Polímeros, vol. 29, no. 4, pp. 1-8, 2020.

[232] A. Murugan and V. Narayanan, "Effect of nanoclay addition and chemical treatment on static and dynamic mechanical analysis of jute fibre composites," Polímeros, vol. 29, 01/01 2019.

[233] S. Arulmurugan and N. Venkateshwaran, "Effect of nanoclay addition and chemical treatment on static and dynamic mechanical analysis of jute fibre composites," Polimeros, vol. 29, no. 4, pp. 1-8, 2019.

[234] M. H. Hasan, M. S. Mollik, and M. M. Rashid, "Effect of nanoclay on thermal behavior of jute reinforced composite," The International Journal of Advanced Manufacturing Technology, journal article vol. 94, no. 5, pp. 1863-1871, February 01 2018.

[235] N. R. R. Anbusagar and K. Palanikumar, "Nanoclay Addition and Core Materials Effect on Impact and Damage Tolerance Capability of Glass Fiber Skin Sandwich Laminates," Silicon, vol. 10, no. 3, pp. 769-779, 2018/05/01 2018.

[236] P. P. Binu, K. E. George, and M. N. Vinodkumara, "Effect of nanoclay, Cloisite15A on the Mechanical Properties and Thermal behavior of Glass Fiber Reinforced Polyester," Procedia Technology, vol. 25, no. 2016, pp. 846-853, 2016.

[237] K. Deepak, S. V. P. Vattikuti, and B. Venkatesh, "Experimental Investigation of Jute FiberReinforcedNano Clay Composite," Procedia Materials Science, vol. 10, pp. 238-242, 2015/01/01/ 2015.

[238] Y. Jaya Vinse Ruban, S. Ginil Mon, and D. Vetha Roy, "Chemical resistance/thermal and mechanical properties of unsaturated polyester-based nanocomposites," Applied Nanoscience, vol. 4, no. 2, pp. 233-240, 2014/02/01 2014.

[239] P. Ramesh, B. D. Prasad, and K. L. Narayana, "Influence of Montmorillonite Clay Content on Thermal, Mechanical, Water Absorption and Biodegradability Properties of Treated Kenaf Fiber/ PLA-Hybrid Biocomposites," Silicon, 2020/02/05 2020.

[240] S. Murugesan and T. Scheibel, "Copolymer/Clay Nanocomposites for Biomedical Applications," Advanced Functional Materials, vol. 30, no. 17, p. 1908101, 2020.

[241] Y. Zhou, A. M. LaChance, A. T. Smith, H. Cheng, Q. Liu, and L. Sun, "Strategic Design of Clay-Based Multifunctional Materials: From Natural Minerals to Nanostructured Membranes," Advanced Functional Materials, vol. 29, no. 16, p. 1807611, 2019.

[242] J. Liu, W. J. Boo, A. Clearfield, and H. J. Sue, "Intercalation and Exfoliation: A Review on Morphology of Polymer Nanocomposites Reinforced by Inorganic Layer

Structures," Materials and Manufacturing Processes, vol. 21, no. 2, pp. 143-151, 2006/04/01 2006.

[243] N. Y. U. P. S. o. Engineering, "A metal composite that will (literally) float your boat," ScienceDaily, New York, USA, 12 May 2015 2015, [Online]. Available: www.sciencedaily.com/releases/2015/05/150512164522.htm, Accessed on: 17 October 2022.

[244] J. Fan and J. Njuguna, "1 - An introduction to lightweight composite materials and their use in transport structures," in Lightweight Composite Structures in Transport, J. Njuguna, Ed.: Woodhead Publishing, 2016, pp. 3-34.

[245] H. N. Dhakal and S. O. Ismail, Sustainable Composites for Lightweight Applications (Woodhead Publishing Series in Composites Science and Engineering). United Kingdom: Woodhead Publishing, 2021.

[246] J. Mohammad and T. Mohamed, Sustainable Composites for Aerospace Applications (Woodhead Publishing Series in Composites Science and Engineering). United Kingdom: Elsevier Ltd. Elsevier Science & Technology, 2018, p. 590.

[247] A. Amiri, Z. Triplett, A. Moreira, N. Brezinka, M. Alcock, and C. Ulven, "Standard density measurement method development for flax fiber," Industrial Crops and Products, vol. 96, pp. 196-202, 02/01 2017.

[248] Y. Saadati, J.-F. Chatelain, G. Lebrun, and Y. Beauchamp, "Comparison of density measurement methods for unidirectional flax-epoxy polymer composites," in European Conference on Multifunctional Structures (EMuS), Barcelona, Spain, 2019.

[249] Standard Test Methods for Density and Specific Gravity (Relative Density) of Plastics by Displacement, 2020.

[250] P. Joyce, "Mechanical Testing of CompositesComposite," U. S. N. Academy, Ed., ed. USA, 2003.

[251] G. Guo, K. H. Wang, C. B. Park, Y. S. Kim, and G. Li, "Effects of nanoparticles on the density reduction and cell morphology of extruded metallocene polyethylene/wood fiber nanocomposites," Journal of Applied Polymer Science, vol. 104, no. 2, pp. 1058-1063, 2007.

[252] H. Mohit and V. Arul Mozhi Selvan, "A comprehensive review on surface modification, structure interface and bonding mechanism of plant cellulose fiber reinforced polymer based composites," Composite Interfaces, vol. 25, no. 5-7, pp. 629-667, 2018/07/03 2018.

[253] M. C. Khoathane, E. R. Sadiku, and C. S. Agwuncha, "Surface Modification of Natural Fiber Composites and their Potential Applications," in Surface Modification of Biopolymers, V. K. Thakur and A. S. Singha, Eds., 2015, pp. 370-400.

[254] I. Shah, L. Jing, Z. Fei, Y. Yuan, M. Farooq, and N. Kanjana, "A Review on Chemical Modification by using Sodium Hydroxide (NaOH) to Investigate the Mechanical Properties of Sisal, Coir and Hemp Fiber Reinforced Concrete Composites," Journal of Natural Fibers, pp. 1-19, 03/18 2021.

[255] S. Kalia, B. S. Kaith, and I. Kaur, "Pretreatments of natural fibers and their application as reinforcing material in polymer composites—A review," Polymer Engineering & Science, vol. 49, no. 7, pp. 1253-1272, 2009.

[256] S. Jayabal, S. Sathiyamurthy, K. T. Loganathan, and S. Kalyanasundaram, "Effect of soaking time and concentration of NaOH solution on mechanical properties of coir–polyester composites," Bull. Mater. Sci., vol. 35, no. 4, pp. 567–574, 2012.

[257] I. N. Nasidi, L. H. Ismail, and E. M. Samsudin, "Effect of Sodium Hydroxide (NaOH) Treatment on Coconut Coir Fibre and its Effectiveness on Enhancing Sound Absorption Properties," Pertanika J. Sci. & Technol., vol. 29, no. 1, pp. 693 - 706, 2021.

[258] M. Khan, S. Rahamathbaba, M. Mateen, D. Ravi Shankar, and M. Manzoor Hussain, "Effect of NaOH treatment on mechanical strength of banana/epoxy laminates," Polymers from Renewable Resources, vol. 10, no. 1-3, pp. 19-26, 2019.

[259] M. Y. Hashim, A. M. Amin, O. M. F. Marwah, M. H. Othman, M. R. M. Yunus, and N. C. Huat, "The effect of alkali treatment under various conditions on physical properties of kenaf fiber," in International Conference on Materials Physics and Mechanics (PHENMA 2017), Jabalpur, India, 2017, vol. 914: IOP Publishing.

[260] A. Karthikeyan, B. Kulendran, and A. Kalpana, "The effect of sodium hydroxide treatment and fiber length on the tensile property of coir fiber-reinforced epoxy composites," Science and Engineering of Composite Materials, vol. 21, 06/01 2014.

[261] Standard Test Method for Compositional Analysis by Thermogravimetry, 2008.

[262] Standard Practice for Plastics: Dynamic Mechanical Properties: Determination and Report of Procedures, 2001.

[263] Standard Test Method for Glass Transition Temperature (DMA Tg) of Polymer Matrix Composites by Dynamic Mechanical Analysis (DMA), 2008.

[264] PerkinElmer, "Dynamic Mechanical Analysis (DMA): A Beginner's Guide," PerkinElmer, Ed., ed. Waltham, MA, USA: PerkinElmer, Inc., 2013.

[265] C. A. Gracia-Fernández, S. Gómez-Barreiro, J. López-Beceiro, J. Tarrío Saavedra, S. Naya, and R. Artiaga, "Comparative study of the dynamic glass transition temperature by DMA and TMDSC," Polymer Testing, vol. 29, no. 8, pp. 1002-1006, 2010/12/01/ 2010.

[266] K. Whitcomb, "Measurement of Glass Transition Temperatures by Dynamic Mechanical Analysis and Rheology," T. Instruments, Ed., ed. USA: TA Instruments.

[267] Standard Test Method for Tensile Properties of Polymer Matrix Composite Materials, 2000.

[268] Standard Test Methods for Flexural Properties of Unreinforced and Reinforced Plastics and Electrical Insulating Materials, 2003.

[269] Standard Test Method for Determining the Charpy Impact Resistance of Notched Specimens of Plastics, 2010.

[270] W. Webo, L. Masu, and M. Maringa, "The Impact Toughness and Hardness of Treated and Untreated Sisal Fibre-Epoxy Resin Composites," Advances in Materials Science and Engineering, vol. 2018, pp. 1-11, 2018.

[271] G. Rajeshkumar et al., "Influence of Sodium Hydroxide (NaOH) Treatment on Mechanical Properties and Morphological Behaviour of Phoenix sp. Fiber/Epoxy Composites," Journal of Polymers and the Environment, vol. 29, no. 3, pp. 765-774, 2021/03/01 2021.

[272] N. F. Ismail, N. A. M. Radzuan, A. B. Sulong, N. Muhamad, and C. H. C. Haron, "The Effect of Alkali Treatment on Physical, Mechanical and Thermal Properties of Kenaf Fiber and Polymer Epoxy Composites," Polymers, vol. 13, no. 2005, pp. 1-17, 2021.

[273] B. Pejic, M. Kostic, P. Skundric, and J. Praskalo, "The effects of hemicelluloses and lignin removal on water uptake behavior of hemp fibers," Bioresource technology, vol. 99, pp. 7152-9, 11/01 2008.

[274] Ikramullah, S. Rizal, S. Thalib, and S. Huzni, "Hemicellulose and lignin removal on typha fiber by alkali treatment," IOP Conference Series: Materials Science and Engineering, vol. 352, p. 012019, 2018/05 2018.

[275] M. Ali, C. Yong, C. Yern Chee, C. H. Chuah, and N.-S. Liou, "Effect of Single and Double Stage Chemically Treated Kenaf Fibers on Mechanical Properties of Polyvinyl Alcohol Film," BioResources, vol. 10, pp. 822-838, 01/01 2015.

[276] T. P. Mohan and K. Kanny, "Water barrier properties of nanoclay filled sisal fibre reinforced epoxy composites," Composites Part A: Applied Science and Manufacturing, vol. 42, no. 4, pp. 385-393, 2011/04/01/ 2011.

[277] H. Alamri and I. M. Low, "Effect of water absorption on the mechanical properties of nanoclay filled recycled cellulose fibre reinforced epoxy hybrid nanocomposites," Composites Part A: Applied Science and Manufacturing, vol. 44, pp. 23-31, 2013/01/01/ 2013.

[278] S. H. Kamarudin, L. C. Abdullah, M. M. Aung, and C. T. Ratnam, "A study of mechanical and morphological properties of PLA based biocomposites prepared with EJO vegetable oil based plasticiser and kenaf fibres," Materials Research Express, vol. 5, no. 8, p. 085314, 2018/07/27 2018.

[279] A. K. Rana, R. K. Basak, B. C. Mitra, M. Lawther, and A. N. Banerjee, "Studies of acetylation of jute using simplified procedure and its characterization," Journal of Applied Polymer Science, vol. 64, no. 8, pp. 1517-1523, 1997.

[280] L. F. C. Nascimento et al., "Charpy impact test of epoxy composites reinforced with untreated and mercerized mallow fibers," Journal of Materials Research and Technology, vol. 7, no. 4, pp. 520-527, 2018/10/01/ 2018.

[281] S. Kamarudin, A. Luqman Chuah, M. M. Aung, and C. Ratnam, "Thermal and Structural Analysis of Epoxidized Jatropha Oil and Alkaline Treated Kenaf Fiber Reinforced Poly(Lactic Acid) Biocomposites," Polymers, vol. 12, p. 2604, 11/06 2020.

[282] E. Jakubowska, M. Gierszewska, J. Kujawa, A. Raszkowska-Kaczor, and W. Kujawski, "Development and Characterization of Polyamide-Supported Chitosan Nanocomposite Membranes for Hydrophilic Pervaporation," Polymers, vol. 10, p. 868, 08/04 2018.

[283] H. Ku, H. Wang, N. Pattarachaiyakoop, and M. Trada, "A review on the tensile properties of natural fiber reinforced polymer composites," Composites Part B: Engineering, vol. 42, no. 4, pp. 856-873, 2011/06/01/ 2011.

[284] O. Samuel, "Assessing Mechanical Properties of Natural Fibre Reinforced Composites for Engineering Applications," 01/01 2012.

[285] R. M. Bajracharya, D. S. Bajwa, and S. G. Bajwa, "Mechanical properties of polylactic acid composites reinforced with cotton gin waste and flax fibers," Procedia Engineering, vol. 200, pp. 370-376, 2017/01/01/ 2017.

[286] E. L. Bourhis and F. Touchard, "Mechanical Properties of Natural Fiber Composites," in Materials Science and Materials Engineering, ed. France: Elsevier, 2021, pp. 1-28.

[287] V. P. Sajna, S. Mohanty, and S. K. Naya, "Hybrid green nanocomposites of poly(lactic acid) reinforced with banana fibre and nanoclay," Reinforced Plastics and Composites, vol. 33, no. 18, pp. 1717–1732, 2014.

[288] P. Ramesh, B. D. Prasad, and K. L. Narayana, "Effect of MMT Clay on Mechanical, Thermal and Barrier Properties of Treated Aloevera Fiber/ PLA-Hybrid Biocomposites," Silicon, 2019/10/17 2019.

[289] S. Salman, Z. Leman, M. T. H. Sultan, M. Ishak, and F. Cardona, "Influence of resin system on the energy absorption capability and morphological properties of plain woven kenaf composites," IOP Conference Series Materials Science and Engineering, vol. 100, p. 012053, 12/22 2015.

[290] A. Erklig, N. F. Dogan, and M. Bulut, "Charpy Impact Response of Glass Fiber Reinforced Composite with Nano Graphene Enhanced Epoxy," Periodicals of Engineering and Natural Sciences, vol. 5, no. 3, pp. 341-346, 2017.

[291] A. A. Pérez-Fonseca, V. O. Ramírez-Herrera, F. J. Fuentes-Talavera, D. Rodrigue, J. A. Silva-Guzmán, and J. R. Robledo-Ortíz, "Crystallinity and impact strength improvement of wood-polylactic acid biocomposites produced by rotational and compression molding," Maderas. Ciencia y tecnología, vol. 23, 2021.

[292] H. Suherman, E. Azwar, Duskiardi, Y. Mahyoedin, and E. Septe, "Properties of Kenaf Fibers/Epoxy Biocomposites: Flexural Strength and Impact Strength," IOP Conference Series: Materials Science and Engineering, vol. 652, p. 012036, 10/29 2019.

[293] J.-H. Lee et al., "Mechanical Properties of Biocomposites Using Polypropylene and Sesame Oil Cake," Polymers, vol. 13, no. 10, p. 1602, 2021.

[294] N. Navaranjan and T. Neitzert, "Impact Strength of Natural Fibre Composites Measured by Different Test Methods: A Review," in ICMSNT 2017 MATEC Web of Conferences, 2017.

[295] k. Chitra and A. Gurusamy, "Fluorescent Silica Nanoparticles in the Detection and Control of the Growth of Pathogen," Journal of Nanotechnology, vol. 2013, p. 7, 09/13 2013.

[296] G. Nallathambi, T. Ramachandran, R. Venkatachalam, and R. Palanivelu, "Effect of Silica Nanoparticles and BTCA on Physical Properties of Cotton Fabrics," Materials Research, vol. 14, pp. 552-559, 12/01 2011.

[297] O. Saber and H. M. Gobara, "Optimization of silica content in alumina-silica nanocomposites to achieve high catalytic dehydrogenation activity of supported Pt catalyst," Egyptian Journal of Petroleum, vol. 23, no. 4, pp. 445-454, 2014/12/01/ 2014.

[298] S. Yaman et al., "Effects of silica nanoparticles on isolated rat uterine smooth muscle," Drug and chemical toxicology, vol. 41, no. 4, pp. 465-475, 2017.

[299] P. Sikora, D. Lootens, M. Liard, and D. Stephan, "The effects of seawater and nanosilica on the performance of blended cements and composites," Applied Nanoscience, 2020/03/09 2020.

[300] T.-J. Chung et al., "The Improvement of Mechanical Properties, Thermal Stability, and Water Absorption Resistance of an Eco-Friendly PLA/Kenaf Biocomposite Using Acetylation," Applied Sciences, vol. 8, no. 3, p. 376, 2018.

[301] M. H. Mat Yazik et al., "Effect of Nanofiller Content on Dynamic Mechanical and Thermal Properties of Multi-Walled Carbon Nanotube and Montmorillonite Nanoclay Filler Hybrid Shape Memory Epoxy Composites," (in eng), Polymers (Basel), vol. 13, no. 5, Feb 25 2021.

[302] R. Zhang, X. He, and G. Huang, "A review of the slow relaxation processes in the glass–rubber transition region of amorphous polymers," Phase Transitions, vol. 88, pp. 1-16, 05/20 2015.

[303] X. Li, W. Rombouts, J. Gucht, R. de Vries, and J. Dijksman, "Mechanics of composite hydrogels approaching phase separation," PLOS ONE, vol. 14, p. e0211059, 01/25 2019.

[304] Z. Sun, L. Zhang, D. Liang, W. Xiao, and J. Lin, "Mechanical and Thermal Properties of PLA BiocompositesReinforced by Coir Fibers," International Journal of Polymer Science, vol. 2017, pp. 1-8, 2017.

[305] J. Chandradass, M. R. Kumar, and R. Velmurugan, "Effect of nanoclay addition on vibration properties of glass fibre reinforced vinyl ester composites," Materials Letters, vol. 61, no. 22, pp. 4385-4388, 2007/09/01/ 2007.

[306] L. A. Pothan, Z. Oommen, and S. Thomas, "Dynamic mechanical analysis of banana fiber reinforced polyester composites," Composites Science and Technology, vol. 63, no. 2, pp. 283-293, 2003/02/01/ 2003.

[307] M. Mohammadi, J. Davoodi, M. Javanbakht, and H. Rezaei, "Glass transition temperature of PMMA/modified alumina nanocomposite: molecular dynamic study," Materials Research Express, vol. 6, no. 3, p. 035309, 2018/12/19 2018.

[308] P. Mach, A. Géczy, R. Polansky, and D. Bušek, "Glass transition temperature of nanoparticle-enhanced and environmentally stressed conductive adhesive materials for electronics assembly," Journal of Materials Science: Materials in Electronics, vol. 30, 03/01 2019.

[309] O. A. Serenko, V. I. Roldughin, A. A. Askadskii, E. S. Serkova, P. V. Strashnov, and Z. B. Shifrina, "The effect of size and concentration of nanoparticles on the glass

transition temperature of polymer nanocomposites," RSC Advances, 10.1039/C7RA08152A vol. 7, no. 79, pp. 50113-50120, 2017.

[310] PerkinElmer, "Dynamic Mechanical Analysis (DMA)," PerkinElmer, Ed., ed. Waltham, USA, 2008.

[311] F. Pinto and M. Meo, "Design and Manufacturing of a Novel Shear Thickening Fluid Composite (STFC) with Enhanced out-of-Plane Properties and Damage Suppression," Applied Composite Materials, vol. 24, no. 3, pp. 643-660, 2017/06/01 2017.

[312] D. Li, R. Wang, F. Guan, Y. Zhu, and F. You, "Enhancement of the quasi-static stab resistance of Kevlar fabrics impregnated with shear thickening fluid," Journal of Materials Research and Technology, vol. 18, pp. 3673-3683, 2022/05/01/ 2022.

[313] M. Wei, K. Lin, and L. Sun, "Shear thickening fluids and their applications," Materials & Design, vol. 216, p. 110570, 2022/04/01/ 2022.

Appendices

Appendix A Fabricated kenaf/nanoclay/PLA biocomposites

Figure 9.1 shows a typical kenaf/nanoclay/PLA biocomposite laminate fabricated in this work.

Figure 9.1 Fabricated kenaf/nanoclay/PLA hybrid biocomposite

Appendix B Impacted specimen

Figure 9.2 shows a damaged kenaf/nanoclay/PLA hybrid biocomposite that was subjected to medium velocity impact.

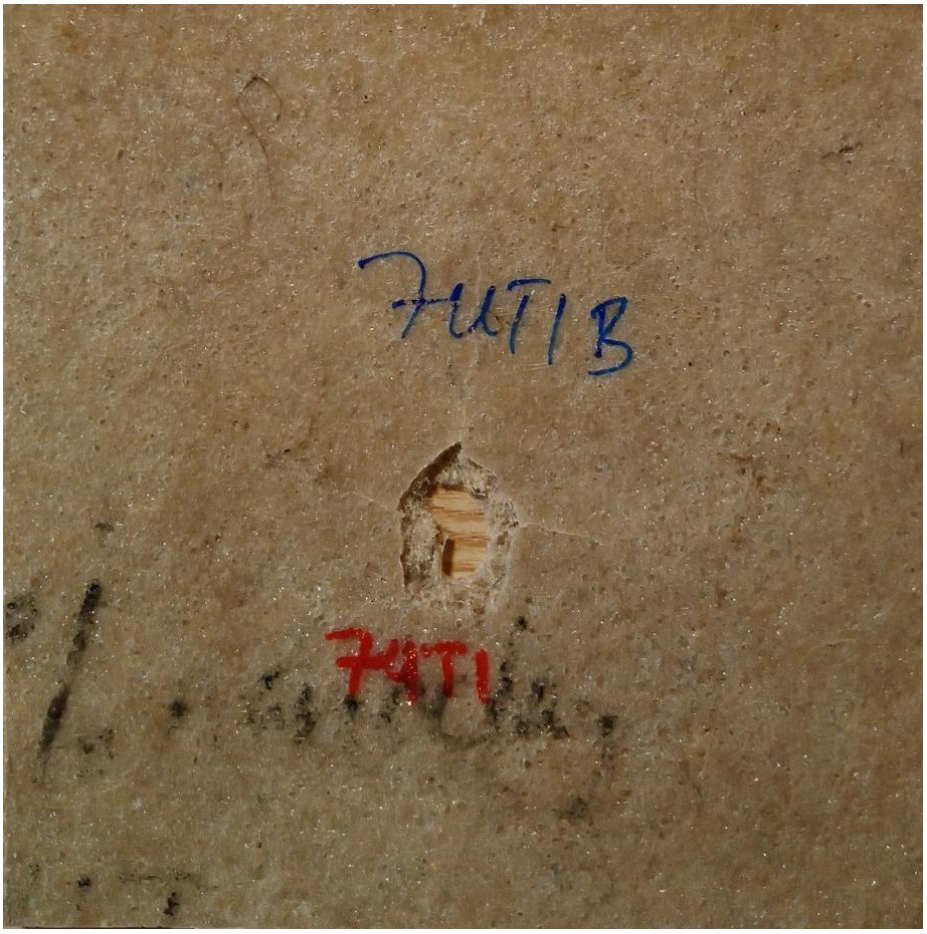

Figure 9.2 Damaged biocomposite after medium velocity impact loading

Appendix C Optical microscope image of damaged composite area

Figure 9.3 shows an optical microscope image of the damaged area of the hybrid composite subjected to medium velocity impact loading.

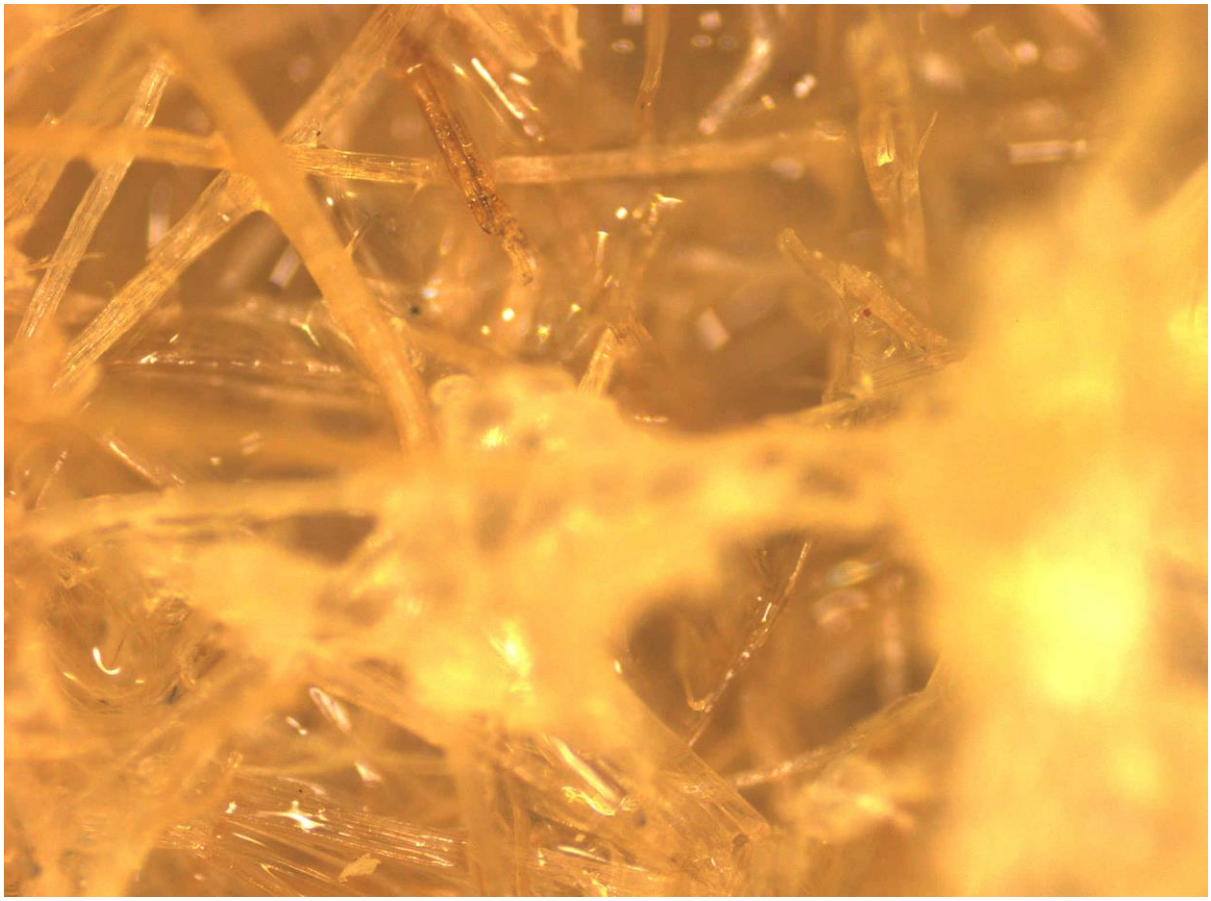

Figure 9.3 Microscopic image of damaged hybrid biocomposite